สารออกฤทธิ์ทางชีวภาพจากรากเมื่อยดูก *Gnetum macrostachyum*

นายปิยวิทย์ ศรีอินทร์

วิทยานิพนธ์นี้เป็นส่วนหนึ่งของการศึกษาตามหลักสูตรปริญญาวิทยาศาสตรมหาบัณฑิต
สาขาวิชาเคมี ภาควิชาเคมี
คณะวิทยาศาสตร์ จุฬาลงกรณ์มหาวิทยาลัย
ปีการศึกษา 2550

BIOACTIVE COMPOUNDS FROM THE ROOTS OF *Gnetum macrostachyum*

Mr. Piyawit Sri-in

A Thesis Submitted in Partial Fulfillment of the Requirements
for the Degree of Master of Science Program in Chemistry
Department of Chemistry
Faculty of Science
Chulalongkorn University
Academic Year 2007

Thesis Title	BIOACTIVE COMPOUNDS FROM THE ROOTS OF *Gnetum macrostachyum*
By	Mr. Piyawit Sri-in
Field of Study	Chemistry
Thesis Advisor	Associate Professor Santi Tip-pyang, Ph.D.
Thesis Co-advisor	Assistant Professor Preecha Phuwapraisirisan, Ph.D.

Accepted by the Faculty of Science, Chulalongkorn University in Partial Fulfillment of the Requirements for the Master's Degree

S. Hannongbua ..... Dean of the Faculty of Science

(Professor Supot Hannongbua, Ph.D.)

THESIS COMMITTEE

Udom Kokpol ..... Chairman

(Professor Udom Kokpol, Ph.D.)

Santi Tip-pyang ..... Thesis Advisor

(Associate Professor Santi Tip-pyang, Ph.D.)

P. Phuwapraisirisan ..... Thesis Co-advisor

(Assistant Professor Preecha Phuwapraisirisan, Ph.D.)

W. Bhanthumnavin ..... Member

(Assistant Professor Worawan Bhanthumnavin, Ph.D.)

A. Shitangkoon ..... Member

(Assistant Professor Aroonsiri Shitangkoon, Ph.D.)

ปิยวิทย์ ศรีอินทร์ : สารออกฤทธิ์ทางชีวภาพจากรากเมื่อยดูก *Gnetum macrostachyum*. (BIOACTIVE COMPOUNDS FROM THE ROOTS OF *Gnetum macrostachyum*) อ. ที่ปรึกษา: รศ.ดร. สันติ ทิพยางค์, อ. ที่ปรึกษาร่วม: ผศ.ดร. ปรีชา ภูวไพรศิริศาล, 78 หน้า.

ในการศึกษาสารออกฤทธิ์ทางชีวภาพจากพืชสมุนไพรไทยในวงศ์ Gnetaceae จึงได้เลือกสิ่งสกัดอะซิโตนจากรากเมื่อยดูกมาแยก ทำให้บริสุทธิ์ และหาสูตรโครงสร้าง จากการแยกสารจากสิ่งสกัดอะซิโตนนี้โดยวิธีทางโครมาโทกราฟี ได้สารสติลบินอยด์ชนิดใหม่ 5 ชนิดคือ macrostachyol A (**6**), B (**7**), C (**11**), D (**13**) และ gnetumacrosin (**9**) พร้อมกับสติลบินอยด์ที่มีรายงานมาแล้ว 8 ชนิดคือ isorhapontigenin (**1**), *trans*-resveratrol (**2**), gnetol (**3**), gnetin C (**4**), latifolol (**5**), parvifolol A (**8**), bisisorhapontigenin B (**10**) และ oxyresveratrol (**12**) พิสูจน์สูตรโครงสร้างของสารทั้งหมดที่แยกได้ โดยวิธีทางสเปกโทรสโกปี และเปรียบเทียบกับข้อมูลที่มีรายงานแล้ว นำสารที่แยกได้ไปทดสอบฤทธิ์ในการยับยั้งการเกิดออกซิเดชัน (ต้านอนุมูลอิสระ DPPH และยับยั้งการเกิดออกซิเดชันของไขมัน) ฤทธิ์ยับยั้งการรวมตัวของเกล็ดเลือด และ ความเป็นพิษต่อเซลล์มะเร็งชนิด HeLa และ KB พบว่า สาร **1, 3, 4, 5,** และ **6** แสดงฤทธิ์ที่ดีในการต้านอนุมูลอิสระ DPPH ด้วยค่า IC_{50} = 0.28, 0.21, 0.24, 0.32 และ 0.33 mM ตามลำดับ สาร **5** และ **6** (IC_{50} = 0.02 mM) มีฤทธิ์ต้านการเกินออกซิเดชันของไขมันมากที่สุด สำหรับฤทธิ์ยับยั้งการรวมตัวของเกล็ดเลือดพบว่าสาร **1-8** (IC_{50} = 0.18-1.26 μM) มีฤทธิ์ที่สูงกว่า ibuprofen (IC_{50} = 11.2 mM) ซึ่งใช้เป็นสารมาตรฐาน นอกจากนั้นพบว่าสาร **1, 2, 9,** และ **10** แสดงความเป็นพิษต่อเซลล์มะเร็งชนิด KB ที่ IC_{50} = 6.90, 8.00, 8.50, และ 12.50 และ HeLa ที่ IC_{50} = 15.00, 15.50, 11.00, และ 14.00 μg/mL, ตามลำดับ

ภาควิชา.....เคมี..... ลายมือชื่อนิสิต.....ปิยวิทย์ ศรีอินทร์.....

สาขาวิชา.....เคมี..... ลายมือชื่ออาจารย์ที่ปรึกษา.....สันติ ทิพยางค์.....

ปีการศึกษา.....2550..... ลายมือชื่ออาจารย์ที่ปรึกษาร่วม.....ปรีชา ภูวไพรศิริศาล.....

4772378923: MAJOR CHEMISTRY

KEY WORD: BIOACTIVE COMPOUNDS / *Gnetum macrostachyum* / STILBENOIDS / RESVERATROL

PIYAWIT SRI-IN: BIOACTIVE COMPOUNDS FROM THE ROOTS OF *Gnetum macrostachyum*. THESIS ADVISOR: ASSOC. PROF. SANTI TIP-PYANG, Ph.D., THESIS CO-ADVISOR: ASST. PROF. PREECHA PHUWAPRAISIRISAN, Ph.D., 78 pp.

In phytochemical investigation for bioactive compounds from Thai medicinal plants in the family Gnetaceae, acetone crude extract from the roots of *Gnetum macrostachyum* was selected for isolation, purification and structure elucidation. The chromatographic separation of acetone crude extract led to the isolation of five new stilbenoids, macrostachyol A (**6**), B (**7**), C (**11**), D (**13**), and gnetumacrosin (**9**) along with eight known stilbenoids, isorhapontigenin (**1**), *trans*-resveratrol (**2**), gnetol (**3**), gnetin C (**4**), latifolol (**5**), parvifolol A (**8**), bisisorhapontigenin B (**10**), and oxyresveratrol (**12**). The structures of all isolated compounds were elucidated by spectroscopic methods as well as comparison with previous literature data. The isolated stilbenoids were tested for inhibitory activity of antioxidant (DPPH radical scavenging and lipidperoxidation inhibition), antiplatelet aggregation, and cytotoxicity on HeLa and KB cell lines. Compounds **1, 3, 4, 5,** and **6** showed antioxidant activity on DPPH radical with IC_{50} value of 0.28, 0.21, 0.24, 0.32, and 0.33 mM respectively. Compound **5** and **6** (IC_{50} = 0.02 mM) also showed highest activity towards on lipid peroxidation inhibition. For antiplatelet aggregation, compounds **1-8** (IC_{50} = 0.18-1.26 μM) more potent than ibuprofen (IC_{50} = 11.2 mM) which was used as a positive control. In addition, compounds **1**, **2**, **9,** and **10** showed mild cytotoxic activity against KB cell line IC_{50} = 6.90, 8.00, 8.50, and 12.50 and against HeLa cell line with IC_{50} = 15.00, 15.50, 11.00, and 14.00 μg/mL, respectively.

Department:.....Chemistry.....Student's signature...Piyawit Sri-in.....
Field of study:.....Chemistry.....Advisor's signature.....Santi Tip-pyang.....
Academic year:....2007.....Co-advisor's signature.....P. Phuwaprai sirisan.....

ACKNOWLEDGEMENTS

I would like to express my faithful gratitude to my advisor, Associate Professor Dr. Santi Tip-pyang, and my co-advisor, Asssistant Professor Dr. Preecha Phuwapraisirisal, for their assistance and encouragement in conducting this research.

I also gratefully acknowledge the members of my thesis committee, Professor Dr. Udom Kokpol, Assistant Professor Dr. Aroonsiri Shitangkoon, and Assistant Professor Dr. Worawan Bhanthumnavin for their discussion and guidance.

The special thank to both Mr. Somkiet Singtong and Miss Kringkaew Nuansri for providing the roots of *Gnetum macrostachyum* in this study.

I would like to thank the staff of Plant of Thailand Research Unit, Department of Botany, Faculty of Science, Chulalongkorn University for plant identification in this study.

My appreciation is also expressed to Mr. Serm Surapinit and Mr. Dech Dokpuang for their help and guidance in anti-platelet aggregation assay.

I would like to express my gratitude to the Natural Product Research Unit, Department of Chemistry, Faculty of Science, Chulalongkorn University, for the support of chemicals and laboratory facilities throughout the course of study. Moreover, thanks are extended to Graduate School of Chulalongkorn University for financial support.

I would also like to express my appreciation to my family for their great support and encouragement throughout my education.

Finally, I would like to thank all of my friends for their friendship and help during my graduate study.

CONTENTS

List of Tables

List of Figures

List of Schemes

List of Abbreviations

^{13}C NMR	carbon 13 nuclear magnetic resonance
^{1}H NMR	proton nuclear magnetic resonance
ADP	adenosine diphosphate
brs	broad singlet (NMR)
c	concentration
COSY	correlated spectroscopy
d	doublet (NMR)
dd	doublet of doublet (NMR)
DPPH	2,2-diphenyl-1-picrylhydrazyl radical
DPPHn	2,2-diphenyl-1-picrylhydrazine
ESIMS	electrospray ionization mass spectrometry
g	gram (s)
HMBC	heteronuclear multiple bond correlation experiment
HMQC	heteronuclear multiple quantum correlation
HRESIMS	high resolution electrospray ionization mass spectrometry
Hz	hertz
IC_{50}	concentration that is required for 50% inhibition in vitro
J	coupling constant
m	multiplet (NMR)
M	molar
MeOH	methanol
mg	milligram (s)
MHz	megahertz
min	minute
mL	milliliter (s)
mult	multiplicity
NMR	nuclear magnetic resonance
NOESY	nuclear overhauser enhancement spectroscopy
s	singlet (NMR)

t	triplet (NMR)
TMS	tetramethylsilane
UV	ultraviolet
VLC	vacuum liquid chromatography
δ	chemical shift
δ_C	chemical shift of carbon
δ_H	chemical shift of proton
ε	molar extinction coefficient
λ_{max}	maximum wavelength
2D NMR	two dimentional nuclear magnetic resonance
$[\alpha]_D^{26}$	specific optical rotation

CHAPTER I
INTRODUCTION

It has been long thought that human can use plants in many ways. Human can obtain numerously valuable benefits from their natural resources. Fortunately, Thailand is located in the tropical region of the world and has abundant kinds of plants, especially herbs which are used as medicinal plants.

Medicinal plants contain various bioactive secondary metabolites. They have especially pharmacological active principle which can be used as therapeutic drugs or herbal medicine. Therefore, medicinal plants still serve as sources for scientists to be developed into new lead and more active compounds.

Medicinal plants are a vital source of medication in developing countries. Despite the wealth of human experience and folklore concerning the medicinal uses of plants, proper scientific investigation has only been applied to a small fraction of the world's plants.

The family of Gnetaceae is known to contain stilbenoids.[1-3] Various species in the family have been used as folk medicine for the treatment of rheumarthritis, arthritis, bronchitis and asthma.[4] The leaves and the fruits are also used as food in many parts of the tropics.[5] The recent isolation of many stilbene oligomers,[6-8] their various biological activities such as blood sugar reduction,[9] induction of apoptosis in colon cancer,[10] *etc.* have been revealed. These revealed the importance of plants containing stilbenoids as resources for the development of new drugs.

1.1 Stilbenoids: distribution and their biosynthesis pathway

Stilbenoids, a large group of natural occurring compounds, are commonly found in plants in the families Dipterocarpaceae[11-12] Vitaceae,[7,13] Cyperaceae,[14] and Gnetaceae.[2, 15-18]

Stilbenoids are secondary metabolites of heartwood formation in trees that can act as phytoalexins. Chemically they are hydroxylated derivatives of stilbene. Biochemically they belong to the family of phenylpropanoids and share most of their biosynthesis pathway with chalcones.[19] An example of stilbenoids is reservatrol which is found in grapes. It has been suggested in many health benefits.[20]

1.1.1 Resveratrol biosynthetic pathway

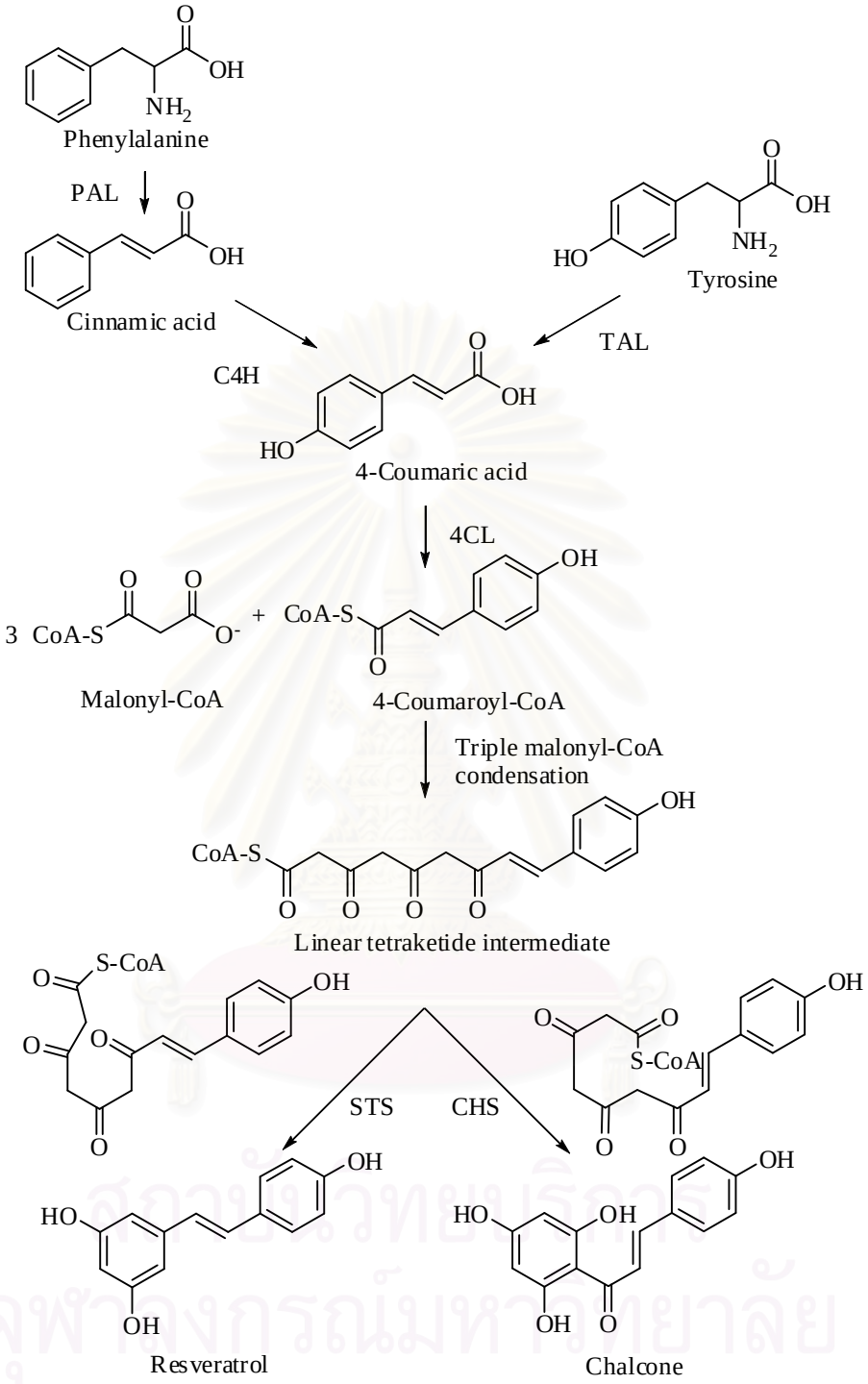

Figure 1.1 Biosynthetic pathway of resveratrol and its derivatives diverge from the flavonoid pathway after the third malonyl-CoA condensation. Cyclization of the polyketide intermediate catalyzed by stilbene synthase (STS) yielded resveratrol.

In some plant species resveratrol branches from the phenylpropanoid-polyketide biosynthesis pathway (Figure 1.1),[21-23] the resveratrol pathway consists of four enzymes:

phenylalanine ammonia lyase (PAL), cinnamic acid 4-hydroxylase (C4H), 4-coumarate-CoA ligase (4CL)-which can be replaced by a single enzyme tyrosine ammonia lyase (TAL) and stilbene synthase (STS). The first two enzymes, PAL and C4H, transform phenylalanine into *p*-coumaric acid (4-coumaric acid). The third enzyme, 4CL, attaches *p*-coumaric acid to the pantetheine group of Coenzyme-A (CoA) to produce 4-coumaroyl-CoA. PAL, C4H and 4CL are members of the common phenylpropanoid pathway in plants, which synthesizes the majority of phenolic compounds found in nature, including lignins for use as cell wall components, anthocyanins as pigments and flavonols as UV-protectants. The final enzyme in the pathway, STS, catalyzes the condensation of resveratrol from one molecule of 4-coumaroyl-CoA and three molecules of malonyl-CoA, which originate from fatty acid biosynthesis, produce resveratrol through a $C2 \rightarrow C7$ aldol condensation. STS is a member of the type III polyketide synthases and has extensive homology to chalcone synthase (CHS). CHS is responsible for the formation of chalcones in many higher plants – chalcones are starting molecules for all flavonoid compounds. Although CHS is ubiquitous in plants, STS is only found in species that accumulate resveratrol and related compounds.

1.2 Stilbenoids constituent from Gnetum species and their biological activities

Stilbenoids have attracted much attention for their unique structures. They are monomer, dimer, oligomer up to octamer. Moreover, many of these compounds have demonstrated a number of interesting biological activities, such as antioxidant,[24-26] anti-platelet aggregation,[24,27] antifungal,[28-29] protein kinase C inhibitory,[30] hepatoprotective and hepatotoxic,[31] anti-HIV, cytotoxic[32-33] and cyclooxygenase (COX I and COX II) inhibitory[34] activities.

Common stilbenoid monomers and dimers found in plants of family Gnetaceae include resveratrol, isorhapontigenin, gnetol, oxyresveratrol, (-)-*e*-viniferin and gnetin C. Stilbenoid dimers and oligomers are formed from oxidative coupling of these compounds.

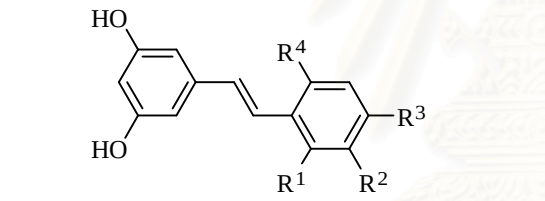

	R^1	R^2	R^3	R^4
resveratrol	H	H	OH	H
isorhapontigenin	H	OMe	OH	H
gnetol	OH	H	H	OH
oxyresveratrol	OH	H	OH	H

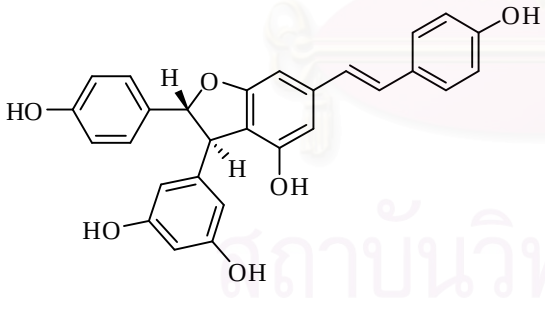

gnetin C

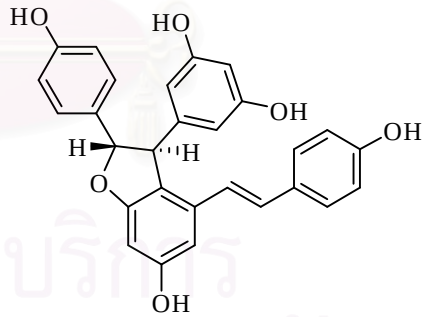

(-)-*e*-viniferin

Figure 1.2 Common stilbenoid monomers and dimers from plants in Gnetaceae family.

Stilbenoids and their oligomers have been isolated from the acetone soluble fraction of linas of *G. latifolium.* They were resveratrol, gnetin C, (-)-*e*-viniferin, gnetin E, gnetin D, and latifolol (Figure 1.3).[18]

Gnetum gnemon have been used as folk medicines for the treatment of arthritis, bronchitis, and asthma.[35] Recently gnemonols A, B, D, E, F, K, L, M, gnetin E, gnemonoside K, (-)-*e*-viniferin, gnetol, isorhapontigenin, gnetifolin E, isorhapontigenin-3-*O*-D-glucopyranoside,[3] resveratrol, and latifolol[18] were isolated from the acetone, methanol and 70% methanol extracts of the root of *G. gnemon* Linn (Figure 1.3).[5,36]

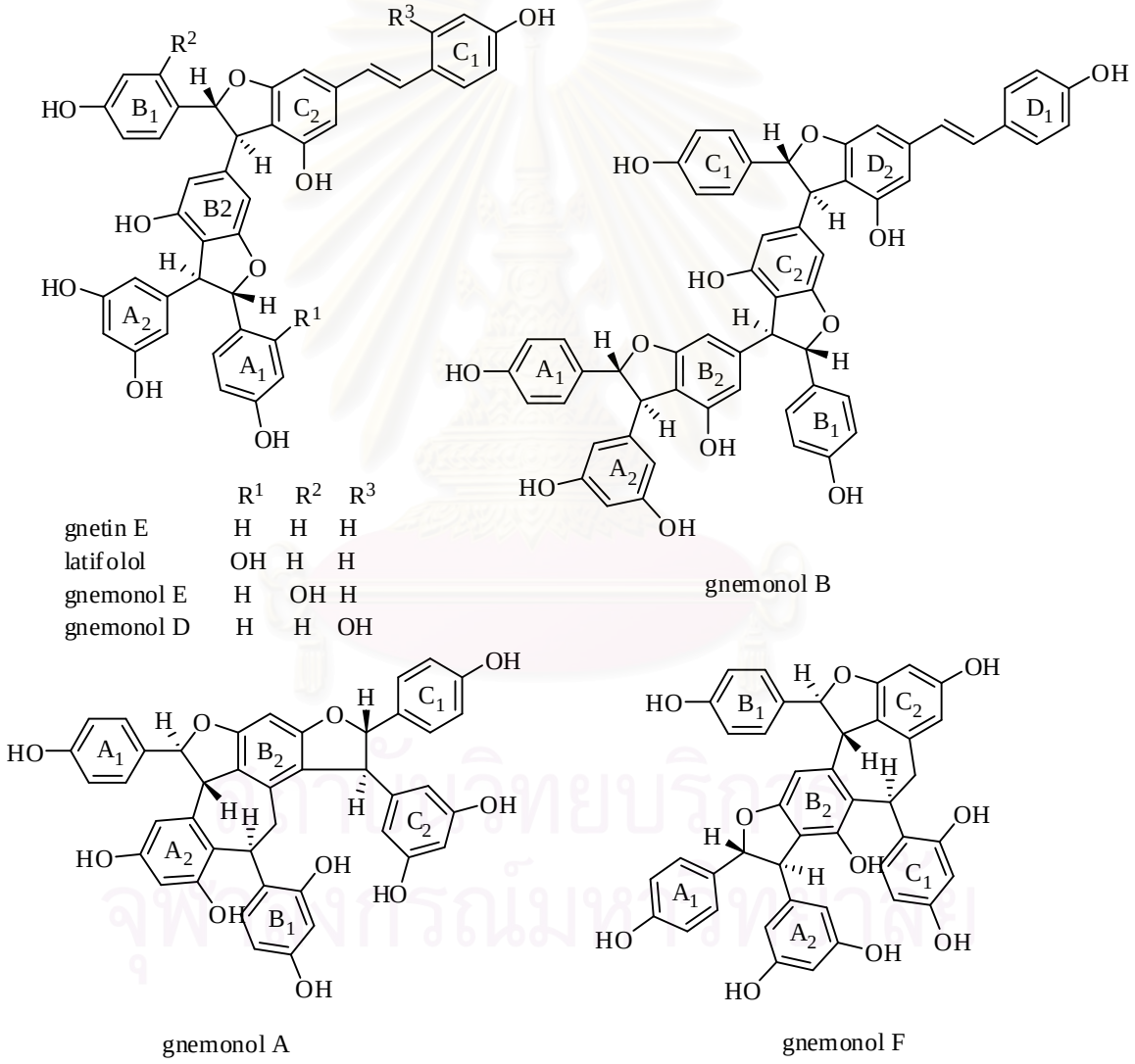

Figure 1.3 Stilbenoids from *G. latilolium* and *G. gnemon*.

Gnemonol B is the first instance of a stilbene tetramer reported from the family of Gnetaceae.[36] The antioxidant activity (super oxide scavenging and lipid peroxidation

activities) of some stilbenoids from *G. gnemon* such as gnemonol K, L, (-)-*e*-viniferin, gnetol, resveratrol, isorhapontigenin and latifolol were stronger than vitamin E.[25] Gnetol was found to be approximately 30-fold stronger than kojic acid (standard) for tyrosinase inhibition. Moreover, it significantly suppressed melanin biosynthesis in murin B 16 melanoma cell.[35]

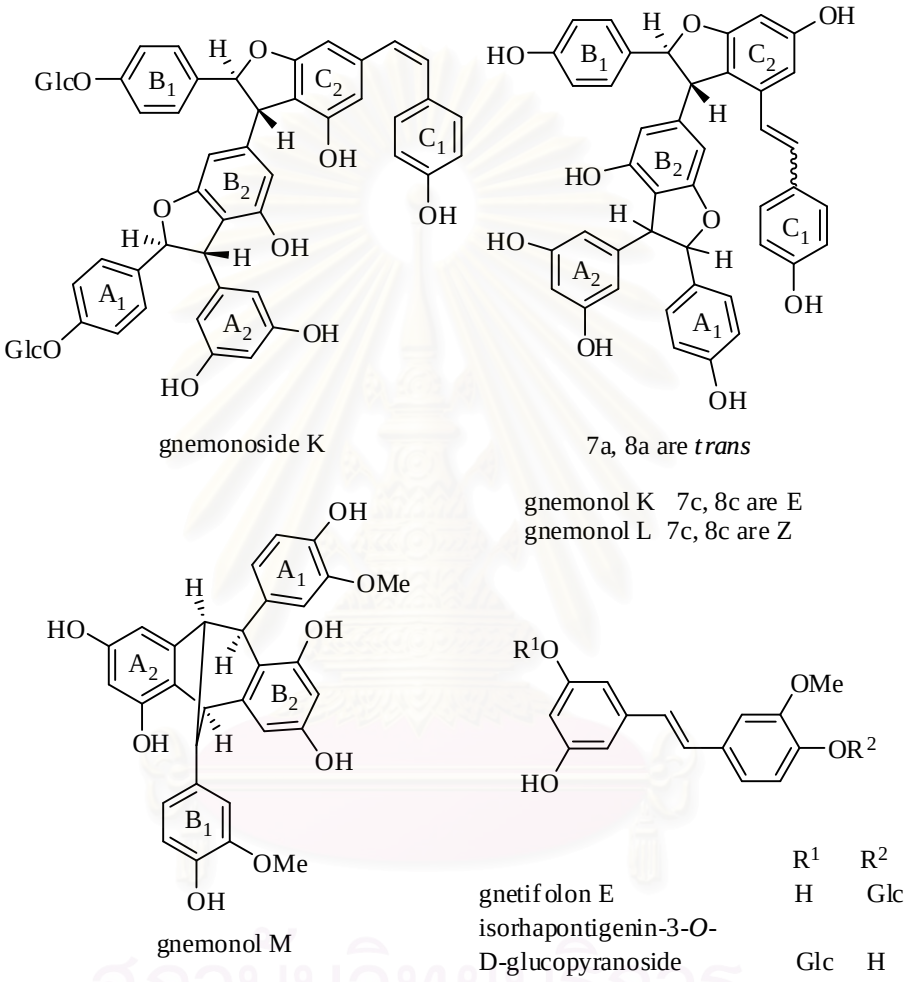

Figure 1.3 Stilbenoids from *G. latilolium* and *G. gnemon*. (cont.)

Many stilbenoids were also isolated from the EtOAc soluble fraction of *G. montanum*[4] and *G. montanum* f. *megalocarpum*.[37] They were gnetifolin M, gnetumontanins A-D, gnetifolin, isorhapontigenin, resveratrol, gnetol, gnetupendin B,[34] (-)-*e*-viniferin, gnetulin, gnetin D, gnetuhainin M, isorhapontigenin 3-*O*-*b*-D-glucoside, and isorhapontigenin 12-*b*-D-glucoside (Figure 1.5).

Gnetumontanin A was the first stilbene dimer derived from two oxyresveratrol units while gnetumontanins C and D were novel skeleton having δ-lactone moieties.

Gnetumontanin B showed tumor necrosis factor inhibitory activities (IC_{50} 1.49 μM while dexanethasone was used as a positive control with an IC_{50} at 1 μM).[37]

Gnetupendins A and B were obtained together with resveratrol and isorhapontigenin from *G. pendulum*.[34] They contained new stilbenoid skeletons, in which the position 2 of 3,5-dihydroxybenzene ring (B) of the isorhapontigenin unit were substituted by 4-hydroxybenzyl and 3,4-dihydroxybenzyl groups, respectively. Moreover, gnetupendin B has cyclooxygenase-II inhibitory activity.

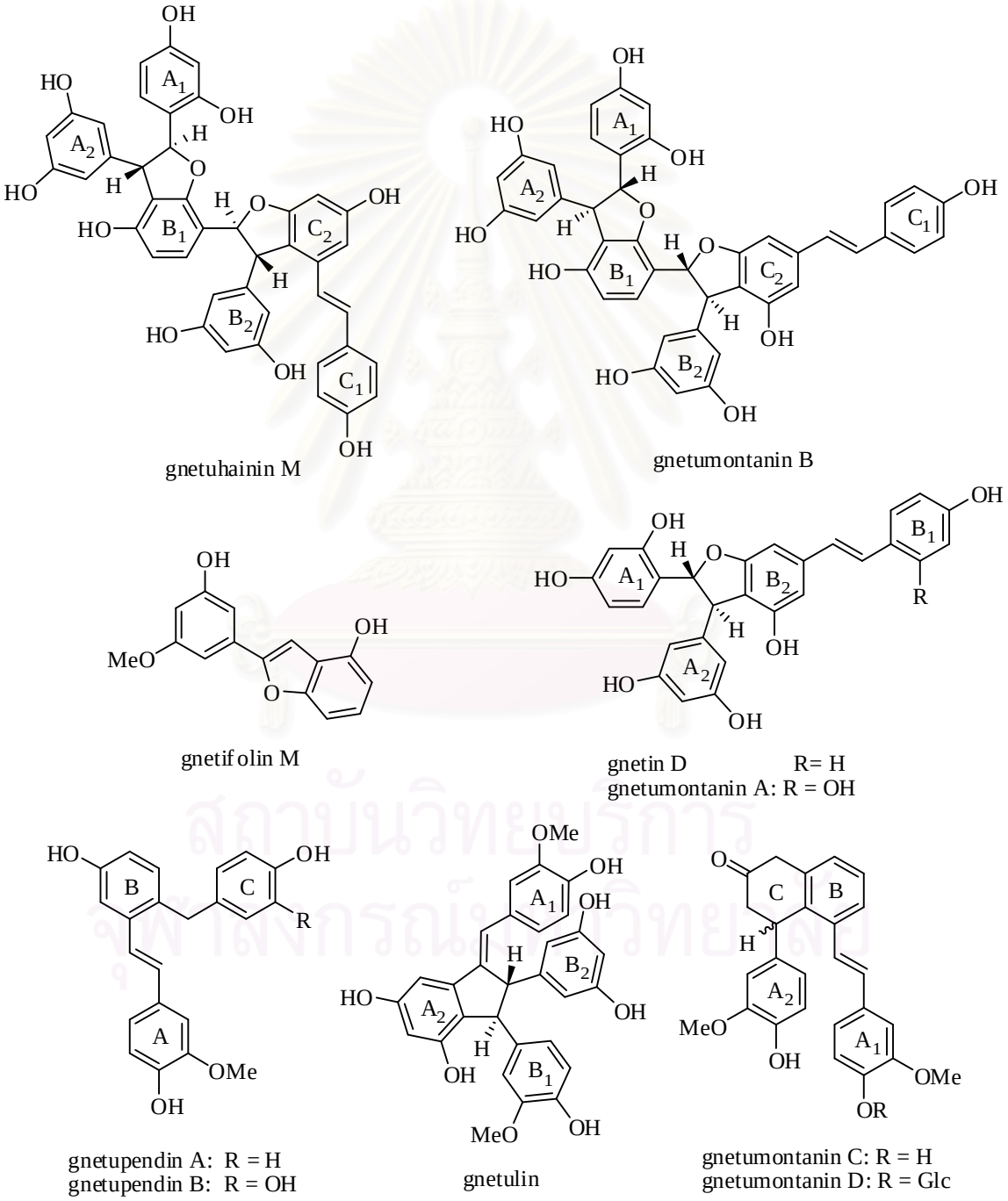

Figure 1.4 Stilbenoids from *G. montanum* and *G. montanum* f. *megalocarpum*.

1.3 Botanical aspect and distribution

Gnetaceae is a monogeneric family, *Gnetum* being the only genus. *Gnetum* is evergreen dioecious (rarely monoecious) trees, shrubs, or woody climbers; There are about 30 species in the tropical lowlands of the world, from northeastern South America, tropical West Africa, south China to Southeast Asia. In Thailand, 8 species are found in rainforests below 1800 metres,[38-39] consist of

G. gnemon Linn. var. *gnemon* (Shrub tree) Pisae (**บีแซ**)

G. gnemon Linn.var. *tenerum* Markgr. (Shrub) Phak miang (**ผักเมี่ยง**)

G. tenuifolium Ridl. (Woody climber) Muai nok (**เมื่อยนก**)

G. macrostachyum Hook. f. (Woody climber) Muai duk (**เมื่อยดูก**)

G. microcarpum Bl. (Woody climber) Muai nok (**เมื่อยนก**)

G. cuspidatum Bl. (Woody climber) Muai dam (**เมื่อยดำ**)

G. leptostachyum Bl. (Woody climber)

G. montanum Markgr. (Woody climber) Muai (**เมื่อย**)

G. latifolium Bl. var. *funiculare* Markgraf. (Woody climber) Mamuai (**มะม่วย**)

Gnetum macrostachyum Hook. f. is the woody climber plant in genus of *Gnetum*, Gnetaceae family.

Leaves: oblong to lanceolate-oblong, coriaceous, brown when dry, 14-16 by 4-5 cm; apex cuspidate; base acute to rounded or sometimes suboblique; secondary nerves curved, distinctly anastomosing; petiole ± 1 cm.

Male inflorescences: axillary, simple, ± 5 by 0.7 cm, sporphylls very short, embedded in the villous indumentum; hair twice as long as the collar. rudimentary ovaries obliquely ovoid, about 10 in each collar.

Female inflorescences: simple cauline, ± 9 by 1 cm, flowers globose, 8-10 in each collar.

Fruits: sessile, ellipsoid, 2 by 1.2 cm, surrounded basally by very striking long brown hairs.

Thailand: North-Eastern: Nong Khai; Eartern: Nakhon Ratchasima, Surin; Central: Nakhon Nayok; South-Eastern: Trat, Chon Buri; Penisular: Ranong, Surat Thani, Nakhon Si Thammarat.

Distribution: Tenasserim, Indochina, Malesia (type, Malaya).

Ecology: Mostly by streams in evergreen forest, alt. 200-900 m.

Flowering: January-February; fruiting February-March.

Vernacular: Muai duk (เมื่อยดูก), Muai (เมื่อย), Muai (ม่วย), Muai luat (ม่วยเลือด).

Compound strobilus of *G. macrostachyum*

Seeds on two cones of *G. macrostachyum*

Linas of *G. macrostachyum*

Figure 1.5 Strobilus, seeds and linas of *G. macrostachyum*

1.4 Biological activities

1.4.1 Antioxidant activities

There are many methods or models to determine the antioxidative properties of the compounds. DPPH is selected in activity directed fractionation of free radical scavenging activity because this model is rapid, convenient, reliable, inexpensive, sensitive, and require little material.[40-41] DPPH is classified as nitrogen centered radical and stable at room temperature because it has virtual of the delocalization of the spare electron over the molecule. The radical scavenging of plant extracts against stable DPPH was determined spectrophotometrically. DPPH radical reacts with antioxidant compound which can donate hydrogen. Antioxidants scavenging DPPH radical by converting DPPH to DPPHn (2,2-diphenyl-1-picrylhydrazine). The changing of color (from deep violet to light yellow) was measured at 517 nm on a visible light spectrophotometer. Radical scavenging activity is reported in term of IC_{50} (Inhibition Concentration at 50 %)

Lipid peroxidation (LPO) is a free radical-related process that in biological system may occur under enzyme control, e.g., for the generation of lipid-derived inflammatory mediator, or nonenzymatically. This latter form is associated mostly with cellular damage as a result of oxidative stress, and a great variety of aldehydes is formed when lipid hydroperoxides break in biological system, among them, malondialdehydes (MDA) and 4-hydroxynonenal (HNE). As MDA, HNE is able to form adducts with free amino acids and many more with proteins. MDA introduces cross-links in proteins which may induce profound alteration in their biological properties. It also been proposed that MDA could react physiologically with several nucleoside (deoxy-guanosine, cytidine). HNE is the major aldehydic product resulting from lipid peroxidation and has been implicated as involved in several pathological conditions, such as atherosclerosis, alcohol-induced liver disease and neurodegenerative disorders,[42-44] both of which can be detected *in vitro*[45] and *in vivo*.[46] This lipid peroxidation product is in tune toxic, causing disruption of cellular enzyme, membrane receptors and transport process.[47-49] The antioxidant potential of lipid peroxidation inhibition is using system *in vitro* by spectrophotometric measurement. In this method, the peroxyl radical generated by metal cation (Fe^{2+}) react with phospholipids to MDA and HNE. MDA can react with thiobarbituric acid (TBA) to

produce the MDA-TBA formation, which change from yellow dye to pink dye and detected spectrophotometrically at 532 nm.

1.4.2 Platelet aggregation

Platelet aggregation is the process that platelet interacts with one another to form hemostatic plug or thrombus. Under normal condition, platelets freely circulate in the blood stream and do not adhere to each other. Following blood vessel wall has been injured, platelets adhere to the exposed subendothelium, become activated and aggregated. The platelet aggregation can be induced or initiated by several agonists such as arachidonic acid, adenosine diphosphate (ADP), collagen, thrombin, epinephrine, etc. Inappropriate platelet activations and subsequent thrombus formation are important in the clinical complication of arterial atherosclerosis and thrombosis.

At the site of a vulnerable coronary plague, platelets attach to the vessel wall and initiate thrombotic occlusion of coronary vessel leading to myocardial ischemia and infarction. Besides thrombus formation in the epicardial arteries, platelet microembolization and accumulation within the microcirculation of the ischemic myocardium play a major role in microcirculation arrest, thus promoting tissue damage and leading to myocardial infarction. The anti-platelet drugs interfere with certain steps in the activation process by selectively blocking key platelet enzyme or receptors reducing the risk of arterial thrombosis. For this reason, stilbenoids from medicinal plants have been evaluated for anti-platelet aggregation.

From the literature review on the chemical constituents and their biological activities of plants in Gnetaceae family, the attractive results of primary screening test based on DPPH radical scavenging activity and no report on chemical constituents and biological activity of *G. macrostachyum* Hook. f., this plant was selected for further investigation.

The objective of the this research:

The objective of this research can be summarized as followed:

1. To extract and isolate compounds from the roots of *G. macrostachyum*.
2. To elucidate the structures of all isolated compounds.
3. To determine the biological activities of the isolated compounds.

CHAPTER II
EXPERIMENTAL

2.1 Plant material

The roots of *Gnetum macrostachyum* were collected from Tah-Utane district, Nakhon Phanom province, Thailand in September 2006. The plant material was identified by the staff of Plant of Thailand Research Unit, Department of Botany, Faculty of Science, Chulalongkorn University.

2.2 General experimental procedures

NMR spectra were recorded with a Varian model Mercury^{+} 400 operated at 400 MHz for ^{1}H and 100 MHz for ^{13}C nuclei. The chemical shift in δ (ppm) was assigned with reference to the signal from the residual protons in deuterated solvents and using TMS as an internal standard in some cases. Most solvents used in this research were commercial grade and were distilled prior to use. Adsorbents such as silica gel 60 Merck cat. No. 7731, 7734, and 7749 were used for quick column chromatography, open column chromatography and radial chromatography, respectively. Thin-layer chromatography (TLC) was performed on precoated Merck silica gel 60 F254 plates (0.25 mm thick layer). Chromatotron® (model 7924 T, Harrison Research) on silica gel plate of 1 mm thickness was used for centrifugal thin layer chromatography. ESIMS data were obtained from mass spectrometer model VG TRIO 2000. High resolution mass spectra were recorded by Micromass LCT and Bruker MICROTOF models. HPLC was conducted on Waters® 600 controller equipped with a Waters® 2996 photodiode array detector (USA). Cosmosil 5C18-ARII column (10 × 250 mm) was used for separation purposes. The pH values were measured by MP220 pH meter Mettler Toledo. UV-visible apsorption spectra were recorded on UV-2552PC UV-Vis spectrometer (Shimadzu, Kyoto, Japan), UV-spectrometer, microtiter plate reader, model sunrise (Tecan, Austria GmbH). Optical rotations were measured on a Jasco P-1010 polarimeter. Platelet aggregation activity was measured by dual channel Aggro-Meter 430 (Coulter Electrics, UK). The blood samples were centrifuged centrifuge model Chermle Z 230A.

2.3 Extraction and purification

The air-dried roots of *Gnetum macrostachyum* (2.5 kg) were collected from Tah-Utane district, Nakhon Phanom province, Thailand in September 2006. They were pulverized and then were axtracted successively in a soxhlet apparatus with CH_2Cl_2 and acetone, respectively. The acetone extract was suspended in acetone and left at room temperature over night. An acetone soluble part was subjected to vacuum liquid chromatography (VLC) eluted with hexane/CH_2Cl_2/EtOAc/ MeOH gradient system to furnish seven main fractions (A-G).

Fraction C was subjected to column chromatography over silica gel and eluted with 10-20% EtOAc/CH_2Cl_2 to provide five fractions (C1-C5). Fraction C2 yielded isorhapontigenin (**1**, 60 mg). Fractions C3 and C4 were combined based on TLC and then subjected to Sephadex LH-20 eluted with 10-20% MeOH/CH_2Cl_2. Final purification was achieved by crystallization in 100% MeOH to give 25 mg of resveratrol (**2**).

Fraction D was further purified by column chromatography over silica gel eluted with 10-20% of EtOAc/CH_2Cl_2 to provide three fractions (D1-D3). Fraction D2 was chromatographed on Chromatotron® (MeOH/EtOAc/CH_2Cl_2, 10:20:70) to provide two fractions (D2.1 and D2.2). Fraction D2.1 yielded isorhapontigenin (**1**, 18 mg). Fraction D2.2 was chromatographed by Chromatotron® eluted with mixture of MeOH/EtOAc/CH_2Cl_2 (5:10:85) to give gnetumacrosin (**9**, 10 mg), bisisorhapontigenin B (**10,** 13 mg) and macrostachyol D (**13,** 8 mg). The crystallization of fraction D3 in 100% MeOH gave gnetol (**3**, 71 mg).

Fraction E was also chromatographed over silica gel eluted with a mixture of EtOAc/CH_2Cl_2 with increasing polarity to provide four fractions (E1-E4).

Fraction E2 was subjected to silica gel column eluted with 30-50% EtOAc/CH_2Cl_2 to give six subfractions (E2.1-E2.6). Subfraction E2.1 yielded gnetol (**3,** 28 mg). Subfraction E2.3 was further fractionated by silica gel column eluted with 12% MeOH/CH_2Cl_2 to afford six fractions (E2.3.1 – E2.3.6). Gnetin C (**4**, 15 mg) and oxyresveratrol (**12,** 5 mg) were obtained from silica gel column (10-50% EtOAc/CH_2Cl_2) of fraction E2.3.2. Fraction E2.3.4 was also chromatographed on silica gel column (10-70% MeOH/CH_2Cl_2), followed by Sephadex LH-20 column chromatography using 30-50% MeOH/CH_2Cl_2 as eluting solvent to afford 1.8 mg of

pavifolol A (**8**). Latifolol (**5,** 555 mg), macrostachyol A (**6,** 235 mg) and B (**7,** 52 mg) were obtained from column chromatography of fraction E2.5 on Sephadex LH-20 (30-80% MeOH/CH_2Cl_2).

Fraction E3 was chromatographed on Sephadex LH-20 and eluted with 40% MeOH/CH_2Cl_2 and then further purified by preparative TLC on silica gel using MeOH/EtOAc/CH_2Cl_2 (10:20:70) to yield 3 mg of macrostachyol C (**11**).

The extraction and purification of all stilbenoids from an acetone soluble part of the roots of *G. macrostachyum* were briefly summarized in **Schemes 2.1** and **2.2.**

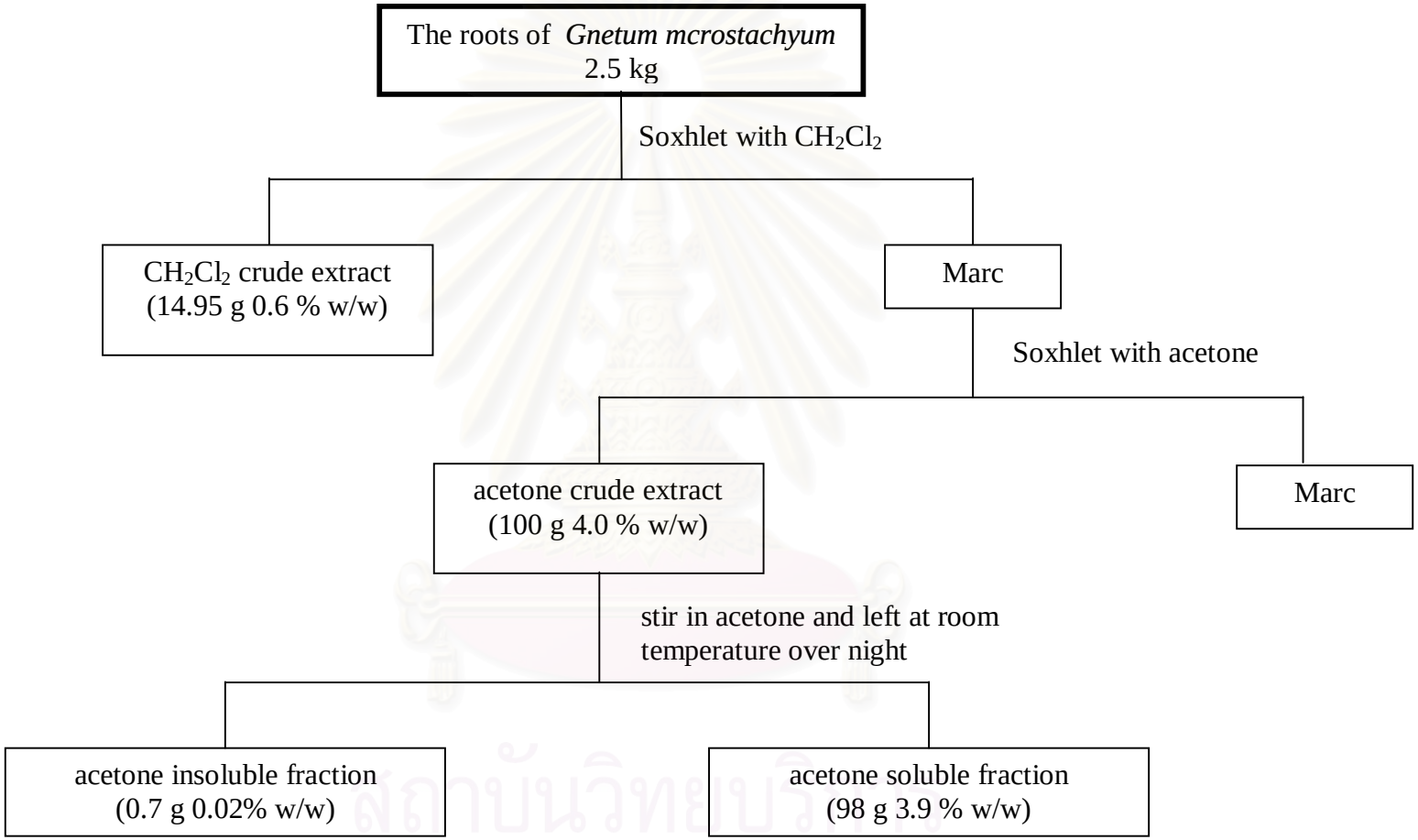

Scheme 2.1 Extraction of *G. macrostachyum* roots.

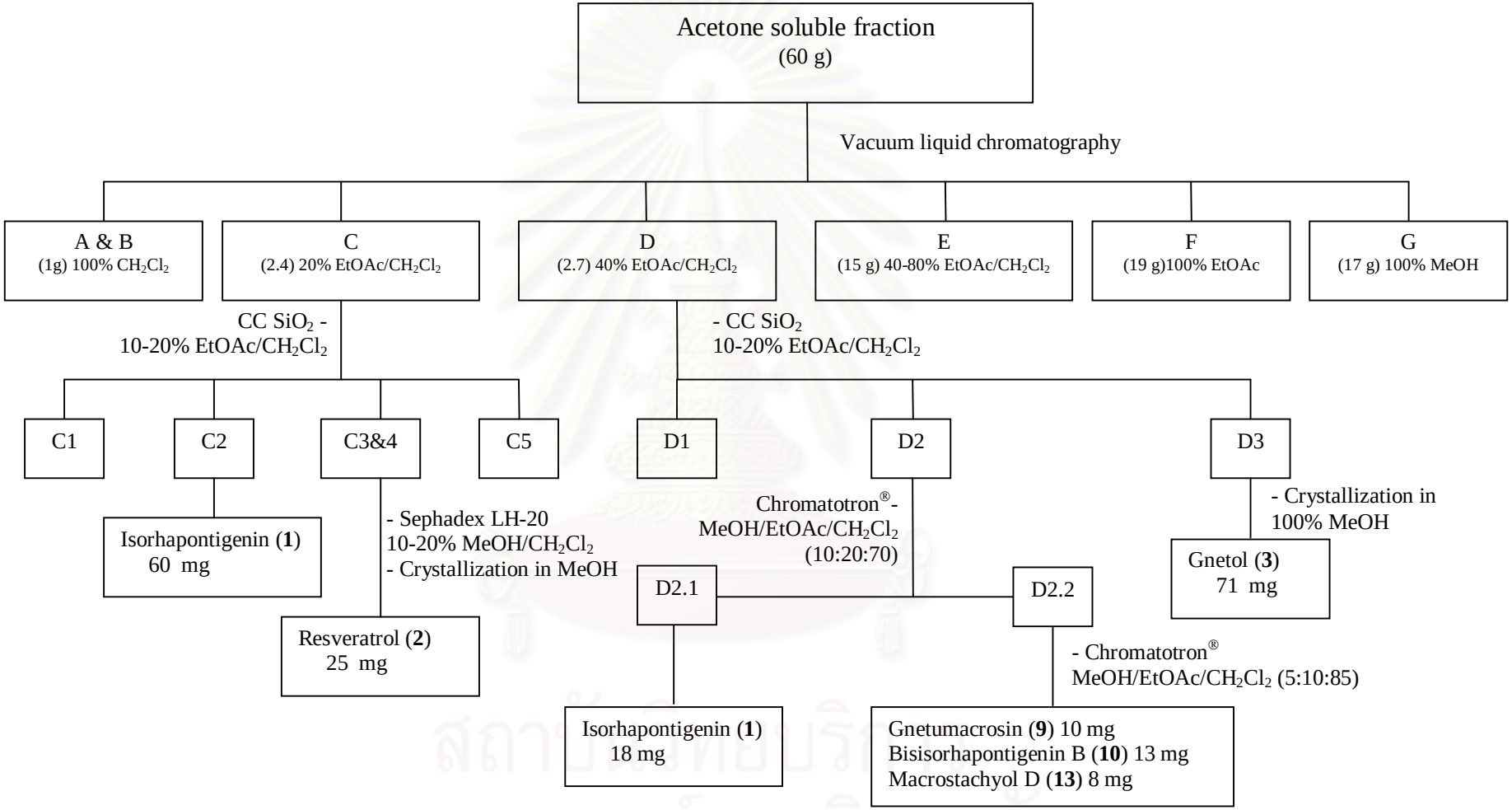

Scheme 2.2 Isolation procedure of the acetone crude extract.

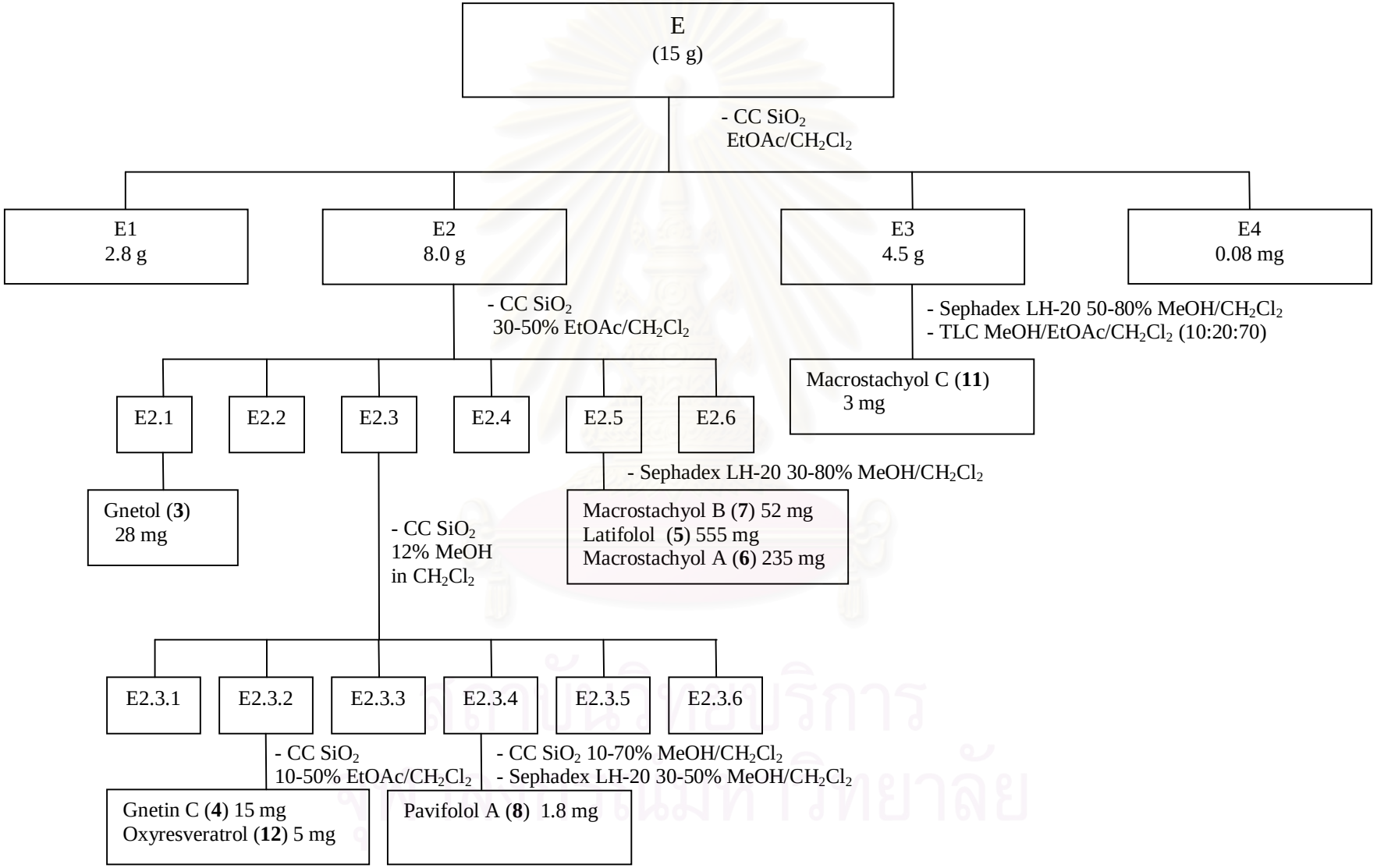

Scheme 2.2 Isolation procedure of the acetone crude extract (cont.)

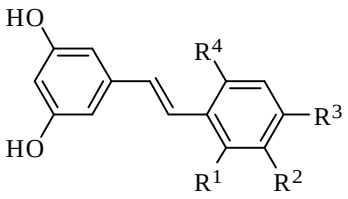

	R^1	R^2	R^3	R^4
isorhapontigenin (**1**)	H	OMe	OH	H
trans-resveratrol (**2**)	H	H	OH	H
gnetol (**3**)	OH	H	H	OH
gnetumacrosin (**9**)	H	OH	H	OMe
oxyresveratrol **(12)**	OH	H	OH	H

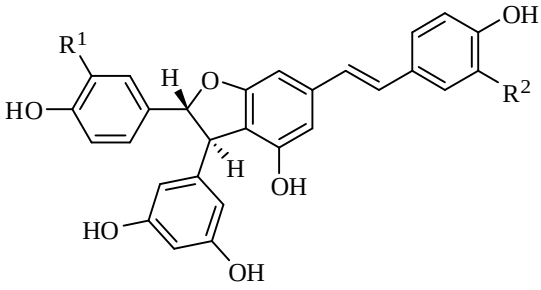

	R^1	R^2
gnetin C (**4**)	H	H
bisisorhapontigenin (**10**)	OMe	OMe
macrostachyol D (**13**)	OMe	H

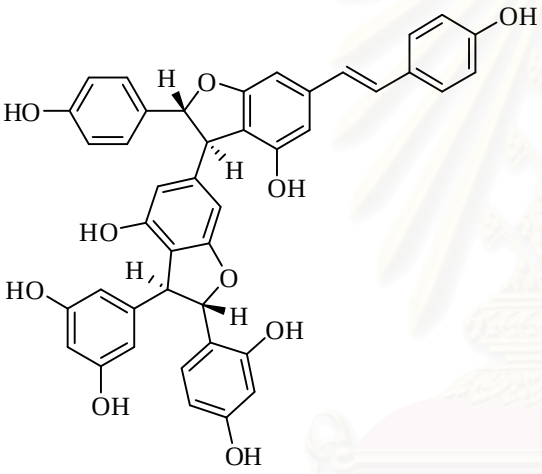

latifolol (**5**)

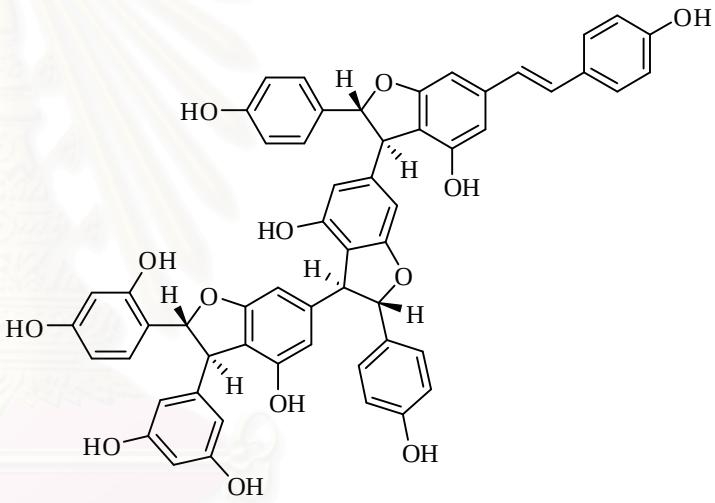

macrostachyol A (**6**)

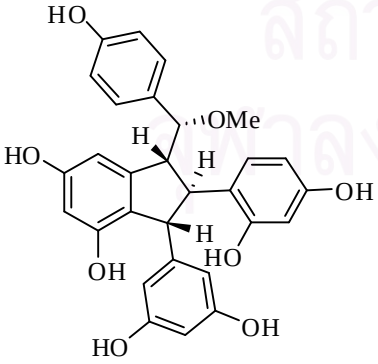

macrostachyol B (**7**)

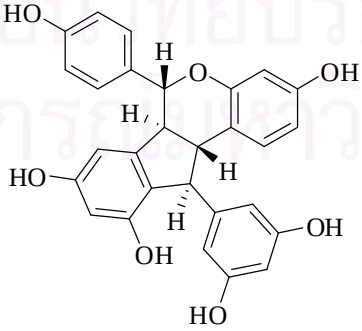

pavifolol A (**8**)

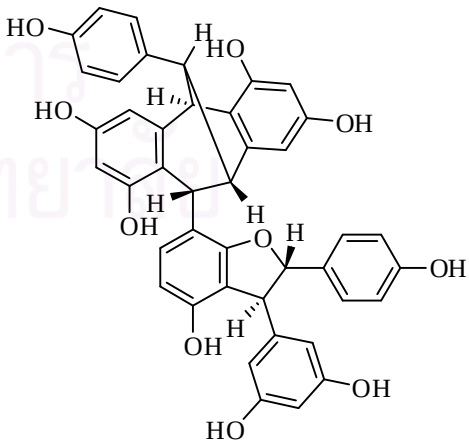

macrostachyol C (**11**)

Figure 2.1 Isolated stilbenoids from *G. macrostachyum* roots.

2.4 Bioassay procedures

2.4.1 DPPH radical scavenging activity

TLC autographic method

2,2-Diphenyl-1-picrylhydrazyl (DPPH) radical as a TLC spray reagent was confirmed to be well suited for the screening of antioxidants in crude plant extracts. The assay involves spraying TLC plates with a 0.2 % DPPH solution in methanol. The plates are considered 30 minutes after spraying. Active compounds occur as yellow spots on a purple background.[50]

Spectrophotometric method

After isolation and purification, activities of pure compounds were quantified in this assay. Various concentrations of sample dissolved in methanolic solution (50 µL) were added to DPPH radical methanolic solution (0.3 mM, 200 µL). After 30 minutes incubation at room temperature in the dark, the absorbance was measured at 517 nm with a UV-Vis spectrophotometer. All tests were run in triplicate and the data were averaged. The scavenging activity was evaluated from the decrease value of 517 nm absorption, which was calculated by the following equation.

$$\% \text{ Radical scavenging} = [1-(A_{sample}/A_{blank})] \times 100$$

The activities was shown as IC_{50} values that donate the concentration of sample required scavenging 50% DPPH free radicals.[51]

2.4.2 Lipid peroxidation inhibition

The assay was conducted by analysis of rat brain lipid peroxidation using documented methods[52] with modification. Protein content in rat brain homogenates (ca 0.5 mg protein/mL) was determined by Lowry's method.[53] Test sample solution (100 µL) was incubated at 37 ^{o}C for 2 h with rat brain homogenate (500 µL) and mixture containing 10 mM KCl (100 µL), 0.05 mM ascorbic acid (100 µL), phosphate buffer pH 7.4 (100 µL) and 5 mM $FeSO_4$ (100 µL). After incubation, the reaction mixture was terminated by adding 3M HCl (500 µL) and 1% thiobarbituric acid (500 µL), respectively, followed by heating at 95 ^{o}C for 20 min. After cooled down, the reaction mixture was centrifuged at 2500 rpm for 5 min. The supernatant was detected

at 532 nm for TBA-MDA formation. The percent inhibition of lipid peroxidation was calculated using the following equation.

$$\% \text{ scavenging activity} = [1-(A_{sample}/A_{blank})] \times 100$$

2.4.3 Platelet aggregation

Platelet aggregation was monitored according to Born's method[54] using dual channel Aggro-Meter 430 (Coulter Electrics, UK) with slight modification. Blood samples were collected from healthy volunteers without taking any medicine at least two weeks. Blood was mixed with 3.2% sodium citrate in a ratio of 9:1 and centrifuged at 160 g for 10 minutes. Supernatant was taken as platelet-rich plasma (PRP), blood residue was further centrifuged at 2000 g for 10 minutes. The supernatant was taken as platelet-poor plasma (PPP). The native PRP was prewarmed at 37ºC for 10 minutes and incubated with 0.2 mM $CaCl_2$ for 1 min. Various concentrations of each test compound or solvent (0.5% DMSO, control) were added into reaction mixture and incubated at 37 °C for two minutes. Aliquot of adenine diphosphate (ADP) was added to 100 µM final concentration and the aggregation was observed for 5 minutes. The final concentration of solvent DMSO was fixed at 0.5% which had no effect on aggregation. The activity of anti-platelet aggregation (%) was calculated by the following equation.[24] Then the IC_{50} value of each compound was calculated and shown as mean ± SD (n = 2).

%anti-platelet aggregation = [1-(platelet aggregation percentage of sample/platelet aggregation percentage of control)] × 100.

2.4.4 The cytotoxic activity against HeLa and KB cell lines by MTT assay

All tested compounds (1 mg each) were examined for cytotoxic activity against HeLa and KB cell lines by MTT assay. This assay was kindly performed by at Natural Products Research Section, Research Division, National Cancer Institute, Thailand.

CHAPTER III
RESULTS AND DISCUSSION

3.1 Primary bioassay screening results of crude extracts

3.1.1 Antioxidant activity of crude extracts

The dichloromethane and acetone crude extracts of *G. macrostachyum* roots were preliminary evaluated using TLC autographic method for screening of antioxidants with 2,2-diphenyl-1-picrylhydrazyl (DPPH). The acetone crude extract showed the most promising activity.

3.1.2 Antioxidant activity of main fractions

An acetone soluble part was subjected on vacuum liquid chromatography (VLC) to furnish seven main fractions (A-G). The antioxidant activity of all main fractions against DPPH radical was expressed as IC_{50} value (mg/mL) by spectroscopic method. The DPPH scavenging activity results of all main fractions are shown in **Table 3.1**.

Table 3.1 DPPH scavenging activity of main fractions.

Fractions	IC_{50} (mg/mL)
dichloromethane fraction	-
Acetone soluble fraction	0.08 ± 0.01
A	1.14 ± 0.14
B	0.13 ± 0.01
C	0.09 ± 0.01
D	0.06 ± 0.01
E	0.16 ± 0.01
F	0.11 ± 0.01
G	0.11 ± 0.00
Ascorbic acid*	0.03 ± 0.01

* Standard antioxidant; - Not determined

3.2 Properties and structural elucidation of isolated compounds

3.2.1 Macrostachyol A (6)

Macrostachyol A was obtained as optically active brown amorphous powder; $[\alpha]_D^{26}$ -29.0° (*c* 0.10, MeOH). The UV spectrum (λ_{max} 325 nm) revealed the presence of a highly conjugated system in the molecule. The positive ESIMS exhibited an $[M+H]^+$ ion peak at *m/z* 923, indicating the molecular weight of 922. The positive pseudomolecular ion in HRESIMS, $[M+Na]^+$ 945.2492 (calcd for $C_{56}H_{42}NaO_{13}$ require 945.2518) established the molecular formula as $C_{56}H_{42}O_{13}$.

The ^1H NMR spectrum exhibited the signals of three sets of *ortho*-coupled protons in the A_2B_2 system on the *p*-substituted phenyl moieties (rings B_1, C_1 and D_1) at δ 7.24 (2H, d, *J* = 9.2 Hz, H-2b, 6b)/6.86 (2H, d, *J* = 8.4 Hz, H-3b, 5b), δ 7.26 (2H, d, *J* = 9.2 Hz, H-2c, 6c)/6.86 (2H, d, *J* = 8.8 Hz, H-3c, 5c) and δ 7.45 (2H, d, *J* = 8.4 Hz, H-2d, 6d)/6.86 (2H, d, *J* = 8.4 Hz, H-3d, 5d); three sets of *meta*-coupled protons in the AB system on 1,3,4,5-tetrasubstituted benzene rings (rings B_2, C_2 and D_2) at δ 6.29 (1H, br s, H-10b)/6.24 (1H, br s, H-14b), δ 6.34 (1H, br s, H-10c)/6.24 (1H, br s, H-14c) and δ 6.73 (1H, br s, H-10d)/6.61 (1H, br s, H-14d) and a set of protons in the A_2X system on the 1,3,5-trisubstituted benzene ring (ring A_2) at δ 6.26 (2H, d, *J* = 2.0 Hz, H-10a, 14a)/6.20 (1H, t, *J* = 1.6 Hz, H-12a) and a set of protons in ABX system on 1,2,4-trisubstituted benzene ring (ring A_1) at δ 7.02 (1H, d, *J* = 8.4 Hz, H-6a)/6.45 (1H, d, *J* = 2.0 Hz, H-3a)/6.30 (1H, dd, *J* = 8.4, 2.0 Hz, H-5a). A set of *trans*-coupled olefinic protons at δ 7.12 (1H, d, *J* = 16.0 Hz, H-7d)/6.99 (1H, d, *J* = 16.0 Hz, H-8d), three sets of mutually coupled aliphatic methine protons at δ 5.74 (1H, d, *J* = 4.0 Hz, H-7a)/4.45 (1H, d, *J* = 4.4 Hz, H-8a), δ 5.44 (1H, d, *J* = 5.2 Hz, H-7b)/4.48 (1H, d, *J* = 4.8 Hz, H-8b) and δ 5.49 (1H, d, *J* = 4.4 Hz, H-7c)/4.49 (1H, d, *J* = 4.0 Hz, H-8c) and ten phenolic hydroxyl protons at δ 8.57 (1H, br s, OH-2a), 8.30 (1H, br s, OH-4a), 8.12 (2H, br s, OH-11a, 13a), 8.49 (1H, br s, OH-4b), 8.04 (1H, br s, OH-13b), 8.49 (1H, br s, OH-4c), 8.22 (1H, br s, OH-13c), 8.55 (1H, br s, OH-4d), 8.32 (1H, br s, OH-13d) were also observed in the spectrum.

The molecular formula ($C_{56}H_{42}O_{13}$) and NMR (^1H and ^{13}C) spectral data revealed that **6** composed of one oxyresveratrol and resveratrol units. The correlations of all protons to the respective carbons were clarified with the help of HMQC and

HMBC spectra. The HMBC correlations between H-7a/C-6a, H-7a/C-2a, H-7a/C-9a, H-8a/C-10a(14a), H-8a/C-1a; H-7b/C-2b(6b), H-7b/C-9b, H-8b/C-1b, H-10b(14b)/C-8b; H-7c/C-2c(6c), H-7c/C-9c, H-8c/C-1c, H-10c(14c)/C-8c; H-7d/C-2d(6d), H-7d/C-9d, H-8d/C-1d, H-10d(14d)/C-8d; (Fig. 3.1) revealed the connectivities between C-1a/C-7a, C-8a/C-9a, C-1b/C-7b, C-8b/C-9b, C-1c/C-7c, C-8c/C-9c and C-8d/C-9d and the correlations between H-7a/H-8a; H-7b/H-8b; H-7c/H-8c; H-7d/H-8d; in the ^{1}H-^{1}H COSY spectrum completely connections in oxyresveratrol unit (unit A) and three resveratrol units (unit B, C and D).

The upfield chemical shift of C-1a (δ119.5) as compared to that of gnemonol B and the appearance of a set of protons in the ABX system based on the 1,2,4-trisubstituted benzene ring (ring A_1) revealed the substitution of the hydroxyl group at C-2a on ring A_1 that was confirmed by correlations between OH-2a/C-2a(1a) and H-7a/C-2a. The chemical shifts of all protons and carbons were assigned by the HMBC correlations (Fig. 3.1). Relative downfield (ca 5 ppm) shifts observed for C-11b (δ_C 162.1), C-11c (δ_C 162.0) and C-11d (δ_C 162.2), compared to C-13b, C-13c and C-13d (δ_C 157.6), supported the replacement of hydroxyl groups by ether linkages at these respective positions. The presence of three dihydrofuran rings (7a-8a-12b-11b-O), (7b-8b-12c-11c-O) and (7c-8c-12d-11d-O) and connectivities pattern of units A-D were supported by HMBC correlations between H-7a/C-11b, H-8a/C-12b; H-7b/C-11c, H-8b/C-12c, H-8b/C-13c and H-7c/C-11d, H-8c/C-12d, H-8c/C-13d. Furthermore, out of the 36 degrees of unsaturation (according to the molecular formula), 33 were satisfied by eight benzene rings and one olefinic moiety. Therefore, the remaining must be attributed to three dihydrofuran rings. Finally, the planar structure of **6** was depicted as in **Fig. 3.1**.

The conformation of dihydrofuran rings was assigned to be *trans*-oriented as in gnemonol B,[36] based on interactions NOESY (Fig. 3.2) between H-7a/H-10a(14a), H-8a/H-6a, H-8a/OH-2a; H-7b/H-10b(14b), H-8b/H-2b(6b) and H-7c/H-10c(14c), H-8c/H-2c(6c). Thus, **6** was found to be 2a-hydroxyl-gnemonol B, a tetramer formed as a result of oxidative coupling of latifolol with a resveratrol unit and it was given the name macrostachyol A.

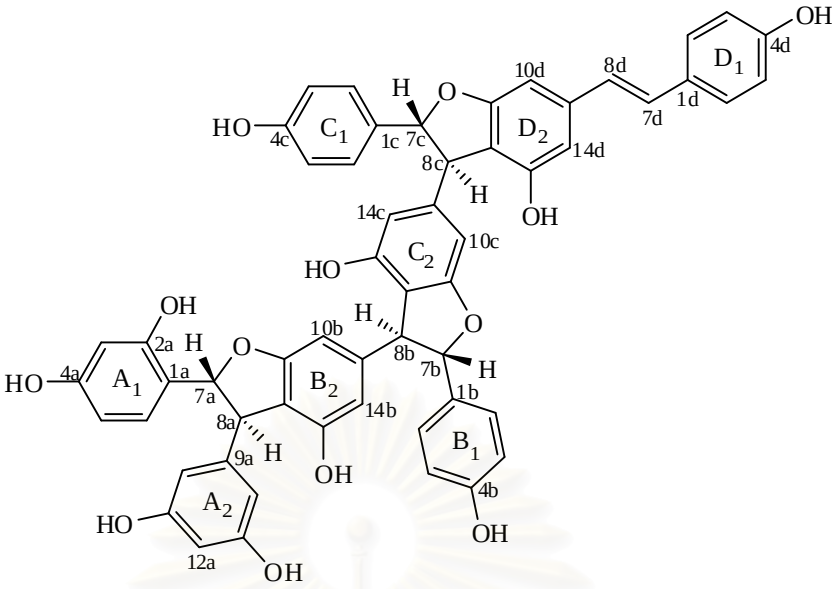

Macrostachyol A (**6**)

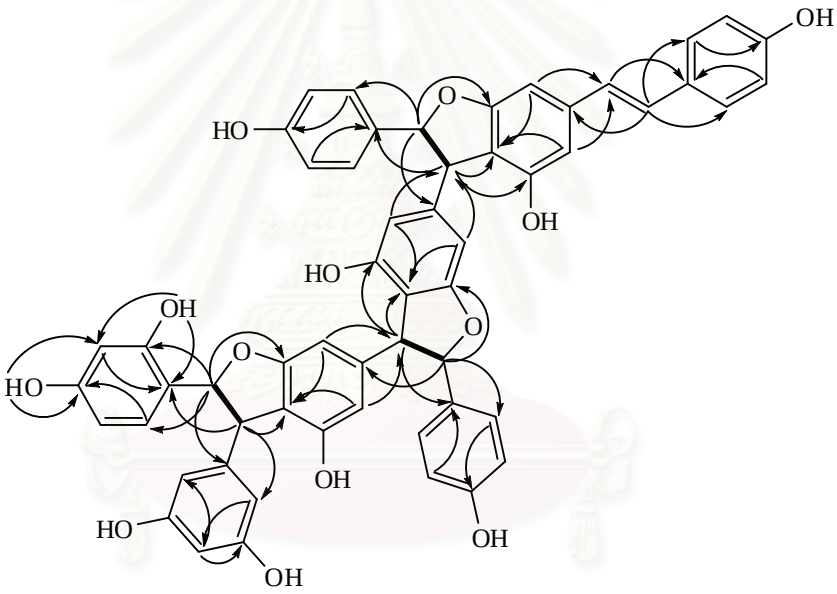

Figure 3.1 Selected HMBC (arrow curves) and COSY (bold lines) correlations of **6**.

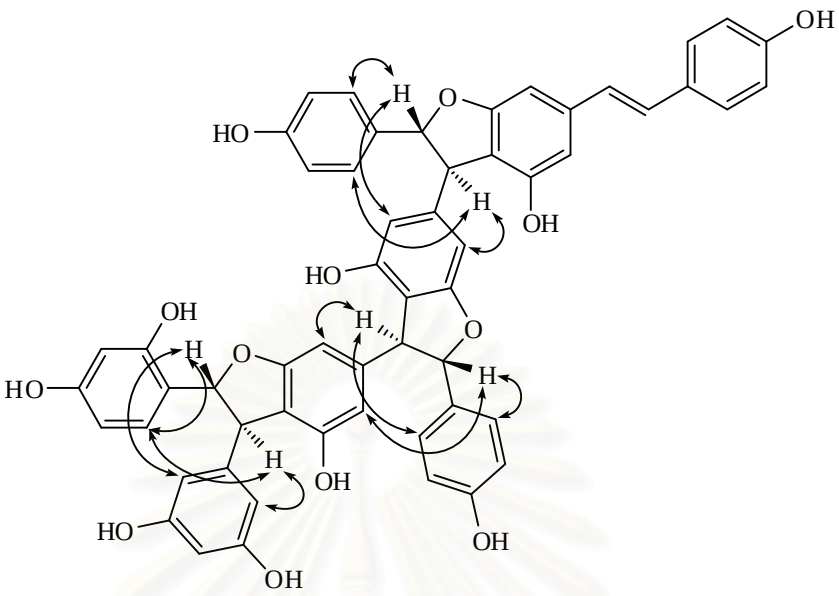

Figure 3.2 Key NOESY correlations for **6.**

Table 3.2 ^{1}H, ^{13}C, HMBC and ^{1}H-^{1}H COSY NMR data of macrostachyol A (**6**) in acetone-d_6

Position	δ_C	δ_H (mult., *J* in Hz)	HMBC	COSY
1a	119.5	-	-	-
2a	155.4	-	-	-
3a	102.6	6.45 (d, 2.0)	C-1a, C-2a, C-4a, C-5a	H-5a
4a	158.1	-	-	-
5a	106.4	6.30 (dd, 8.4, 2.0)	C-1a, C-3a	H-3a, H-6a
6a	127.3	7.02 (d, 8.4)	C-2a, C-4a, C-7a	H-5a
7a	88.3	5.74 (d, 4.0)	C-1a, C-2a, C-6a, C-8a, C-9a, C-11b, C-12b	H-8a
8a	53.4	4.45 (d, 4.4)	C-1a, C-7a, C-9a, C-10a,14a, C-11b, C-12b	H-7a
9a	145.9	-	-	-
10a, 14a	106.2	6.26 (d, 2.0)	C-8a, C-11a,13a, C-12a	H-12a
11a, 13a	158.4	-	-	-
12a	100.8	6.20 (t, 1.6)	C-10a,14a, C-11a,13a	H-10a,14a
1b	132.9	-	-	-
2b, 6b	127.1	7.24 (d, 9.2)	C-2b,6b C-3b,5b, C-4b, C-7b	H-3b,5b
3b, 5b	115.3[a]	6.86[f] (d, 8.4)	C-1b, C-3b,5b, C-4b	H-2b,6b
4b	157.3[b]	-	-	-
7b	93.0	5.44 (d, 5.2)	C-1b, C-2b,6b, C-8b, C-9b C-11c, C-12c	H-8b
8b	55.1[c]	4.48 (d, 4.8)	C-1b, C-7b, C-8b, C-10b, C-14b, C-11c, C-12c, C-13c	H-7b
9b	145.1	-	-	-

Position	δ_C	δ_H (mult., *J* in Hz)	HMBC	COSY
10b	100.3[d]	6.29 (brs)	C-8b, C-11b, C-12b, C-13b, C-14b	-
11b	162.1	-	-	-
12b	114.0	-	-	-
13b	154.6[e]	-	-	-
14b	107.3[*]	6.24[g] (brs)	C-8b, C-10b, C-11b, C-12b, C-13b,	-
1c	133.2	-	-	-
2c, 6c	126.9	7.26 (d, 9.2)	C-7c, C-2c,6c, C-4c	H-3c,5c
3c, 5c	115.3[a]	6.86[f] (d, 8.8)	C-1c, C-3c,5c, C-4c	H-2c,6c
4c	157.3[b]	-	-	-
7c	92.7	5.49 (d, 4.4)	C-1c, C-2c,6c, C-8c, C-9c, C-11d, C-12d	H-8c
8c	55.1[c]	4.49 (d, 4.0)	C-1c, C-9c, C-10c, C-14c, C-11d, C-12d, C-13d	H-7c
9c	145.7	-	-	-
10c	100.3[d]	6.34 (brs)	C-8c, C-10c, C-11c, C-12c, C-13c	-
11c	162.0	-	-	-
12c	113.3	-	-	-
13c	154.6[e]	-	-	-
14c	107.4	6.24[g] (brs)	C-8c, C-11c, C-12c, C-14c	-
1d	129.0	-	-	-
2d, 6d	127.9	7.45 (d, 8.4)	C-2d,6d, C-3d,5d, C-4d, C-7d	H-3d,5d
3d, 5d	115.5	6.86[f] (d, 8.4)	C-1d, C-3d,5d, C-4d	H-2d,6d
4d	157.3[b]	-	-	-
7d	128.3	7.12 (d, 16.0)	C-1d, C-2d,6d, C-8d, C-9d	H-8d
8d	125.8	6.99 (d, 16.0)	C-1d, C-9d, C-10d, C-14d,	H-7d
9d	140.4	-	-	-
10d	98.3	6.73 (brs)	C-8d, C-11d, C-12d, C-13d, C-14d,	H-14d
11d	162.2	-	-	-
12d	114.2	-	-	-
13d	154.6[e]	-	-	-
14d	107.2[*]	6.61 (brs)	C-8d, C-10d, C-12d, C-13d	H-10d
2a-OH		8.57 (brs)	C-1a, C-2a, C-3a	
4a-OH		8.30 (brs)	C-3a,5a, C-4a	
11a, 13a-OH		8.12 (brs)	C-10a,14a, C-11a,13a, C-12a	
4b-OH		8.49[h] (brs)	C-3b,5b, C-4b	
13b-OH		8.04 (brs)	C-12b, C-13b, C-14b	
4c-OH		8.49[h] (brs)	C-3c,5c, C-4c	
13c-OH		8.22 (brs)	C-12c, C-13c, C-14c	
4d-OH		8.55 (brs)	C-3d,5d, C-4d	
13d-OH		8.32 (brs)	C-12d, C-13d, C-14d	

[a-h] Overlaped

[*] Data can be interchanged

3.2.2 Macrostachyol B (7)

Macrostachyol B was obtained as optically active brown amorphous powder with $[\alpha]_D^{26}$ +34.0° (*c* 0.10, MeOH). It molecular formula was established as $C_{29}H_{26}O_8$ by mean of HREIMS data [*m/z* 525.1504 $[M+Na]^+$ (calcd for $C_{29}H_{26}NaO_8$, 525.1520)].

The ^{1}H NMR spectrum exhibited the presence of one set of *ortho*-coupled H-atoms in A_2B_2 system on *p*-substituted phenyl moiety (ring A_1) at δ 7.03 (2H, d, *J* = 8.4 Hz, H-2a, 6a)/ 6.80 (2H, d, *J* = 8.4 Hz, H-3a, 5a). The spectrum also showed one set of *meta*-coupled H-atoms in AB system on tetrasubstituted benzene ring (ring A_2) at δ 6.24 (1H, d, *J* = 2.0 Hz, H-12a)/5.23 (1H, d, *J* = 1.6 Hz, H-14a); one set of A_2B H-atoms on 1,3,5-trisubstituted benzene ring (ring B_2) at δ 6.18 (1H, d, *J* = 2.0 Hz, H-12b)/6.16 (2H, d, *J* = 2.0 Hz, H-10b, 14b) and one set of ABX H-atoms on 1,2,4-trisubstituted benzene ring (ring B_1) at δ 6.40 (1H, d, *J* = 2.4 Hz, H-3b)/6.22 (1H, dd, *J* = 8.4, 2.4 Hz, H-5b)/6.72(1H, d, *J* = 8.4 Hz, H-6b). The ^{1}H NMR spectrum also displayed four signals in an aliphatic region at δ 4.50 (1H, s, br, H-8b), 3.96 (1H, d, *J* = 10.0 Hz, H-7a), 3.82 (1H, t, *J* = 1.9 Hz, H-7b) and 3.11 (1H, dd, *J* = 9.6, 1.2 Hz, H-8a), one methoxy at δ 3.00 (3H, s), and seven phenolic hydroxyl protons at δ 8.40, 8.09 (2H), 8.08, 8.03, 7.94 and 7.78.

The ^{13}C NMR spectrum revealed the presence of five aliphatic carbons in addition to 24 aromatic carbons, one of which appeared at δ 87.0 and was assigned as an oxygenated carbon. Considering the molecular formula ($C_{29}H_{26}O_8$), ^{1}H and ^{13}C NMR spectral data (Table 3.3), **7** could be assigned as a dimer of a resveratrol and oxyresveratrol units.

Significant long-range correlations were observed in HMBC spectrum of **7** (Fig 3.3) between H-7a (δ3.96) and three carbon signals at δ 55.5 (OCH_3) and 129.3 (C-2a, 6a) indicating that the methoxy group and the *p*-hydroxy substituted benzene ring (ring A_1) were located at C-7a. Another significant interaction was observed between H-8b/C-10b and H-8b/C-14b, therefore, the 3,5-dihydroxybenzene ring (ring B_2) was connected at C-8b. The correlations between H-7b/C-2b, H-8b/C-1b and H-6a/C-1b revealed that the 2,4-dihydroxybenzene ring (B_1) was connected at C-7b.

The relative stereochemistry of **7** was determined by analysis of its NOESY spectrum (Fig 3.4). The NOE interactions between H-7b/OMe-7a and H-8a/H-8b suggested a *cis* orientation for H-7b and OMe-7a as well as H-8a and H-8b, and NOE

interaction between H-8b/H-6b revealed the *trans* relationship of H-7b and H-8b. Based on these data, compound **7** was characterized as 7-*O*-methyl gnetuhainin D[16] or trivially named macrostachyol B.

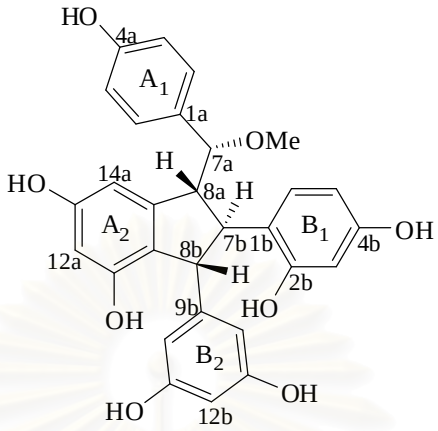

Macrostachyol B (**7**)

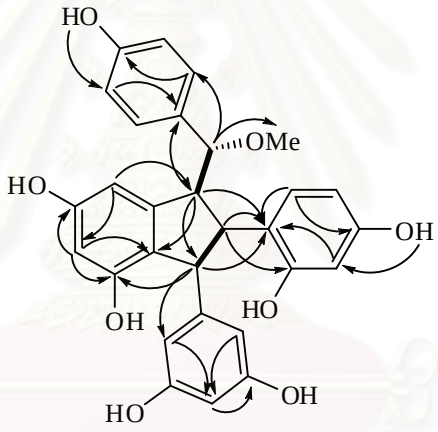

Figure 3.3 Selected HMBC (arrow curves) and COSY (bold lines) correlations of **7**.

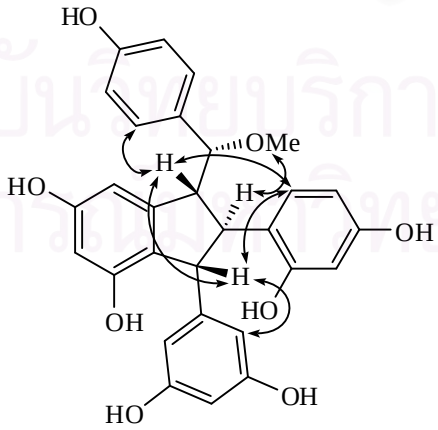

Figure 3.4 Key NOESY correlations for **7**.

Table 3.3 ^{1}H, ^{13}C, HMBC and ^{1}H-^{1}H COSY NMR data of macrostachyol B (**7**) in acetone-d_6

Position	δ_C	δ_H (mult., *J* in Hz)	HMBC	COSY
1a	130.4			
2a, 6a	129.3	7.03 (d, 8.4)	C-2a,6a C-3a,5a, C-4a, C-7a	H-3a,5a
3a, 5a	114.8	6.80 (d, 8.4)	C-1a, C-3a,5a C-4a	H-2a,6a
4a	157.2			
7a	87.0	3.96 (d, 10.0)	C-2a,6a, C-8a, C-7a-OMe C-7b	H-8a
8a	61.1	3.11 (dd, 9.6,1.2)	C-1a, C-7a, C-10a, C-1b, C-8b	H-7a
9a	149.3	-		
10a	121.8	-		
11a	154.2	-		
12a	101.7	6.24 (d, 2.0)	C-10a, C-11a, C-13a, C-14a	H-14a
13a	157.7	-		
14a	105.1	5.23 (d, 1.6)	C-8a, C-10a, C-12a, C-13a	H-12a
1b	123.7	-		
2b	155.3	-		
3b	103.2	6.40 (d, 2.4)	C-1b, C-2b, C-4b, C-5b	H-5b
4b	156.8	-		
5b	106.5	6.22 (dd, 8.4, 2.4)	C-1b, C-3b	H-6b, H-3b
6b	126.7	6.72 (d, 8.4)	C-2b, C-4b, C-7b	H-5b
7b	51.0	3.82 (t, 1.9)	C-7a, C-8a, C-9a, C-10a, C-1b, C-2b, C-6b, C-8b, C-9b	H-8b
8b	51.8	4.50 (brs)	C-8a, C-9a, C-10a, C-11a, C-1b, C-7b, C-9b, C-10b,14b	H-7b
9b	144.8	-		
10b, 14b	106.2	6.16 (d, 2.0)	C-8b, C-10b,C-14b, C-11b,13b, C-12b	
11b, 13b	158.4	-		
12b	100.2	6.18 (d, 2.0)	-	
7a-OMe	55.4	3.00 (s)	C-7a	
4a-OH		8.40 (s)	C-3a,5a, C-4a	
11a-OH		7.78 (s)	C-10a, C-11a, C-12a	
13a-OH		7.94 (s)	C-12a, C-13a, C-14a	
2b-OH		8.08 (s)	C-1b, C-2b, C-3b	
4b-OH		8.03 (s)	C-3b, C-4b, C-5b	
11b, 13b-OH		8.09 (s)	C-10b,14b, C-11b,13b, C-12b	

3.2.3 Gnetumacrosin (9)

Gnetumacrosin (**9**) was obtained as inseparable mixture. The ^{1}H NMR indicated that there were **9** and resveratrol (**2**) in a ratio of 3:2. The positive ESIMS exhibited an $[M+H]^+$ ion peak at *m/z* 259, indicating the molecular weight of 258. The positive HRESIMS of $[M+H]^+$ ion (259.0974 calcd for $C_{15}H_{15}O_4$ require a 259.0970) etablished a molecular formula $C_{15}H_{15}O_4$. The ^{1}H NMR spectrum of this mixture was subtracted with ^{1}H NMR spectrum of resveratrol (**2**). The structure of gnetumacrosin (**9**) could be assigned (Table 3.4 and Fig 3.5).

The ^{1}H NMR spectrum (Table 3.4) exhibited the presence of one set of protons in the A_2X system on the 1,3,5-trisubstituted benzene ring at δ 6.57 (2H, d, *J* = 2.0 Hz, H-2′, 6′)/6.29 (1H, t, *J* = 2.0 Hz, H-4′) and one set of protons in ABX system on 1,2,5-trisubstituted benzene ring at δ 6.85 (1H, d, *J* = 8.8 Hz, H-3)/6.73 (1H, dd, *J* = 8.8, 3.2 Hz, H-4)/7.12 (1H, d, *J* = 3.2 Hz, H-6). A set of *trans*-coupled olefinic protons at δ 7.35 (1H, d, *J* = 16.4 Hz, H-*α*)/6.97 (1H, d, *J* = 16.8 Hz, H-*b*), one methoxy at δ 3.81 (3H, s, OMe-2), and three phenolic hydroxyl protons at δ 8.00 (1H, br s, OH-5), 8.31 (2H, br s, OH-3′, 5′) were also observed in the spectrum. The ^{13}C NMR spectrum (Table 3.4) showed signals of one methoxy carbon at δ 55.7 (OMe-2), twelve aromatic carbons at δ 102.1-158.7 and two olefinic carbons at δ 122.9 (C-*α*) and δ 128.8 (C-*b*). In the HMBC experiment (Fig 3.5), the correlations between methoxy group at δ 3.81 and C-2 and H-*α*/C-2 suggested that the methoxy group was attached to C-2, which was further confirmed by the correlations among the protons at δ 3.81 (OMe) and δ 6.85 (H-3) in the NOE experiment. The upfield chemical shift of C-6 (δ112.3) as compared to that of oxyresveratrol (**12**) and the appearance of a set of protons in the ABX system on the 1,2,5-trisubstituted benzene ring revealed the substitution of the hydroxyl group at C-5 that was confirmed by correlations between OH-5/C-4, OH-5/C-5, OH-5/C-6 and H-3/C-5. Therefore, structure of **9** was assigned to be 5,3′,5′-trihydroxy-2-methoxystilbene or trivially named gnetumacrosin.

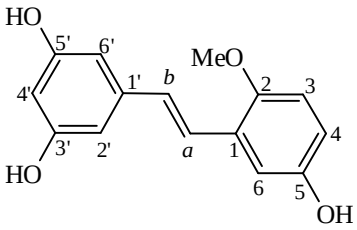

Gnetumacrosin (**9**)

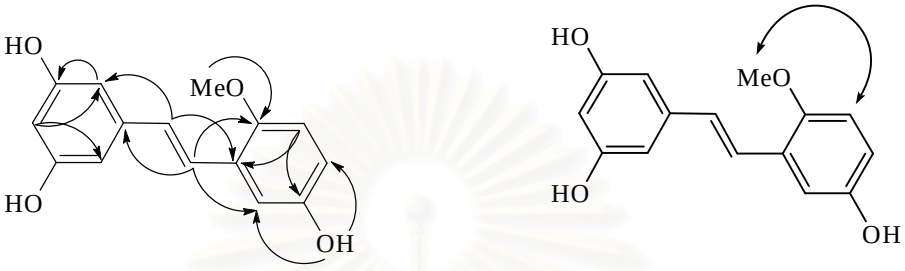

a b

Figure 3.5 Selected HMBC (a) and NOE correlations (b) of **9**.

Table 3.4 ^{1}H, ^{13}C, HMBC and ^{1}H-^{1}H COSY NMR data of gnetumacrosin (**9**) in acetone-d_6

Position	δ_C	δ_H (mult., *J* in Hz)	HMBC	COSY
1	126.8	-		
2	150.7	-		
3	112.6	6.85 (d, 8.8)	C-1, C-5	H-4
4	115.2	6.73 (dd, 8.8, 3.2)	C-2, C-6	H-3, H-6
5	151.3	-		
6	112.3	7.12 (d, 3.2)	C-2, C-4, C-*α*	H-4
A	122.9	7.35 (d, 16.4)	C-2, 6, C-1′	H-*b*
b	128.8	6.97 (d, 16.8)	C-1, C-1′, C-2′,6′	H-*α*
1′	139.9	-		
2′, 6′	105.0	6.57 (d, 2.0)	C-*b*, C-2′, 6′, C-3′,5′ C-4′	H-4′
3′, 5′	158.7	-		
4′	102.1	6.29 (t, 2.0)	C-2′,6′, C-3′,5′	H-2′,6′
2-OMe	55.7	3.81 (s)	C-2	
5-OH		8.00 (s)	C-4, C-5, C-6	
3′, 5′-OH		8.31 (s)	C-2′,6′, C-4′	

3.2.4 Macrostachyol C (11)

Macrostachyol C was obtained as optically active brown amorphous powder; $[\alpha]_D^{26}$ -30.0° (*c* 0.10, MeOH). The positive ESIMS exhibited an $[M+H]^+$ ion peak at *m/z* 697. The positive ion HRESIMS *m/z*: $[M+H]^+$ 697.2076 (calcd for $C_{42}H_{33}O_{10}$ require 697.2073)

The ^{1}H NMR spectrum exhibited the signals of two sets of *ortho*-coupled protons in the A_2B_2 system on the *p*-substituted phenyl moieties (rings A_1 and C_1) at δ 7.23 (2H, d, *J* = 8.4 Hz, H-2a, 6a)/6.89 (2H, d, *J* = 8.4 Hz, H-3a, 5a), δ 7.10 (2H, d, *J* = 8.0 Hz, H-2c, 6c)/6.73 (2H, d, *J* = 8.0 Hz, H-3c, 5c), two sets of *meta*-coupled protons in the AB system on 1,2,3,5-tetrasubstituted benzene rings (rings B_2 and C_2) at δ 6.11 (1H, d, *J* = 2.4 Hz, H-12b)/6.35 (1H, d, *J* = 2.0 Hz, H-14b), δ 6.07 (1H, d, *J* = 2.0 Hz, H-12c)/6.65 (1H, br s, H-14c), a set of protons in the A_2X system on the 1,3,5-trisubstituted benzene ring (ring A_2) at δ 6.05 (2H, d, *J* = 2.0 Hz, H-10a, 14a)/6.17 (1H, t, *J* = 2.0 Hz, H-12a) and *ortho*-coupled doublets at δ 6.10 (1H, d, *J* = 8.4 Hz, H-5b)/6.60 (1H, d, *J* = 8.8 Hz, H-6b) on a 1,2,3,4-tetrasubstituted benzene ring (ring B_1). Four benzylic methine appearance as singlets at δ 3.87 (1H, s, H-7b), 4.30 (1H, s, H-8b), 4.22 (1H, br s, H-7c), 3.56 (1H, br s, H-8c), and a set of mutually coupled aliphatic methine protons assignable to the dihydrofuran ring at δ 5.31 (1H, d, *J* = 5.2 Hz, H-7a)/4.32 (1H, d, *J* = 5.2 Hz, H-8a). However, nine phenolic hydroxyl groups were not observed in the ^{1}H NMR spectrum.

All the protonated carbons were assigned by HMBC and HMQC (Table 3.5). The HMBC correlations between H-7a/C-2a,(6a), H-7a/C-9a, H-8a/C-10a(14a), H-8a/C-1a, and the correlation between H-7a and H-8a in the ^{1}H-^{1}H COSY spectrum established the structure of resveratrol unit (unit A). The connectivities between C-1b/C-7b, C-8b/C-9b and C-1c/C-7c, C-8c/C-9c of oxyresveratrol unit (unit B) and resveratrol unit (unit C) were supported by the correlations between H-7b/C-2b, H-7b/C-9b; H-8b/C-1b, H-8b/C-10b, H-8b/C-14b; H-7c/C-2c(6c), H-7c/C-9c; H-8c/C-7c, H-8c/C-10c in HMBC data (Fig. 3.6). The presence of dihydrofuran ring (7a-8a-3b-2b-O) and connectivities of units A and B were supported by the HMBC correlations between H-7a/C-2b, H-7a/C-3b, H-8a/C-3b. The HMBC correlations between H-7b/C-10c, H-8b/C-10c; H-7c/C-10b, H-8c/C-10b supported connectivities of unit B to unit C through 7b/10c and 10b/8c respectively, and correlations between

H-8b/C-8c, H-7c/C-7b, H-7c/C-10b supported that C-7b was carbon bridge of dibenzobicyclo[3,2,1]octadiene ring system like ampelopsin F.[55]

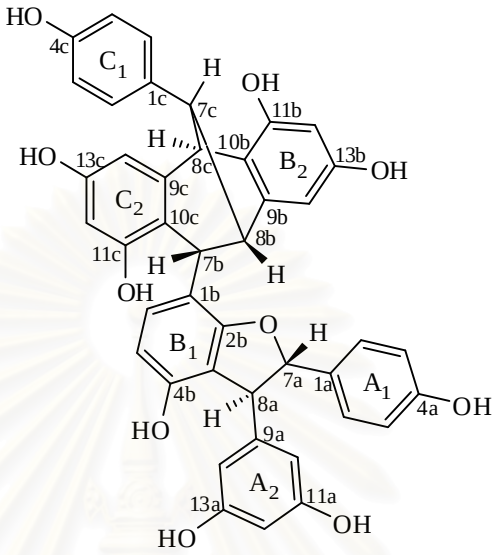

Macrostachyol C (**11**)

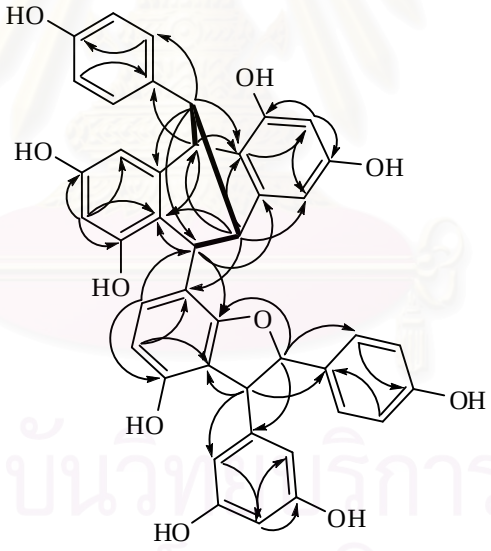

Figure 3.6 Selected HMBC (arrow curves) and COSY (bold lines) correlations of **11**.

On this basic skeleton, H-8b and H-8c gave *W*-type relationships, so a coupling between H-8b and H-8c was observed in the ^{1}H-^{1}H COSY spectrum. The ^{1}H-^{1}H COSY spectrum (Fig. 3.6) showed the correlations between four benzylic methines protons H-7b/H-8b; H-7c/H-8c and their appearance as singlets revealed that all dihedral angles were almost 90 degrees. The NOESY interactions (Fig 3.7)

between H-7b/H-8b and H-7c/H-8c suggested that H-7b/H-8b and H-7c/H-8c were *cis*-oriented, while orientation of dihydrofuran rings was found to be *trans* by the interactions between H-7a/H-2a(6a), H-7a/H-10a(14a), H-8a/H-10a(14a). The orientation of ring C_1 was found to be pseudoequatorial of five member ring (8b-9b-10b-8c-7c) and *cis* configuration to H-7b by the interactions between H-2c(6c)/H-7b, H-2c(6c)/H-8c in the NOESY experiment (Fig. 3.7). Moreover, the NOESY interactions between H-8b/H-2a(6a) and H-8c/H-6b suggested that orientation of ring B_1 and unit A were determined as shown in **Fig 3.7**. Thus the structure 11 was determined, and it was assigned the trivially mane macrostachyol C.

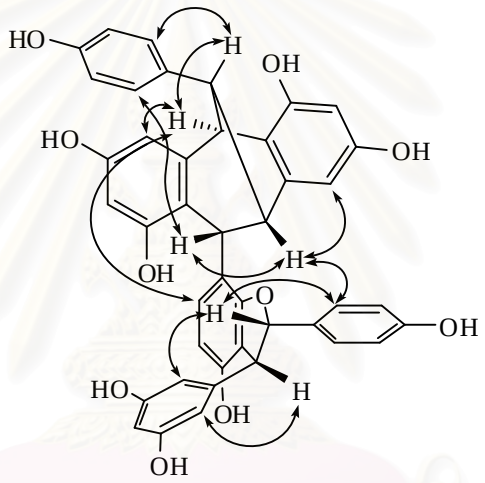

Figure 3.7 Key NOESY correlations of **11**.

Table 3.5 ^{1}H, ^{13}C, HMBC and ^{1}H-^{1}H COSY NMR data of macrostachyol C (**11**) in acetone-d_6

Position	δ_C	δ_H (mult., *J* in Hz)	HMBC	COSY
1a	133.4	-		
2a, 6a	126.4	7.23 (d, 8.4)	C-4a, C-2a,6a, C-7a	H-3a,5a
3a, 5a	115.0	6.89 (d, 8.4)	C-1a, C-4a	H-2a,6a
4a	156.8	-		
7a	92.1	5.31 (d, 5.2)	C-1a, C-2a,6a, C-9a, C-2b	H-8a
8a	55.1	4.32 (d, 5.2)	C-1a, C-7a, C-9a, C-10a,14a, C-2b, C-3b	H-7a
9a	145.5	-		
10a, 14a	105.5	6.05 (d, 2.0)	C-8a, C-10a,14a, C-11a,13a, C-14a	H-12a
11a, 13a	158.3	-		
12a	100.6[a]	6.17 (t, 2.0)	C-10a,14a, C-11a,13a,	H-10a,14a
1b	116.0	-		
2b	159.6	-		
3b	113.2	-		
4b	152.6	-		
5b	107.5	6.10 (d, 8.4)	C-1b, C-3b	H-6b
6b	127.7	6.60 (d, 8.8)	C-2b, C-4b, C-7b	H-5b
7b	44.5	3.87 (s)	C-1b, C-2b, C-8b, C-9b, C-7c, C-10c	H-8b
8b	48.4	4.30 (s)	C-1b, C-9b, C-10b, C-14b, C-8c, C-10c	H-7b, H-8c
9b	147.2	-		
10b	112.3	-		
11b	152.7	-		
12b	100.6[a]	6.11 (d, 2.4)	C-10b, C-11b, C-13b, C-14b	H-14b
13b	155.9	-		-
14b	104.7	6.35 (d, 2.0)	C-8b, C-10b, C-12b	H-12b
1c	137.1	-		
2c, 6c	128.9	7.10 (d, 8.0)	C-2c,6c, C-4c, C-7c	H-3c,5c
3c, 5c	114.5	6.73 (d, 8.0)	C-1c, C-3c5c, C-4c	H-2c,6c
4c	155.0	-		
7c	45.9	4.22 (brs)	C-1c, C-2c,6c, C-8c, C-9c, C-7b, C-10b	H-8c
8c	54.0	3.56 (brs)	C-7c, C-10c, C-8b, C-10b	H-8b, H-7c
9c	147.0	-		
10c	126.8	-		
11c	152.6	-		
12c	100.6[a]	6.07 (d, 2.0)	C-10c, C-11c, C-13c, C-14c	H-14c
13c	157.3	-		
14c	102.5	6.65 (brs)	C-10c, C-12c	H-12c

[a] Overlaped

3.2.5 Macrostachyol D (13).

Macrostachyol D was yielded as optically active greenish amorphous powder; $[\alpha]_D^{26}$ -39.0° (*c* 0.10, MeOH). The UV spectrum (λ_{max} 327 nm) revealed the presence of a highly conjugated system in the molecule. The positive ESIMS exhibited an $[M+H]^+$ ion peak at *m/z* 485, indicating the molecular weight to be 484. The positive ion HRESIMS *m/z*: $[M+H]^+$ 485.1591 (calcd for $C_{29}H_{25}O_7$ required 485.1600). Therefore, the molecular formula was $C_{29}H_{24}O_7$.

The ^{1}H NMR spectrum exhibited the signals of methoxyl at δ 3.82 (3H, s, OMe-3a); a sets of *ortho*-coupled protons in the A_2B_2 system on the *p*-substituted phenyl moieties (rings B_1) at δ 7.44 (2H, d, *J* = 8.0 Hz, H-2b, 6b)/6.85 (2H, d, *J* = 8.4 Hz, H-3b, 5b); a sets of *meta*-coupled protons in the AB system on 1,3,4,5-tetrasubstituted benzene rings (rings B_2) at δ 6.70 (1H, br s, H-10b)/6.60 (1H, br s, H-14b); a set of protons in the A_2X system on the 1,3,5-trisubstituted benzene ring (ring A_2) at δ 6.18 (2H, d, *J* = 1.6 Hz, H-10a, 14a)/6.24 (1H, t, *J* = 1.6 Hz, H-12a) and a set of protons in ABX system on 1,3,4-trisubstituted benzene ring (ring A_1) at δ 6.99 (1H, br, s, H-2a)/6.84 (1H, m, H-5a)/6.85-6.82 (1H, m, H-6a). A set of *trans*-coupled olefinic protons at δ 7.11 (1H, d, *J* = 16.4 Hz, H-7b) /6.97 (1H, d, *J* = 16.0 Hz, H-8b); three sets of mutually coupled aliphatic methine protons at δ 5.38 (1H, d, *J* = 5.2 Hz, H-7a)/4.42 (1H, d, *J* = 5.2 Hz, H-8a) due to a dihydrobenzofuran moiety. However, five phenolic hydroxyl groups were not observed in the ^{1}H NMR spectrum.

The molecular formula ($C_{29}H_{24}O_7$) and NMR (^{1}H and ^{13}C) spectral data revealed that **13** is a dimer of resveratrol and isorhapontigenin units. The correlations of all protons to the respective carbons were compared to bisisorhapontigennin (**10**) and clarified with the help of HMQC and HMBC spectra. The HMBC correlations between H-7a/C-2a H-7a/C-6a, H-7a/C-9a; H-8a/C-1a, H-8a/C-10a(14a); H-7b/C-2b(6b), H-7b/C-9b, H-8b/C-1b, H-8a/C-10b H-8b/C-14b (Fig. 3.8) revealed the connectivities between C-1a/C-7a, C-8a/C-9a, C-1b/C-7b, C-8b/C-9b, and the correlations between H-7a/H-8a; H-7b/H-8b in the ^{1}H-^{1}H COSY spectrum suggested connectivities between units A and B.

The upfield chemical shift of C-3a (δ 147.5) as compared to that of gnetin C (**4**) and the appearance of a set of protons in the ABX system on the 1,3,4-trisubstituted benzene ring (A_1) revealed the substitution of the methoxyl group at C-

3a on ring A_1 that was confirmed by correlations between OMe-3a/C-3a and H-2a/C-3a. The chemical shifts of all protons and carbons were assigned by the HMBC correlations (Fig. 3.8). A large downfield shift (ca 8 ppm) observed for C-11b (δ_C 162.3) compared to C-13b (δ_C 154.5) supported the replacement of hydroxyl groups by ether linkages at these respective positions. The presence of a dihydrofuran ring (7a-8a-12b-11b-O) and connectivity pattern of units A-B were supported by the HMBC correlations between H-7a/C-11b, H-8a/C-12b and H-8a/C-13b. Finally, the planar structure of **13** was determined as shown in **Fig. 3.8.**

The configuration of dihydrofuran ring was assigned to be *trans* as in gnetin C (**4**) and bisisorhapontigenin B (**10**) on the basis of NOESY interactions between H-7a/H-2a, H-7a/H-6a, H-7a/H-10a(14a), H-8a/H-2a, H-8a/H-6a, and H-8a/H-10a(14a) (Fig 3.9). Thus, **13** was found to be a dimer trivially named macrostachyol D formed as a result of oxidative coupling of resveratrol and isorhapontigenin units.

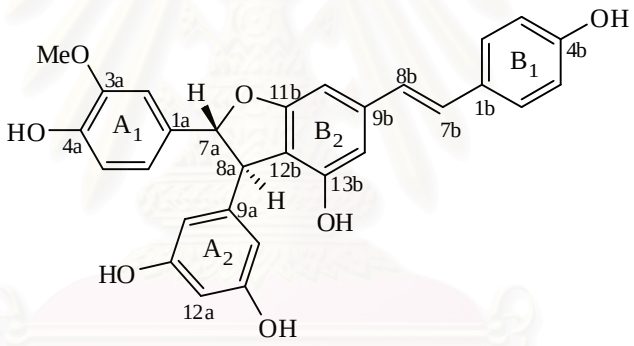

Macrostachyol D (**13**)

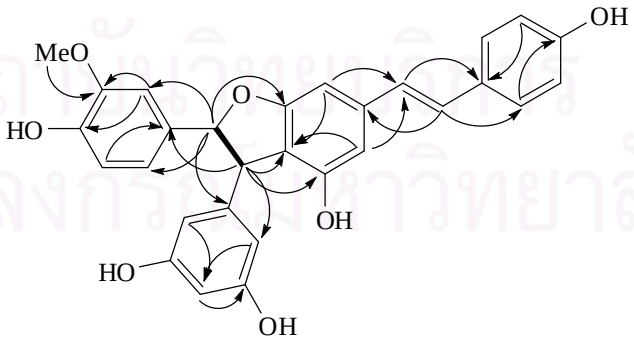

Figure 3.8 Selected HMBC (arrow curves) and COSY (bold lines) correlations of **13**.

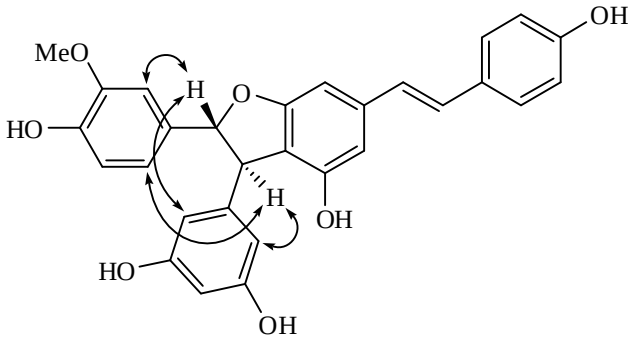

Figure 3.9 Key NOESY correlations for **13**.

Table 3.6 ^{1}H, ^{13}C, HMBC and ^{1}H-^{1}H COSY NMR data of macrostachyol D (**13**) in acetone-d_6

Position	δ_C	δ_H (mult., *J* in Hz)	HMBC	COSY
1a	133.2	-		
2a	109.3	6.99 (brs)	C-3a, C-4a, C-6a, C-7a	H-6a
3a	147.5	-		
4a	146.5	-		
5a	114.9	6.84 (m)[a]	C-1a, C-3a	
6a	118.4	6.85-6.82 (m)[a]	C-2a, C-4a, C-7a	H-2a
7a	93.0	5.38 (d, 5.2)	C-2a, C-6a, C-8a, C-9a, C-11b, C-12b,	H-8a
8a	55.1	4.42 (d, 5.2)	C-1a, C-7a, C-9a, C-10a,14a, C-11b, C-12b, C-13b	H-7a
9a	145.3	-		
10a, 14a	105.9	6.18 (d, 1.6)	C-8a, C-10a,14a, C-11a,13a, C-12a	H-12a
11a, 13a	158.7	-		
12a	101.1	6.24 (brt)	C-10a,14a, C-11a,13a	H-10a, 14a
1b	129.1	-		
2b, 6b	127.9	7.44 (d, 8.0)	C-2b,6b, C-3b,5b, C-12b, C-7b	H-3b, 5b
3b, 5b	115.5	6.85 (d, 8.4)[a]	C-1b, C-3b,5b, C-12b	H-2b, 6b
4b	157.3	-		
7b	128.3	7.11 (d, 16.4)	C-2b,6b, C-8b, C-9b	H-8b
8b	125.8	6.97 (d, 16.4)	C-1b, C-7b C-9b C-10b C-14b	H-7b
9b	140.3	-		
10b	98.2	6.70 (brs)	C-8b, C-11b, C-12b, C-13b, C-14b	H-14b
11b	162.3	-		
12b	114.2	-		
13b	154.5	-		
14b	107.2	6.60 (brs)	C-8b, C-10b, C-12b, C-13b	H-10b
3a-OMe	55.4	3.82 (s)	C-3a	

[a] Overlap

Isorhapotigenin (1): Brown oil; ^{1}H NMR (CD_3COCD_3, 400 MHz): δ 8.35 (2H, brs, OH-3′, 5′), 7.80 (1H, brs, OH-4), 7.20 (1H, brs, H-2), 7.02 (1H, d, *J* = 16.4 Hz, H-*α*), 7.01 (1H, brd, *J* = 6.4 Hz, H-6), 6.91 (1H, d, *J* = 16.4 Hz, H-*b*), 6.83 (1H, d, *J* = 8.0 Hz, H-5), 6.51 (2H, brd, *J* = 1.8 Hz, H-2′, 6′), 6.30 (1H, brt, *J* = 1.6 Hz, H-4′), 3.88 (3H, s, OMe-3). ^{13}C NMR (CD_3COCD_3, 100 MHz): δ 158.7 (C-3′, 5′), 147.7 (C-3), 146.7 (C-4), 140.0 (C-1′), 129.6 (C-1), 128.6 (C-*α*), 126.2 (C-*b*), 120.3 (C-6), 114.1 (C-5), 109.3 (C-2), 104.8 (C-2′, 6′), 101.8 (C-4′), 55.4 (OMe-3).

***trans*-resveratrol (2):** white crystals; ^{1}H NMR (CD_3COCD_3, 400 MHz): δ 7.41 (2H, d, *J* = 8.0 Hz, H-2′, 6′), 7.01 (1H, d, *J* = 16.4 Hz, H-*b*), 6.88 (1H, d, *J* = 16.4 Hz, H-*α*), 6.83 (2H, d, *J* = 8.4 Hz, H-3′, 5′), 6.53 (2H, d, *J* = 2.0 Hz, H-2, 6), 6.26 (1H, d, *J* = 2.0 Hz, H-4). ^{13}C NMR (CD_3COCD_3, 100 MHz): δ 159.4 (C-3, 5), 158.5 (C-4′), 140.9 (C-1), 130.5 (C-1′), 129.3 (C-*b*), 128.9 (C-2′, 6′), 127.8 (C- *α*), 116.5 (C-3′, 5′), 105.7 (C-2, 6), 103.1 (C-4).

Gnetol (3): white crystals; ^{1}H NMR (CD_3COCD_3, 400 MHz): δ 8.49 (2H, s, OH-2, 6), 8.03 (2H, s, OH-3′, 5′), 7.43 (1H, d, *J* = 16.8 Hz, H-*b*), 7.34 (1H, d, *J* = 16.4 Hz, H-*α*), 6.74 (1H, d, *J* = 8.0 Hz, H-4) 6.41 (2H, d, *J* = 2.0 Hz, H-2′, H-6′), 6.31 (2H, d, *J* = 8.0 Hz, H-3, H-5), 6.12 (1H, t, *J* = 2.0 Hz, H-4′). ^{13}C NMR (CD_3COCD_3, 100 MHz): δ 158.6 (C-3′, C-5′), 156.7 (C-2, C-6), 141.7 (C-1′), 131.2 (C-*b*), 127.9 (C-4), 120.5 (C-*α*), 112.0 (C-1), 107.2 (C-3, C-5), 104.7 (C-2′, C-6′), 101.5 (C-4′).

Gnetin C (4): greenish amorphous powder; ^{1}H NMR (CD_3COCD_3, 400 MHz): δ 7.30 (2H, d, *J* = 8.8 Hz, H-2b, 6b), 7.07 (2H, d, *J* = 8.8 Hz, H-2a, 6a), 6.98 (1H, d, *J* = 16.4 Hz, H-7b), 6.82 (1H, d, *J* = 16.4 Hz, H-8b), 6.71 (2H, d, *J* = 8.4 Hz, H-3a, 5a), 6.71 (2H, d, *J* = 8.4 Hz, H-3b, 5b), 6.59 (1H, s, H-10b), 6.48 (1H, s, H-14b), 6.10 (1H, t, *J* = 2.0 Hz, H-12a), 6.01 (2H, d, *J* = 2.0 Hz, H-10a, 14a), 5.21 (1H, d, *J* = 4.8 Hz, H-7a), 4.21 (1H, d, *J* = 4.8 Hz, H-8a). ^{13}C NMR (CD_3COCD_3, 100 MHz): δ 163.8 (C-11b), 160.2 (C-11a, 13a), 158.8 (C-4a), 158.8 (C-4b), 156.1 (C-13b), 146.9 (C-9a), 141.9 (C-9b), 134.7 (C-1a), 130.6 (C-1b), 129.8 (C-7b), 129.4 (C-2b, 6b), 128.5 (C-2a, 6a), 127.4 (C-8b), 117.1 (C-3b, 5b), 116.8 (C-3a, 5a), 114.0 (C-12b), 108.7 (C-14b), 107.3 (C-10a, 14a), 102.6 (C-12a), 99.8 (C-10b), 94.3 (C-7a), 56.6 (C-8a).

Latifolol (5): brown amorphous powder; ^{1}H NMR (CD_3COCD_3, 400 MHz): δ 8.56 (1H, s, OH-2a), 8.53 (1H, brs, OH-4c), 8.47 (1H, s, OH-4b), 8.29 (1H, brs, OH-4a), 8.29 (1H, brs, OH-13b), 8.10 (2H, s, OH-11a, 13a), 8.06 (1H, s, OH-13c), 7.45 (2H, d, *J* = 8.8 Hz, H-2c, 6c), 7.25 (2H, d, *J* = 8.4 Hz, H-2b, 6b), 7.12 (1H, d, *J* = 16.0 Hz, H-7c), 7.03 (1H, d, *J* = 8.4 Hz, H-6a), 6.99 (1H, d, *J* = 16.4 Hz, H-8c), 6.86 (2H, d, *J* = 8.4 Hz, H-3b, 5b), 6.85 (2H, d, *J* = 8.4 Hz, H-3c, 5c), 6.73 (1H, s, H-10c), 6.61 (1H, s, H-14c), 6.44 (1H, d, *J* = 2.0 Hz, H-3a), 6.33 (1H, brs, H-10b), 6.30 (1H, dd, *J* = 8.4, 2.0 Hz, H-5a), 6.26 (2H, d, *J* = 2.0 Hz, H-10a, 14a), 6.20 (1H, d, *J* = 2.0 Hz, H-12a), 6.19 (1H, brs, H-14b), 5.75 (1H, d, *J* = 4.0 Hz, H-7a), 5.46 (1H, d, *J* = 4.4 Hz, H-7b), 4.48 (1H, d, *J* = 4.4 Hz, H-8b), 4.44 (1H, d, *J* = 4.0 Hz, H-8a). ^{13}C NMR (CD_3COCD_3, 100 MHz): δ 162.3 (C-11c), 162.2 (C-11b), 158.3 (C-11a, 13a), 158.1 (C-4a), 157.3 (C-4b), 157.3 (C-4c), 155.4 (C-2a), 154.6 (C-13b), 154.6 (C-13c), 145.9 (C-9a), 145.3 (C-9b), 140.4 (C-9c), 133.2 (C-1b), 129.1 (C-1c), 128.3 (C-7c), 127.9 (C-2c, 6c), 127.2 (C-6a), 126.9 (C-2b, 6b), 125.8 (C-8c), 119.5 (C-1a), 115.5 (C-3c, 5c), 115.3 (C-3b, 5b), 114.1 (C-12b), 114.1 (C-12c), 107.3 (C-14c), 107.1 (C-14b), 106.4 (C-5a), 106.2 (C-10a, 14a), 102.6 (C-3a), 100.8 (C-12a), 100.2 (C-10b), 98.3 (C-10c), 92.8 (C-7b), 88.3 (C-7a), 55.1 (C-8b), 52.4 (C-8a).

Macrostachyol A (6): brown amorphous powder; $[\alpha]_D^{26}$ -29.0° (*c* 0.10, MeOH); UV (MeOH) λ_{max} (log ε): 234 (4.6), 285 (4.2), 325 (4.2) nm; positive ion ESIMS *m/z*: 923 [M+H$^+$]; positive ion HRESIMS *m/z*: [M+Na]$^+$ 945.2492 (calcd for $C_{56}H_{42}Na_1O_{13}$, 945.2518); ^{1}H NMR (CD_3COCD_3, 400 MHz) and ^{13}C NMR (CD_3COCD_3, 100 MHz) see Table 3.2.

Macrostachyol B (7): brown amorphous powder; $[\alpha]_D^{26}$ +34.0° (*c* 0.10, MeOH); UV (MeOH) λ_{max} (log ε): 238 (4.0), 281 (4.0) nm; positive ion ESIMS *m/z*: 525 [M+Na$^+$]; positive ion HRESIMS *m/z*: [M+Na]$^+$ 525.1504 (calcd for $C_{29}H_{26}Na_1O_8$, 525.1520); ^{1}H NMR (CD_3COCD_3, 400 MHz) and ^{13}C NMR (CD_3COCD_3, 100 MHz) see Table 3.3.

Parvifolol A (8): brown amorphous powder; ^{1}H NMR (CD_3COCD_3, 400 MHz): δ 8.46 (1H, s, OH-4a), 8.24 (1H, s, OH-4b), 8.17 (2H, s, OH-11b, 13b), 7.99 (1H, s, OH-13a), 7.18 (2H, d, *J* = 8.4 Hz, H-2a, 6a), 6.84 (2H, d, *J* = 8.4 Hz, H-3a, 5a), 6.76 (1H, s, OH-11a), 6.64 (1H, d, *J* = 8.4 Hz, H-6b), 6.32 (1H, m, H-3b), 6.32 (1H, m, H-5b), 6.29 (2H, brs, H-10b, 14b), 6.29 (1H, brs, H-12b), 6.12 (1H, d, *J* = 2.0 Hz, H-12a), 5.58 (1H, d, *J* = 1.2 Hz, H-14a), 4.66 (1H, d, *J* = 8.8 Hz, H-7a), 4.14 (1H, d, *J* = 8.0 Hz, H-8b), 3.54 (1H, m, H-8a), 3.52 (1H, m, H-7b). ^{13}C NMR (CD_3COCD_3, 100 MHz): δ 158.7 (C-11b, 13b), 157.5 (C-13a), 157.2 (C-4a), 156.8 (C-4b), 155.5 (C-2b), 154.2 (C-11a), 146.5 (C-9b), 145.1 (C-9a), 130.9 (C-1a), 130.1 (C-6b), 129.3 (C-2a, 6a), 121.8 (C-10a), 115.7 (C-1b), 114.8 (C-3a, 5a), 108.3 (C-5b), 106.9 (C-10b, 14b), 104.7 (C-14a), 102.9 (C-3b), 102.1 (C-12a), 101.0 (C-12b), 78.3 (C-7a), 56.4 (C-8b), 49.5 (C-7b), 48.4 (C-8a).

Gnetumacrosin (9): mixture with resveratrol; UV (MeOH) λ_{max} (log ε): 215 (4.1), 304 (4.0) nm; positive ion ESIMS *m/z*: 259 [M+H$^+$]; positive ion HRESIMS *m/z*: [M+H]$^+$ 259.0974 (calcd for $C_{15}H_{14}O_4$+H$^+$, 259.0970); ^{1}H NMR (CD_3COCD_3, 400 MHz) and ^{13}C NMR (CD_3COCD_3, 100 MHz) see Table 3.4.

Bisisorhapontigenin B (10): greenish amorphous powder; ^{1}H NMR (CD_3COCD_3, 400 MHz): δ 8.28 (1H, s, OH-11, 13a), 8.25 (1H, s, OH-13b), 7.84 (1H, s, OH-4b), 7.77 (1H, s, OH-4a), 7.11 (1H, d, *J* = 16.4 Hz, H-7b), 7.24 (1H, d, *J* = 1.6 Hz, H-2b), 7.04 (1H, dd, *J* = 8.0, 2.4 Hz, H-6b), 7.02 (1H, d, *J* = 16.4 Hz, H-8b), 6.99 (1H, brs, H-2a), 6.84 (1H, d, *J* = 8.0 Hz, H-15b), 6.83 (1H, m, H-5a), 6.83 (1H, m, H-6a), 6.71 (1H, brs, H-10b), 6.61 (1H, d, *J* = 1.2 Hz, H-14b), 6.26 (1H, d, *J* = 2.4 Hz, H-12a), 6.20 (2H, d, *J* = 2.0 Hz, H-10a, 14a), 5.39 (1H, d, *J* = 16.4 Hz, H-7a), 4.43 (1H, d, *J* = 16.4 Hz, H-8a), 3.89 (3H, s, OMe-3b), 3.82 (3H, s, OMe-3a). ^{13}C NMR (CD_3COCD_3, 100 MHz): δ 162.2 (C-11b), 158.7 (C-11a, 13a), 154.6 (C-13b), 147.7 (C-3b), 147.5 (C-3a), 146.7 (C-4b), 146.5 (C-4a), 145.3 (C-9a), 140.3 (C-9b), 133.5 (C-1a), 129.6 (C-1b), 128.6 (C-7b), 126.1 (C-8b), 120.3 (C-6b), 118.4 (C-6a), 115.1 (C-5b), 115.0 (C-5a), 114.2 (C-12b), 109.3 (C-2a), 109.3 (C-2b), 107.2 (C-14b), 105.9 (C-10a, 14a), 101.1 (C-12a), 98.3 (C-10b), 93.0 (C-7a), 55.4 (OMe-3a), 55.4 (OMe-3b), 55.1 (C-8a).

Macrostachyol C (11): brown amorphous powder; $[\alpha]_D^{26}$ -30.0° (*c* 0.10, MeOH); UV (MeOH) λ_{max} (log ε): 207 (4.9), 280 (4.1) nm; positive ion ESIMS *m/z*: 697 $[M+H]^+$; positive ion HRESIMS *m/z*: $[M+H]^+$ 697.2076 (calcd for $C_{42}H_{33}O_{10}$, 697.2073); ^1H NMR (CD_3COCD_3, 400 MHz) and ^{13}C NMR (CD_3COCD_3, 100 MHz) see Table 3.5.

Oxyresveratrol (12): white crystals;^1H NMR (CD_3COCD_3, 400 MHz): δ 7.41 (1H, d, *J* = 8.8 Hz, H-6), 7.34 (1H, d, *J* = 16.4 Hz, H-α), 6.89 (1H, d, *J* = 16.4 Hz, H-β), 6.52 (2H, d, *J* = 2.0 Hz, H-2′, 6′), 6.44 (1H, d, *J* = 2.4 Hz, H-3), 6.38 (1H, dd, *J* = 8.4, 2.4 Hz, H-5), 6.23 (1H, t, *J* = 2.0 Hz, H-4′).

Macrostachyol D (13): greenish amorphous powder; $[\alpha]_D^{26}$ -39.0° (*c* 0.10, MeOH); UV (MeOH) λ_{max} (log ε): 207 (4.6), 327 (4.2) nm; positive ion ESIMS *m/z*: 485 $[M+H^+]$; positive ion HRESIMS *m/z*: $[M+H]^+$ 485.1591 (calcd for $C_{29}H_{25}O_7$, 485.1600); ^1H NMR (CD_3COCD_3, 400 MHz) and ^{13}C NMR (CD_3COCD_3, 100 MHz) see Table 3.6.

3.3 Bioassay activity of isolated compounds

3.3.1 Antioxidant activity of isolated compounds

The isolation and purification of acetone crude extracts from *G. macrostrachyum* roots yielded thirteen stilbeniods including five new stilbenoids (**6**, **7**, **9**, **11**, and **13**). The antioxidant activity of isolated stilbeniods were evaluated for inhibitory activity on DPPH radical scavenging activity and lipid peroxidation. The activity were expressed as IC_{50} (mM) by spectroscopic method. The biological activity results of all tested stilbeniods are shown in **Table 3.7**.

Table 3.7 Antioxidant activity of isolated stilbenoids.

Isolated compounds	IC_{50} (mM)	
	DPPH scavenging	**Lipid peroxidation**
Isorhapotigenin (**1**)	0.28 ± 0.01	0.10 ± 0.01
trans-resveratrol (**2**)	0.44 ± 0.04	0.29 ± 0.01
Gnetol (**3**)	0.21 ± 0.00	0.42 ± 0.03
Gnetin C(**4**)	0.24 ± 0.04	0.12 ± 0.00
Latifolol (**5**)	0.32 ± 0.01	0.02 ± 0.00
Macrostachyol A (**6**)	0.33 ± 0.02	0.02 ± 0.00
Macrostachyol B (**7**)	0.82 ± 0.09	0.23 ± 0.01
Parvifolol A (**8**)	1.14 ± 0.12	0.03 ± 0.00
Gnetumacrosin (**9**)	-	-
Bisisorhapotigenin B (**10**)	-	-
Macrostachyol C (**11**)	-	-
Oxyresveratrol (**12**)	-	-
Macrostachyol D (**13**)	-	-
Curcumin*	-	0.02 ± 0.00
Ascorbic acid*	0.14 ± 0.01	-

* Standard antioxidant

-: Not determined

Antioxidant activities of isolated stilbenoids were tested against various radical sources by UV-Vis spectroscopy. Anti-radical property of stilbenoids was examined with DPPH, which is widely used for assessing the ability of polyphenol to transfer labile H-atom to radicals. The greater effectiveness of compounds was possible due to the presence *ortho*-dihydroxy groups (catechol) which upon donating hydrogen radicals will give higher stability to their radical forms.[56] The vicinal dihydroxyl groups could transfer to quinone easily by releasing two electrons in **Scheme 3.1**.[57]

Preliminary, the IC_{50} value of fractions D, and C (IC_{50} = 0.06, and 0.09 mg/mL) showed the antioxidant activity two to three time less than ascorbic acid (IC_{50} = 0.03 mg/mL), and lower than another fractions (Table 3.1). Compounds **3**, **4**, and **1** were isolated from main fraction C and D. The IC_{50} of compounds **3, 4,** and **1** (IC_{50} = 0.21, 0.24, and 0.28 mM) showed two time less than ascorbic acid (IC_{50} = 0.14 mM) which was used as a positive control (Table 3.7). The all of tested stilbenoids were non catecholic compounds. They showed DPPH radical scavenging activity weaker than ascorbic acid (IC50 = 0.21 – 1.14 mM).

Lipid peroxidation, the nonenzymatic autocatalytic interaction of polyunsaturated fatty acids (PUFA) with molecular oxygen, is a process typical of all biological systems. Products generated as a consequence of lipid peroxidation are involved in pathophysiological diseases such as cancer, atherosclerosis and aging.[58] In order to clarify the active component of *G. macrostachyum*, the thirteen isolated stilbenoids were examined *in vitro.*

The lipid peroxidation inhibition results in **Table 3.7**, showed that compounds **5**, **6**, and **8** (IC_{50} = 0.02, 0.02, 0.03 mM) were remarkable inhibitory of malondialdehyde (MDA) formation of lipid peroxidation. Compounds **1**, **2**, **3, 4**, and **7** (IC_{50} = 0.10 - 0.42 mM) showed activity weaker than curcumin (IC_{50} = 0.02 mM), which was used as reference antioxidant.

3.3.2 Anti-platelet aggregation activity of isolated compounds

The antiplatelet aggregration activity of isolated stilbeniods determined by Born's method,[54] were expressed as IC_{50} (μM). The biological activity results of all test stilbeniods are shown in **Table 3.8**.

Table 3.8 Inhibitory effect of isolated stilbeniods from *G. macrostachyum* on platelet aggregation induced by adenosine diphophate (ADP).

Isolated compounds	IC_{50} (µM)[a]
Isorhapotigenin (**1**)	0.368 ± 0.034
trans-resveratrol (**2**)	1.256 ± 0.054
Gnetol (**3**)	0.636 ± 0.085
Gnetin C(**4**)	0.704 ± 0.423
Latifolol (**5**)	0.500 ± 0.005
Macrostachyol A (**6**)	0.180 ± 0.021
Macrostachyol B (**7**)	0.721 ± 0.170
Parvifolol A (**8**)	0.776 ± 0.079
Gnetumacrosin (**9**)	-
Bisisorhapotigenin B (**10**)	-
Macrostachyol C (**11**)	-
Oxyresveratrol (**12**)	-
Macrostachyol D (**13**)	-
Ibuprofen (Standard drug)	11200.00

[a] n = 2

-: Not determined

From phytochemical investigation of *G. macrostachyum* roots extracts, thirteen stilbenoids were isolated and evaluated for anti-platelet aggregation activity (Table 3.8). Macrostacyol A (**6**) was the most effective compound among the isolated stibenoids. From the anti-platelet activity evaluation, all test stilnenoids were more potent (IC_{50} = 0.18-1.26 µM) than ibuprofen (IC_{50} = 11.2 mM) which was used as a positive control.

Inhibitory effects on platelet aggregation of stilbenoids from plant sources have been investigated. In addition, several of stilbenoids exhibited anti-platelet aggregation. Some stilbenoid oligomers such as ampelopsin C, miyabenol A, and vitisinols C inhibited arachidonic acid-induced platelet aggregation.[(24)] The inhibitory effect of piceid and rhaponticin when platelet aggregation induced by collagen or ADP were less than of *trans*-resveratrol.[(27)]

This study revealed all of tested stilbenoids exhibited strong inhibitory effect on platelet aggregation induced by ADP. However, the mode of inhibition of all test stilbenoids must be further clarified by using other type of aggregation agents such as arachidonic acid, collagen, thrombin, etc.

3.3.3 Cytotoxic activity against Hela and KB cell lines of isolated compounds

The cytotoxic activity against HeLa and KB cell lines of isolated stilbenoids were determined using MTT assay and the result was shown in **Table 3.9**.

Table 3.9 Cytotoxic Activity Against HeLa and KB Cell lines of Isolated Compounds.

Isolated compounds	**IC_{50} (µg/mL)**	
	KB cell line	**HeLa cell line**
Isorhapotigenin (**1**)	8.50	15.00
trans-resveratrol (**2**)	8.00	15.50
Gnetol (**3**)	10.00	38.00
Gnetin C (**4**)	-	-
Latifolol (**5**)	49.00	54.00
Macrostachyol A (**6**)	>100.00	>100.00
Macrostachyol B (**7**)	53.00	95.00
Parvifolol A (**8**)	60.00	>100.00
Gnetumacrosin (**9**)	6.90	11.00
Bisisorhapotigenin B (**10**)	12.50	14.00
Macrostachyol C (**11**)	-	-
Oxyresveratrol (**12**)	-	-
Macrostachyol D (**13**)	-	-

-: Not determined

KB cell line: Human epidermoid carcinoma

HeLa cell line: Human cervical carcinoma

Note: Standard agent (Adriamycin IC_{50} = 0.018 μg/mL)

From **Table 3.9**, all of tested stilbenoids showed cytotoxic activity against the KB cell more than HeLa cell. In addition, gnetumacrosin (**9**) was the most effective stilbenoid. Compounds **1**, **2**, and **9** showed mild cytotoxic activity against KB cell line IC_{50} = 8.50, 8.00, and 6.90 and against HeLa cell line with IC_{50} = 15.00, 15.50, and 11.00, μg/mL, respectively. Compounds **5**, **6**, **7**, and **8** could be regarded as inactive. Thus, there are definite correlations between the degree of cytotoxicity and molecular size of tested stilbenoids.

CHAPTER IV
CONCLUSION

In conclusion, the isolation of the acetone crude extract from the roots of *Gnetum macrostachyum* yielded thirteen stilbenoids. They were five new stilbenoids, macrostachyol A (**6**), B (**7**), C (**11**), D (**13**), and gnetumacrosin (**9**), along with eight known stilbenoid; isorhapontigenin (**1**), *trans*-resveratrol (**2**), gnetol (**3**), gnetin C (**4**), latifolol (**5**), parvifolol A (**8**), bisisorhapotigenin B (**10**), and oxyresveratrol (**12**). The chemical structures of all isolated compounds were characterized by means of NMR and MS experiments as well as comparison with the previous reports.

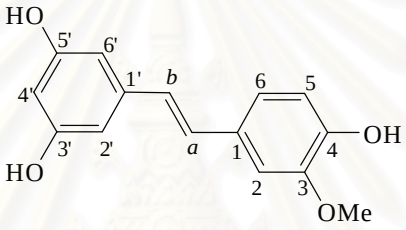

isorhapontigenin (**1**)

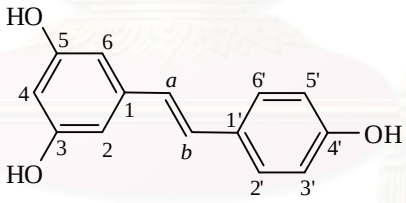

trans-resveratrol (**2**)

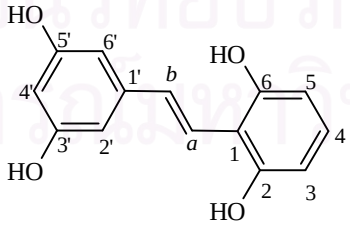

gnetol (**3**)

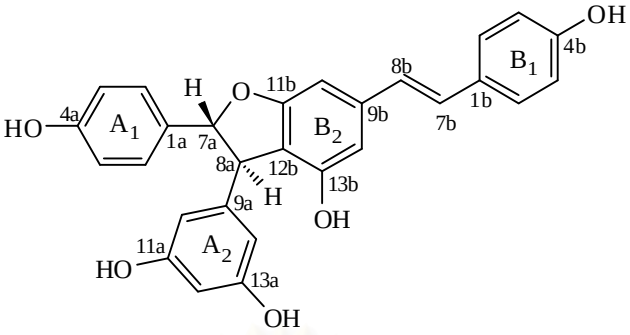

gnetin C (**4**)

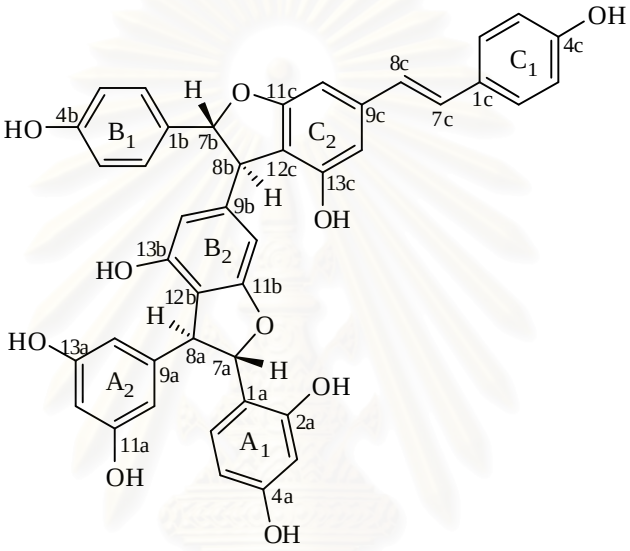

latifolol (**5**)

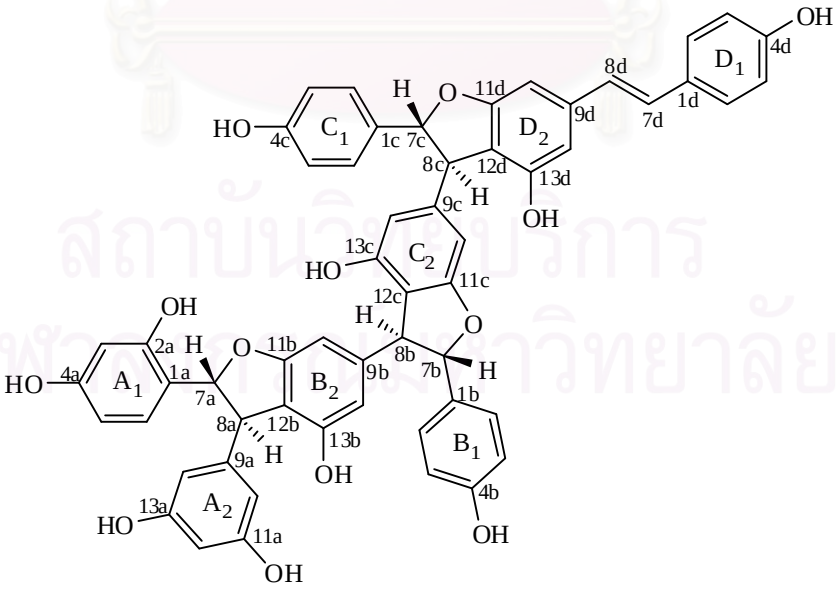

macrostachyol A (**6**, New compound)

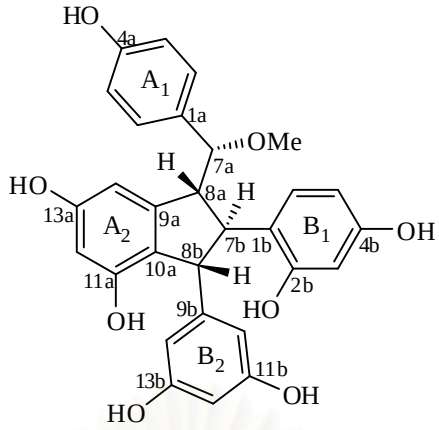

macrostachyol B (**7**, New compound)

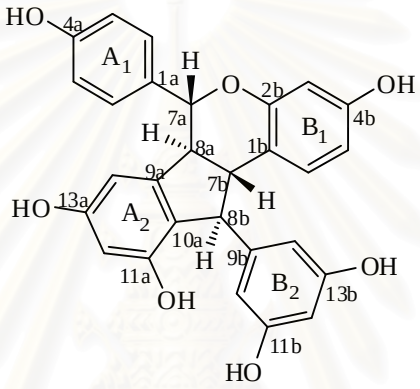

pavifolol A (**8**)

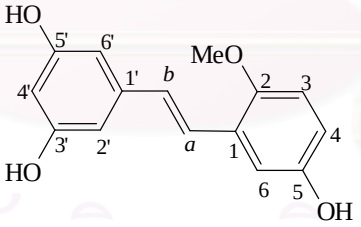

gnetumacrosin (**9**, New compound)

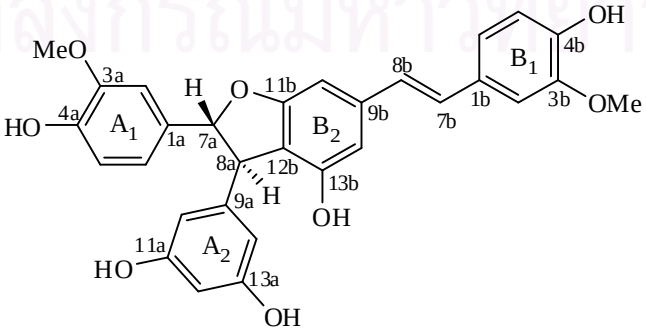

bisisorhapotigenin B (**10**)

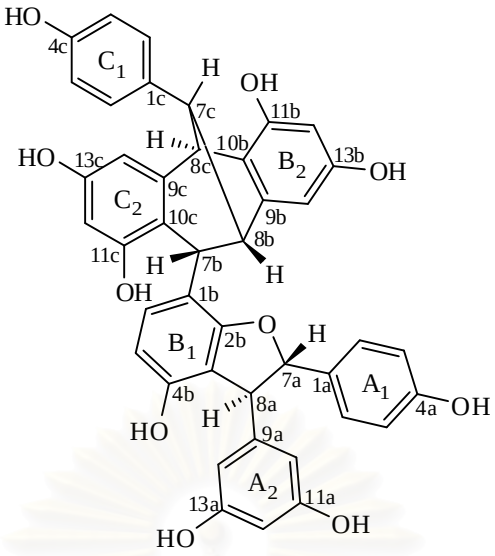

macrostachyol C (**11**, New compound)

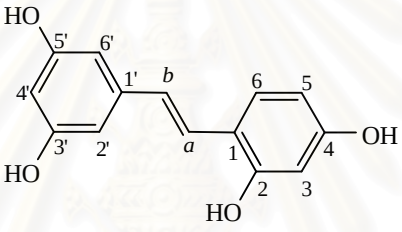

oxyresveratrol (**12**)

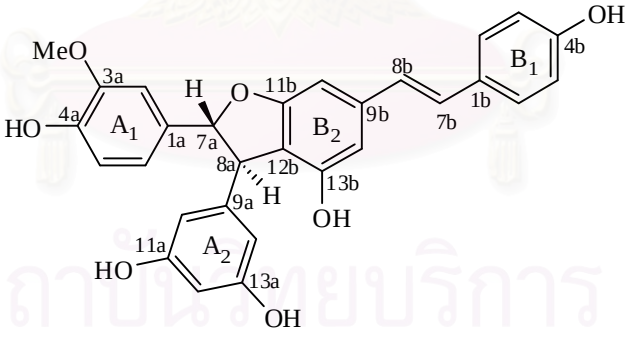

macrostachyol D (**13**, New compound)

The DPPH radical scavenging activity indicated that the IC_{50} of compounds **3, 4,** and **1** (IC_{50} = 0.21, 0.24, and 0.28 mM) showed two time less active than ascorbic acid (IC_{50} = 0.14 mM) which was used as a positive control. In addition, compounds **5**, **6**, **2**, **7**, and **8** also showed antioxidant activity on DPPH radical (IC_{50} = 0.32, 0.33, 0.44, 0.82, and 1.14 mM). Moreover, both compounds **5** and **6** (IC_{50} = 0.02 mM) showed the most effective on lipid peroxidation inhibition activity followed by compounds **8** (IC_{50} = 0.03

mM), **1** (IC_{50} = 0.10 mM), **4** (IC_{50} = 0.12 mM), **7** (IC_{50} = 0.23 mM), **2** (IC_{50} = 0.29 mM), and **3** (IC_{50} = 0.42 mM), respectively.

The evaluation for anti-platelet aggregation using ADP as aggregating agent indicated that macrostachyol A (**6**) was the most effective compound in inhibiting platelet aggregation among the isolated stilbenoids. Furthermore, the IC_{50} value of all tested stilbenoids, compounds **1-8** were found that (IC_{50} = 0.18-1.26 µM) more potent than ibuprofen (IC_{50} = 11.2 mM) which was used as a positive control.

The investigation for cytotoxic activity against KB and HeLa cell lines of all compounds indicated that compound **9** was the most effective stilbenoid. Compounds **1**, **2**, **9,** and **10** showed mild cytotoxic activity against KB cell line IC_{50} = 6.90, 8.00, 8.50, and 12.50 and against HeLa cell line with IC_{50} = 15.00, 15.50, 11.00, and 14.00 μg/mL, respectively.

REFERENCES

[1] Sotheeswaran, S. and Pasupathy, V. Distribution of resveratrol oligomers in plants. *Phytochemistry* **1993**, *32*, 1083-1092.

[2] Lins, A. P.; Ribeiro, M. N. D. S.; Gottlieb, O. R. and Gottlieb, H. E. Gnetins: resveratrol oligomers from Gnetum species. *J. Nat. Prod*. **1982**, *45*, 754-761.

[3] Lin, M.; Li, J. B. Li, S. Z.; Yu, D. Q. and Liang, X. T. A dimeric stilbene from *Gnetum parvifolium*. *Phytochemistry* **1992**, *31*, 633-638.

[4] Xianga, W.; Jianga, B.; Lib, X.–M.; Zhanga, H.–J.; Zhaoa, Q.–S.; Lia, S.–H.; and Sun, H.–D. Constituents of *Gnetum montanum*. *Fitoterapia* **2002**, *73*, 40-42.

[5] Iliya, I.; Ali, Z.; Tanaka, T.; Iinuma, M.; Furasawa, M.; Nakaya, K.–I.; Shirataki, Y.; Murata, J.; Danaedi, D.; Matsuura N. and Ubukata, M. Three new trimeric stilbenes from *Gnetum gnemon*. *Chem. Pharm. Bull*. **2003**, *51*, 85-88.

[6] Luo, H. F.; Zheng, L. P. and Hu, C. Q. Five novel oligostilbenes from the roots of *Caragana sinica*. *Tetrahedron* **2001**, *57*: 4849-4854.

[7] Huang, K. S.; Lin, M.; Yu, L. N. and Hong, M. Four novel oligostilbenes from the roots of *Vitis amurensis*. *Tetrahedron* **2000**, *56*, 1321-1329.

[8] Ito, T.; Tanaka, T.; Nakaya, K.; Iinuma, M.; Takahashi, Y.; Nagawa, H.; Ohyama, M.; Nakanishi, Y.; Bastow, K. F. and Lee, K. H., A novel bridged stilbenoid trimer and four highly condensed stilbenoid oligomers in *Vatica rassak*. *Tetrahedron* **2001**, *57*, 7309-7321.

[9] Huang, K. S.; Li, R. L.; Wang, Y. H. and Lin, M. Three new stilbene trimers from the lianas of *Gnetum hainanense*. *Planta Med.* **2001**, *67*, 61-64.

[10] Ito, T.; Akao, Y.; Tanaka, T.; Iinuma, M. and Nozawa, Y. Vaticanol C, A novel resveratrol tetramer, inhibits cell growth through induction of apoptosis in colon cancer cell lines. *Biol. Pharm. Bull.* **2002**, *25*, 147-148.

[11] Ito, T.; Tanaka, T.; Iinuma, M.; Nakaya, K.–I.; Takahashi, Y.; Sawa, R.; Naganawa, H. and Chelladurai, V. Two new oligostilbenes with dihydrobenzofuran from the stem bark of *Vateria indica*. *Tetrahedron* **2003**, *59*, 1255-1264.

[12] Ge, H. M.; Huang, B.; Tan, S. H.; Shi, D. H.; Song, Y. C. and Tan, R. X.

Bioactive oligostilbenoids from the stem bark of *Hopea exalata*. *J. Nat. Prod*. **2006**, *69*, 1800-1802.

[13] Huang, K.–S.; Lin, M. and Cheng, G.–F. Anti-inflammatory tetramers of resveratrol from the roots of *Vitis amurensis* and the conformations of the seven-membered ring in some oligostilbenes. *Phytochemistry* **2001**, *58*, 357-362.

[14] Yamada, M.; Hayashi, K.-I.; Hayashi, H..; Ikeda, S.; Hoshino, T.; Tsutsui, K.; Tsutsui, K.; Iinuma, M. and Nozaki, H. Stilbenoids of *Kobresia nepalensis* (Cyperaceae) exhibiting DNA topoisomerase II inhibition. *Phytochemistry* **2006**, *67*, 307-313.

[15] Tanaka, T.; Iliya, I.; Ito, T.; Furusawa, M.; Nakaya, K.–I.; Iinuma, M.; Shirataki, Y.; Matsuura, N.; Ubukata, M.; Murata, J.; Simozono, F. and Hirai, K. Stilbenoids in lianas of *Gnetum parvifolium*. *Chem. Pharm. Bull*. **2001**, *49*, 858-862.

[16] Huang, K.–S.; Wang, Y.–H.; Li, R.–L. and Lin, M. Five new stilbene dimers from the lianas of *Gnetum hainanense*. *J. Nat. Prod*. **2000**, *63*, 86-89.

[17] Lin, M., Li, J. B., Wu, B. and Zheng, Q. T. A stilbene derivative from *Gnetum parvifolium. Phytochemistry* **1991**, *30*, 4201-4203.

[18] Iliya, I.; Ali, Z.; Tanaka, T.; Iinuma, M.; Furusawa, M.; Nakaya, K.–I.; Jin Murata, J. and Darnaedi, D. Stilbenoids from the stem of *Gnetum latifolium* (Gnetaceae). *Phytochemistry* **2002**, *61*, 959–961.

[19] Sobolev, A. S.; Horn, B. W.; Potter, T. L.; Deyrup, S. T. and Gloer, J. B. Production of stilbenoids and phenolic acids by the peanut plant at early stages of growth. *J. Agric. Food Chem*. **2006**, *54*, 3505-3511.

[20] Jang, M.; Cai, L.; Udeani, G. O.; Slowing, K. V.; Thomas, C. F.; Beecher, C. W. W.; Fong, H. H. S.; Farnsworth, N. R.; Kinghorn, A. D.; Mehta, R. G.; Moon, R. C. and Pezzuto, J. M. Cancer chemopreventive activity of resveratrol, a natural product derived from grapes. *Science* **1997**, *275*, 218-220.

[21] Halls, C. and Yu, O. Potential for metabolic engineering of resveratrol biosynthesis. *Trends Biotechnol*. **2008**, *26*, 77-81.

[22] Ragab, A. S.; Fleet, J. V.; Jankowski, B.; Park, J.–H. and Bobzin, S. C. Detection

and quantitation of resveratrol in tomato fruit (*Lycopersicon esculentum* Mill.). *J. Agric. Food Chem*. **2006**, *54*, 7175-7179.

[23] Likhitwitayawuid, K. and Sritularak, B. A new dimeric stilbene with tyrosinase inhibitiory activity from *Artocarpus gomezianus*. *J. Nat. Prod*. **2001**, *64*, 1457-1459.

[24] Huang, Y.–L.; Tsai, W.–J.; Shen, C.–C. and Chen, C.–C. Resveratrol derivatives from the roots of *Vitis thunbergii*. *J. Nat. Prod*. **2005**, *68*, 217-220.

[25] Iliya, I.; Ali, Z.; Tanaka, T.; Iinuma, M.; Furusawa, M.; Nakaya, K.–I.; Murata, J.; Darnaedi, D.; Matsuura, N. and Ubukata, M. Stilbene derivatives from *Gnetum gnemon* Linn. *Phytochemistry* **2003**, *62*, 601-606.

[26] Xiang, T.; Uno, T.; Ogino, F.; Ai, C.; Duo, J. and Sankawa, U. Antioxidant constituents of *Caragana tibetica. Chem. Pharm. Bull*., **2005**, *53*, 1204-1206.

[27] Aburjai, T. A. Anti-platelet stilbenes from aerial parts of *Rheum palaestinum. Phytochemistry* **2000**, *55*, 407-410.

[28] Langcake, P. and Pryce, R.J. A new class of phytoalexins from grapevines. *Experientia*. **1977**, *33*, 151-152.

[29] Ducrot, P. H.; Kollmann, A.; Balla, A. E.; Majira, A.; Kerhoas, L.; Delorne, R. and Einhorn, J. Cyphostemmins A-B, two new antifungal oligostilbenes from *Cyphostemma crotalarioides* (Vitaceae). *Tetrahedron Lett*. **1998**, *39*, 9655-9658.

[30] Kulanthaivel, P.; Janzen, W. P.; Ballas, L. M.; Jiang, J. B.; Hu, C. Q.; Darges, J. W.; Seldin, J. C.; Cofield, D. J. and Adams, L. M. Naturally occurring protein kinase inhibitors; II. Isolation of oligomeric stilbenes from *Caragana sinica. Planta Med*. **1995**, *61*, 41-44.

[31] Oshima, Y.; Namao, K.; Kamijou, A.; Matsuoka, S.; Nakano, M.; Terao, K. and Ohizumi, Y. Powerful hepatoprotective and hepatotoxic plant oligostilbenes, isolated from the oriental medicinal plant *Vitis coignetiae* (Vitaceae). *Experientia* **1995**, *51*, 63-66.

[32] Dai, J. R.; Hallock, Y. F.; Cardellina, II, J. H. and Boyd, M. R. HIV-inhibitory and cytotoxic oligostilbenes from the leaves of *Hopea malibato. J. Nat. Prod*. **1998**, *61*, 351–353.

[33] Cichewicz, R. H.; Kouzi, S. A. and Hamann, M. T. Dimerization of resveratrol by

the grapevine pathogen *Botrytis cinerea*. *J. Nat. Prod*. **2000**, *63*, 29–33.

[34] Li, X.–M.; Wang, Y.–H. and Lin, M. Stilbenoids from the lianas of *Gnetum pendulum*. *Phytochemistry* **2001**, *58*, 591-594.

[35] Ohguchi, K.; Tanaka, T.; Iliya, I.; Ito, T.; Iinuma, M.; Matsumoto, K.; Akao, Y. and Nozawa, Y. Gnetol as a potent tyrosinase inhibitoe from genus Gnetum. *Biosci. Biotechnol. Biochem*., **2003**, *67*, 663-665.

[36] Iliya, I.; Tanaka, T.; Iinuma, M.; Ali, Z.; Furasawa, M.; Nakaya, K.–I.; Shirataki, Y.; Murata, J. and Danaedi, D. Stilbene derivatives from two species of Gnetaceae. *Chem. Pharm. Bull*. **2002**, *50*, 796-801.

[37] Li, X.–M.; Lin, M.; Wang, Y.–H. and Liu, X. Four new stilbenoids from the lianas of *Gnetum montanum* f. *megalocarpum*. *Planta. Med*. **2007**, *70*, 160-165.

[38] Smitinand, T.; Larsen, K. Flora of Thailand **1975**, *2*, 207.

[39] เต็ม สมิตินันท์. *ชื่อพรรณไม้แห่งประเทศไทย (ชื่อวิทยาศาสตร์-ชื่อพื้นเมือง)*. **2523**, 166.

[40] Fazilatun, N.; Zhai, I.; Nornish, M.; Mas Rose mal, H.M.H. Free radical-scavenging activity of organic extracts and pure flavonoid of *Blumea balsamifera* DC leaves. *Food Chem*. **2004**, *88*, 243-252.

[41] Aligiannis, N.; Mitaku, S.; Tsitsa-Tsardis, E.; Harvala, C.; Tsaknis, I.; Lalas, S. and Haroutounian, S. Methanolic extract of *Verbascum macrurum* as a source of natural preservatives against oxidative rancidity. *J. Agric. Food Chem*. **2003**, *51*, 7308-7312.

[42] Kalinich, J. F.; Ramakrishnan, R.; McClain, D. E. and Ramakrishnan, N. 4-Hydroxynonenal, an end-product of lipid peroxidation, induces apoptosis in human leukemia T- and B-cell lines. *Free Rad. Res*. **2000**, *33*, 349-358.

[43] Esterbauer, H.; Schaur, R. J. and Zollner, H. Chemistry and biochemistry of 4-hydroxynonenal, malonaldehyde and related aldehydes. *Free Radic. Biol. Med*. **1991**, *11*, 81-128.

[44] Francisco, J. R.; Francisco, B.–M.; Maria, J. R.; Enrique, J. J.; Belén, R. Nuria, M. and Joaquin, R. Lipid peroxidation products and antioxidants in human Disease. *Environ. Health Perspect*. **1998**, *106*, 1229-1234.

[45] Zaleska, M. A. and Floyd, R. A. Reginal lipid peroxidation in rat brain *in vitro*: possible role of endogenous iron. *Neurochem. Res*. **1985**, *10*, 397-410.

[46] Kogure, K. B.; Watson, B.; Busto, R. and Abe, K. Potentiation of lipid peroxides

by ischemia in rat brain. *Neurochem. Res.* **1982**, *7*, 437-454.

[47] Braughler, J. M. Lipid peroxidation-induced inhibition of GABA uptake in rat brain synaptosomes: protection by glucocorticoids. *J. Neurochem.* **1985**, *44*, 1282-1288.

[48] Picklo, M. J.; Amarnath, V.; McIntyre, J. O.; Graham, D. G. and Montine, T. J. 4-Hydroxy-2(E)-nonenol inhibits CNSS mitochondrial respiration at multiple sites. *J. Neurochem.* **1999**, *72*, 1617-1624.

[49] Brown-Galatola, C. H. and Hall, N. D. Impaired suppressor cell activity due to surface sulphydryl oxidation in rheumatoid arthritis. *Br. J. Rheumatol.* **1992**, *31*, 599-603.

[50] Hostettmann, K.; Terreaux, C.; Marston, A. and Potterat, O. The role of planar chromatography in the rapid screening and isolation of bioactive compounds from medicinal plants. *J. Plan. Chromatogr.* **1997**, *10*, 251-257.

[51] Yen, G. C. and Hsieh, C. L. Antioxidant effects of dopamine and related compounds. *Biosci. Biotechnol. Biochem.* **1997**, *61*, 1646-4649.

[52] Hung, C. Y. and Yen, G. C. Antioxidant activity of phenolic compounds isolated from *Mesona procumbens* Hemsl. *J. Agric. Food Chem.* **2002**, *50*, 2993-2997.

[53] Lowry, O. H., Rosebrough, N. J., Farr, A. L., and Randall, R. J. Protein measurement with the folin phenol reagent *J.Biol.Chem.* **1951**, *193*, 265-275.

[54] Born, G. V. R. Aggregation of blood platelets by adenine diphosphate and its reversal. *Nature.* **1962**. *194*, 927-929.

[55] Oshima, Y., Ueno, Y., Hisamichi, K., and Takeshita, M. Ampelopsins F and G, novel bridged plant oligostilbenes from *Ampelopsis brevipedunculata* var. *hancei* roots (vitaceae) *Tetrahedron* **1993**, *49*, 801-804.

[56] Mahabusarakum, W.; Nvangnaowarat, W. Taylor, W. C. Xanthones derivertives from *Cratoxylum cochinchinense* roots. *Phytochemistry* **2006**, *67*, 470-474.

[57] Pietta, P. G. Flavonoids as antioxidants. *J. Nat. Prod.* **2000**, *63*, 1035-1042.

[58] Phuwapraisirisan. P.; Surapinit, S. and Tip-pyang, S. A novel furanoumarin from *Feroniella lucida* exerts protective effect against lipid peroxidation. *Phytother. Res.* **2006**, *20*, 708-710.

APPENDICES

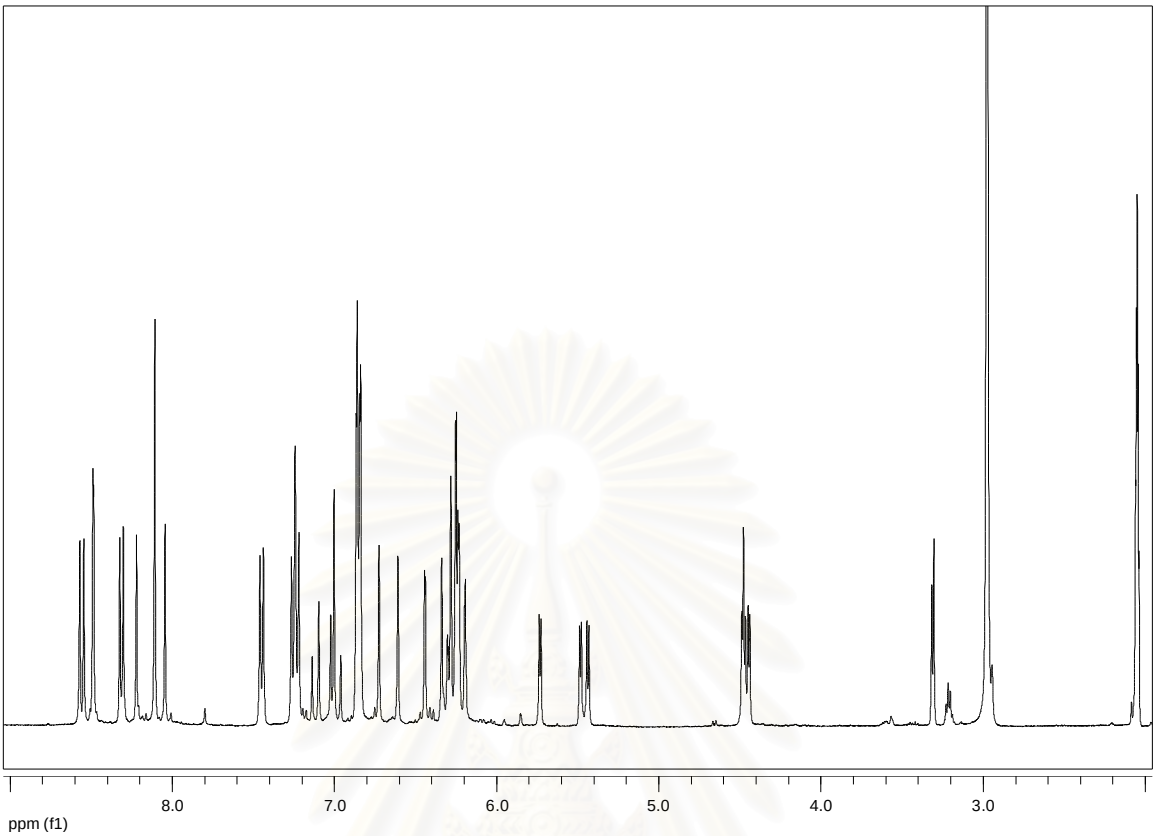

Figure A-1.1 ^{1}H NMR spectrum (acetone-d_6) of macrostachyol A (**6**).

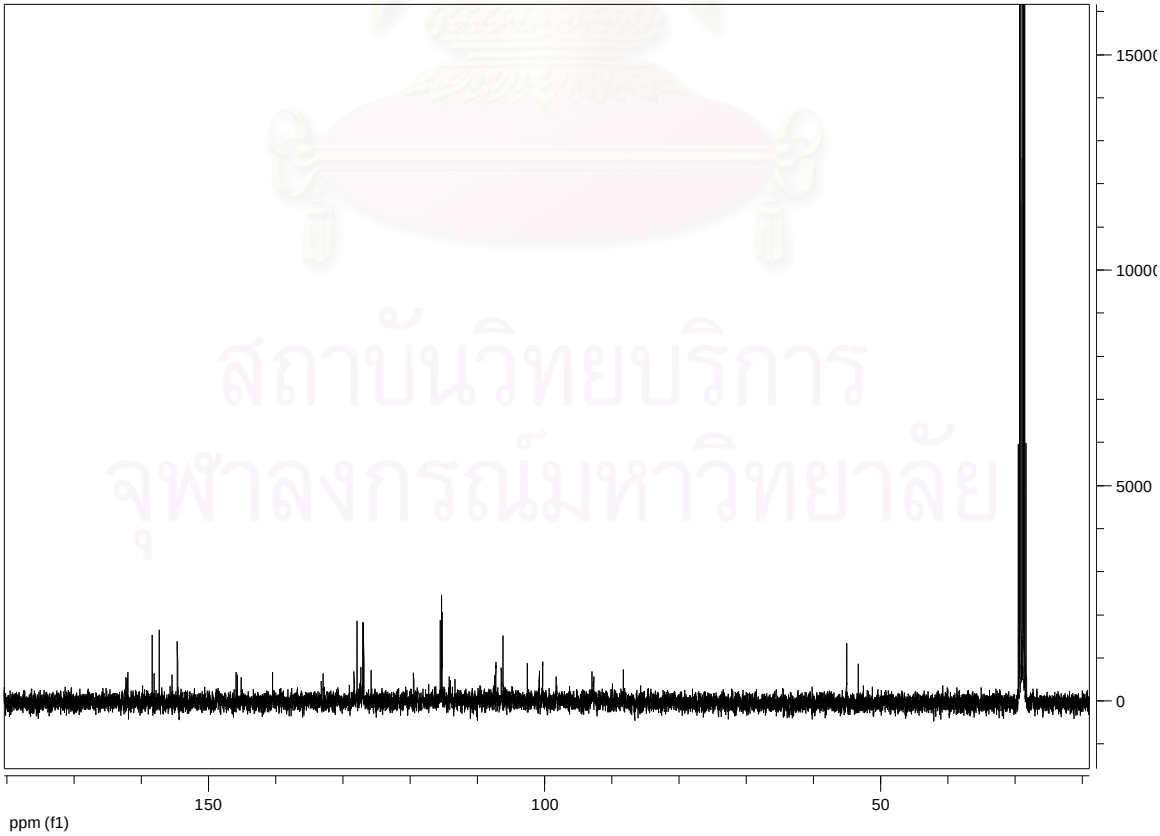

Figure A-1.2 ^{13}C NMR spectrum (acetone-d_6) of macrostachyol A (**6**).

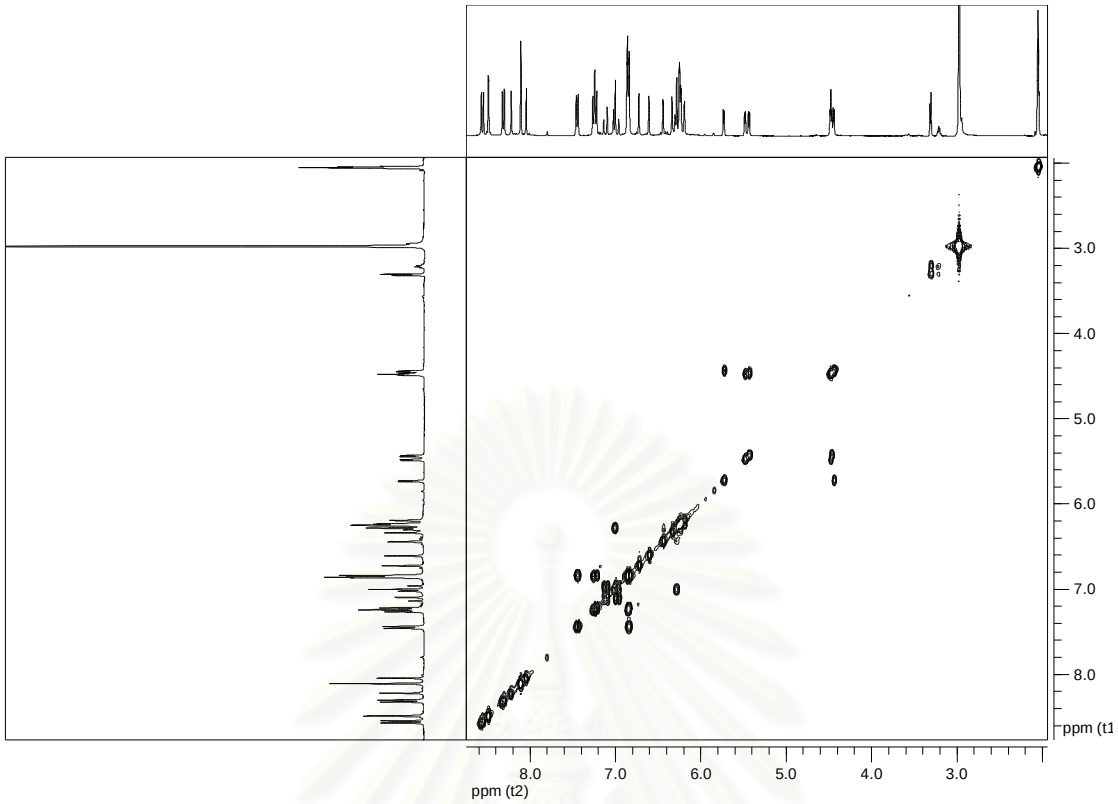

Figure A-1.3 COSY spectrum (acetone-d_6) of macrostachyol A (**6**).

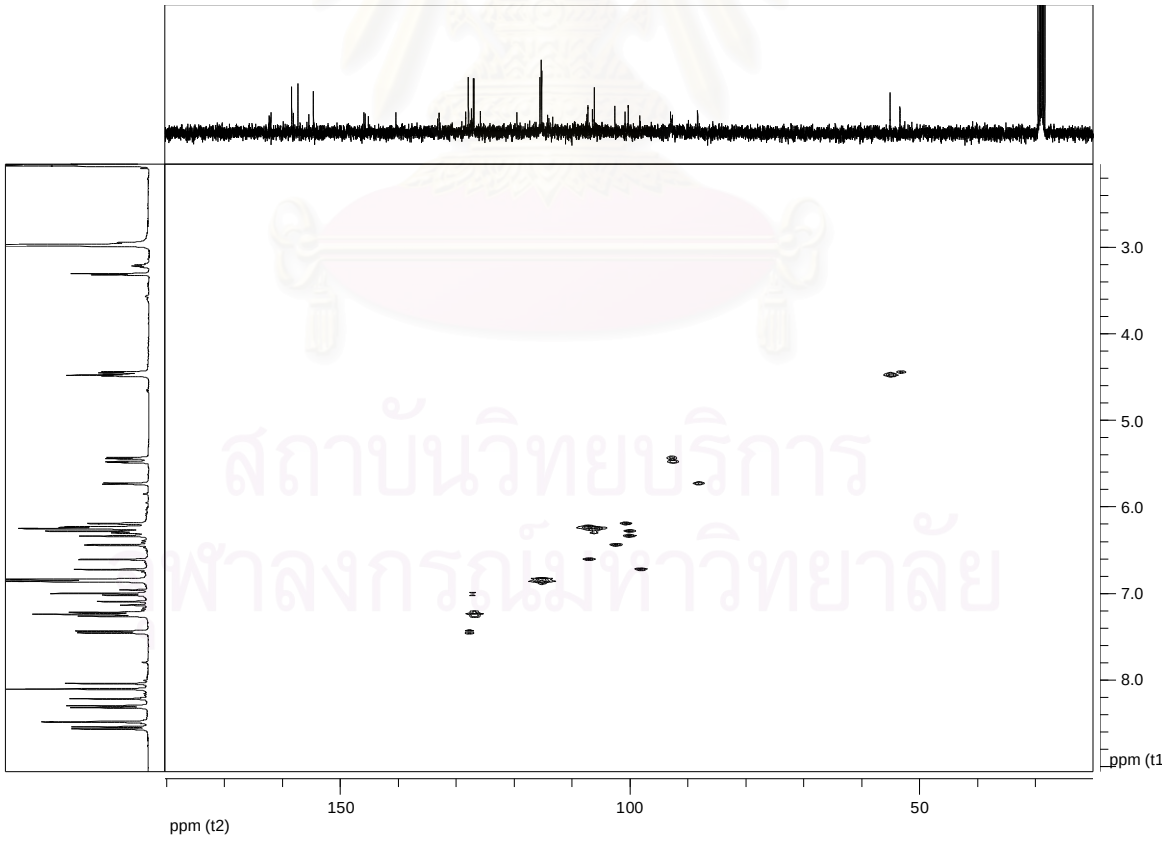

Figure A-1.4 HMQC spectrum (acetone-d_6) of macrostachyol A (**6**).

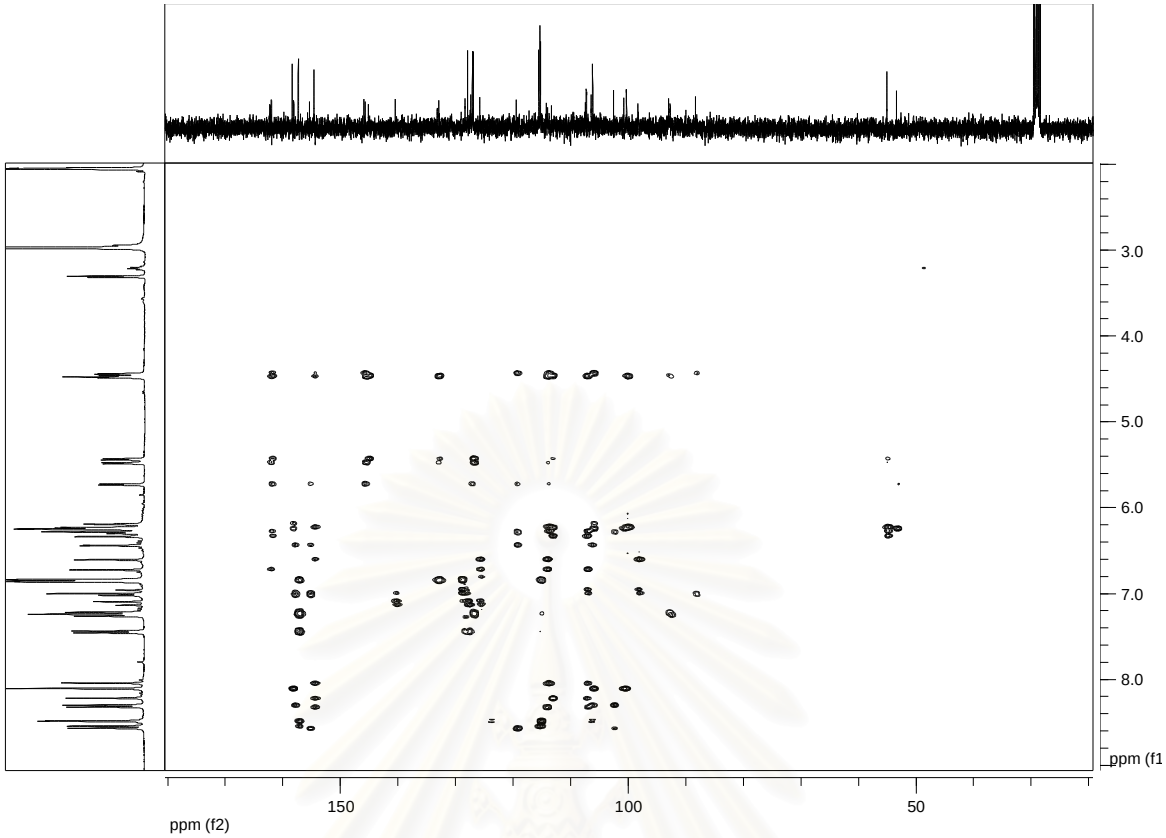

Figure A-1.5 HMBC spectrum (acetone-d_6) of macrostachyol A (**6**).

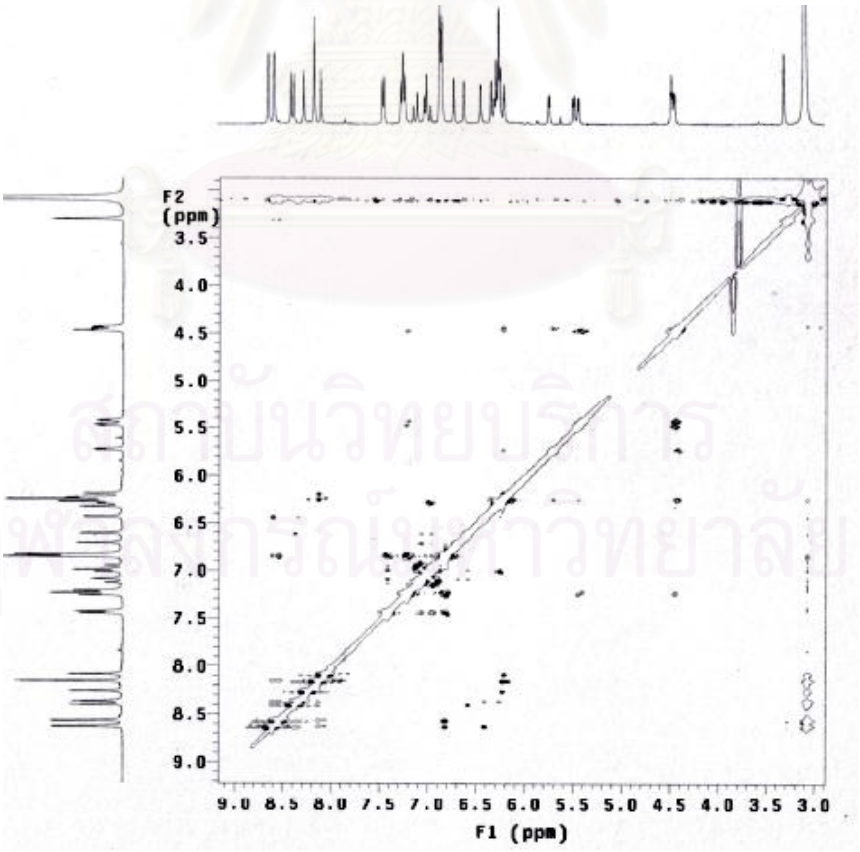

Figure A-1.6 NOESY spectrum (acetone-d_6) of macrostachyol A (**6**).

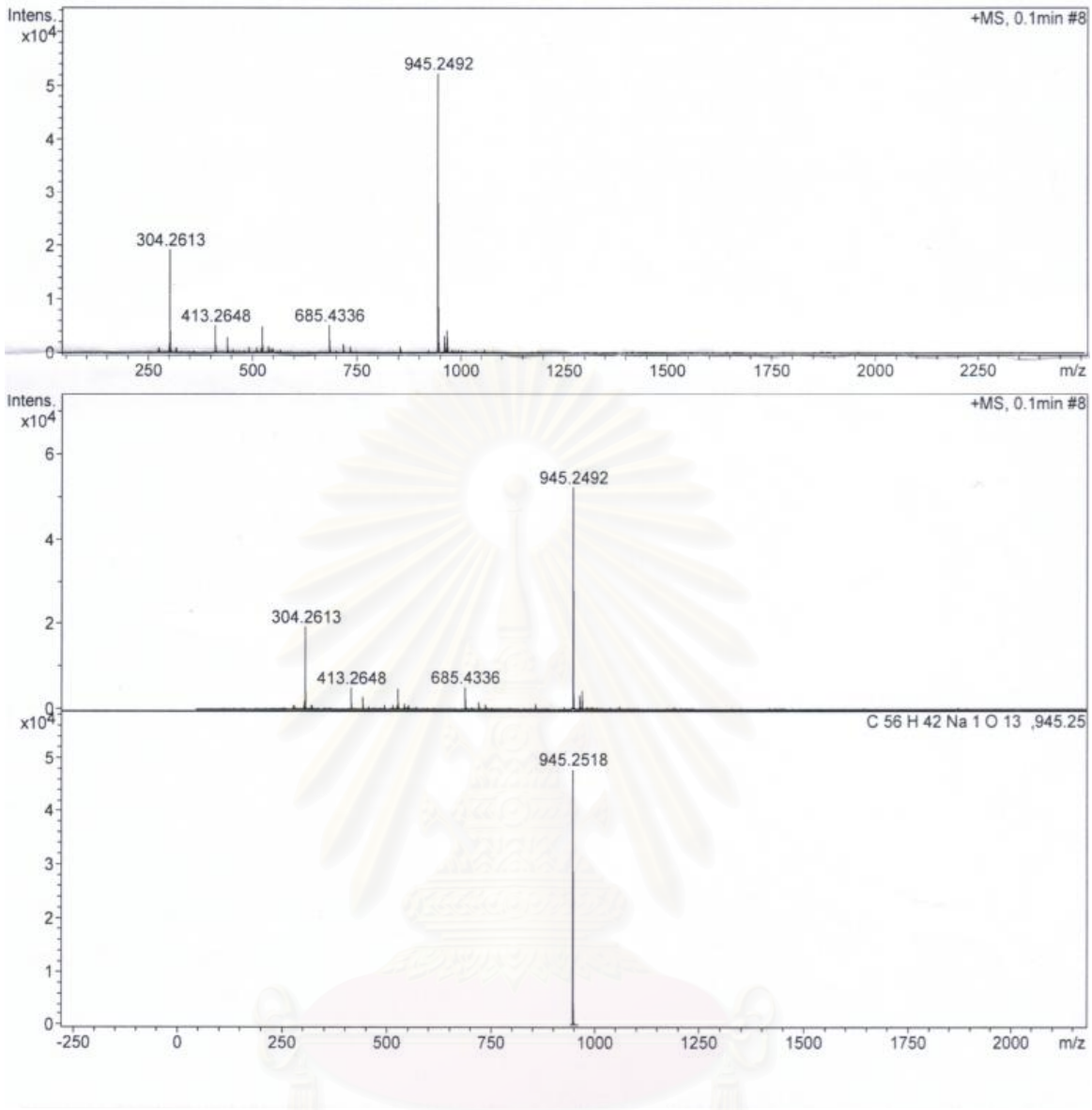

Figure A-1.7 High resolution mass spectrum of macrostachyol A (**6**).

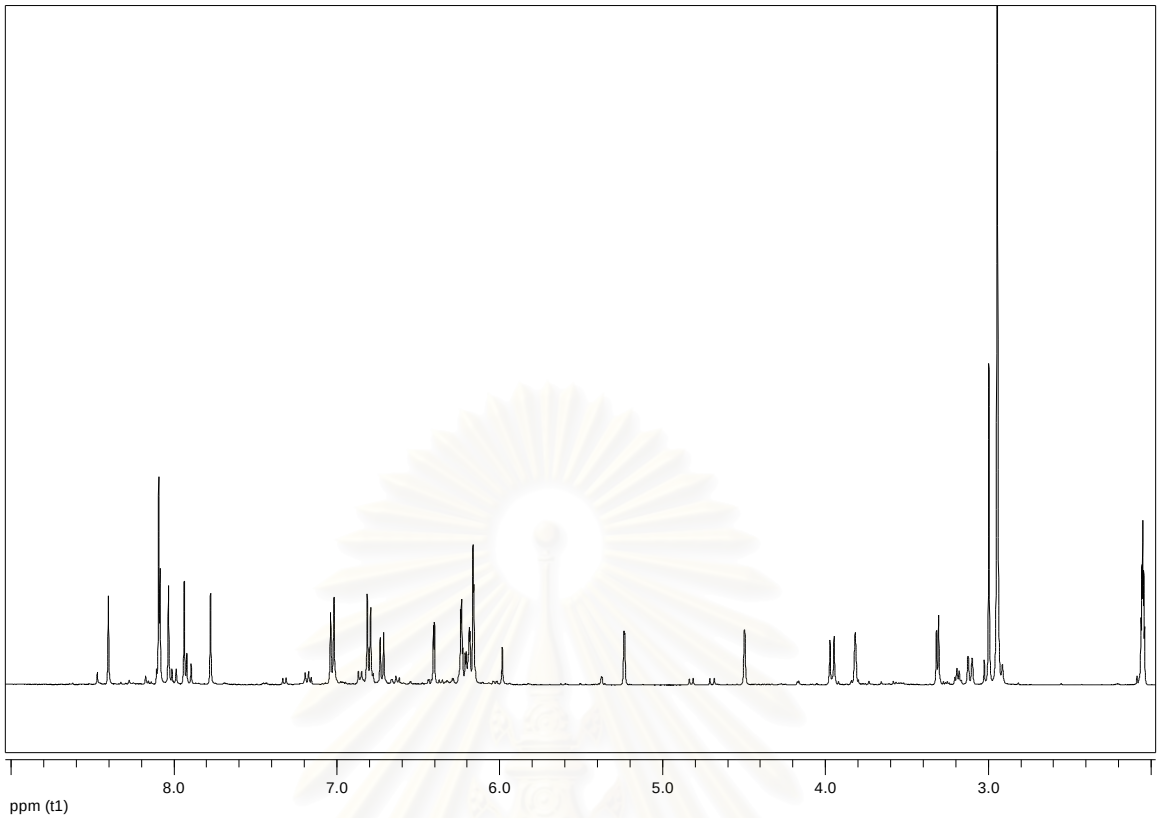

Figure A-2.1 ^{1}H NMR spectrum (acetone-d_6) of macrostachyol B (**7**).

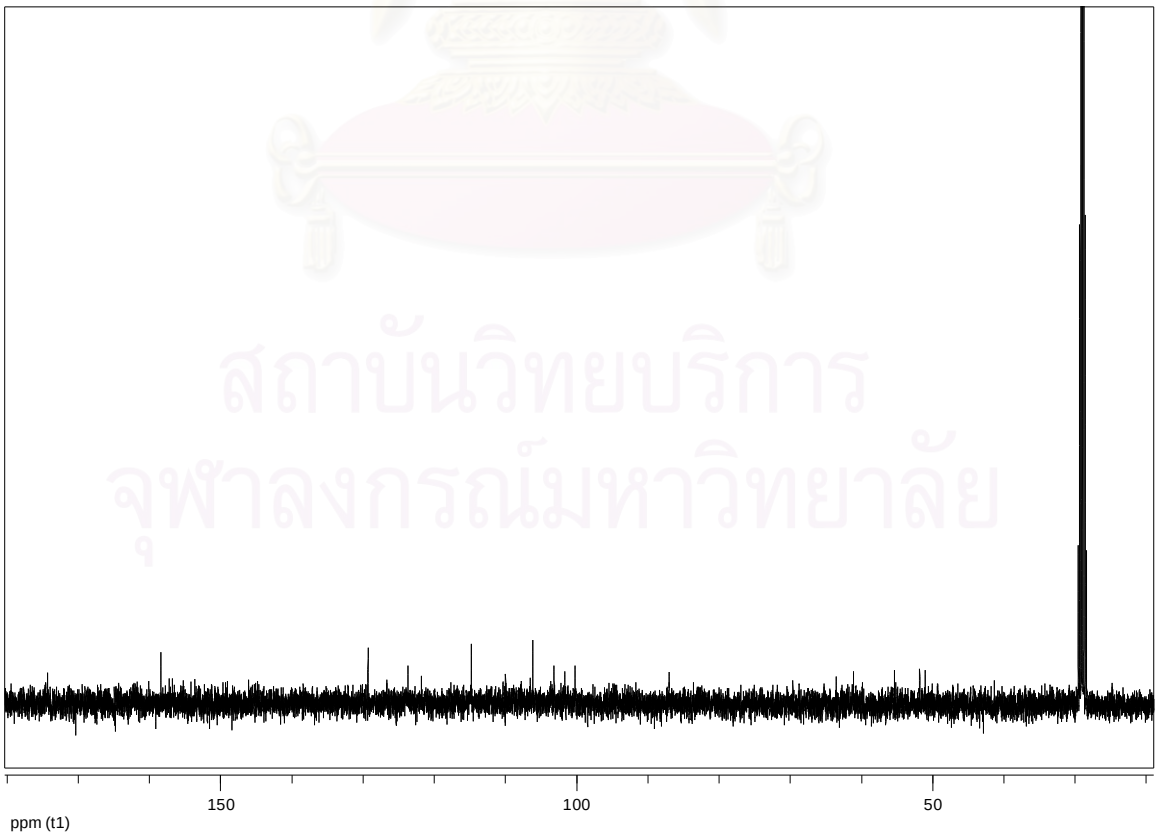

Figure A-2.2 ^{13}C NMR spectrum (acetone-d_6) of macrostachyol B (**7**).

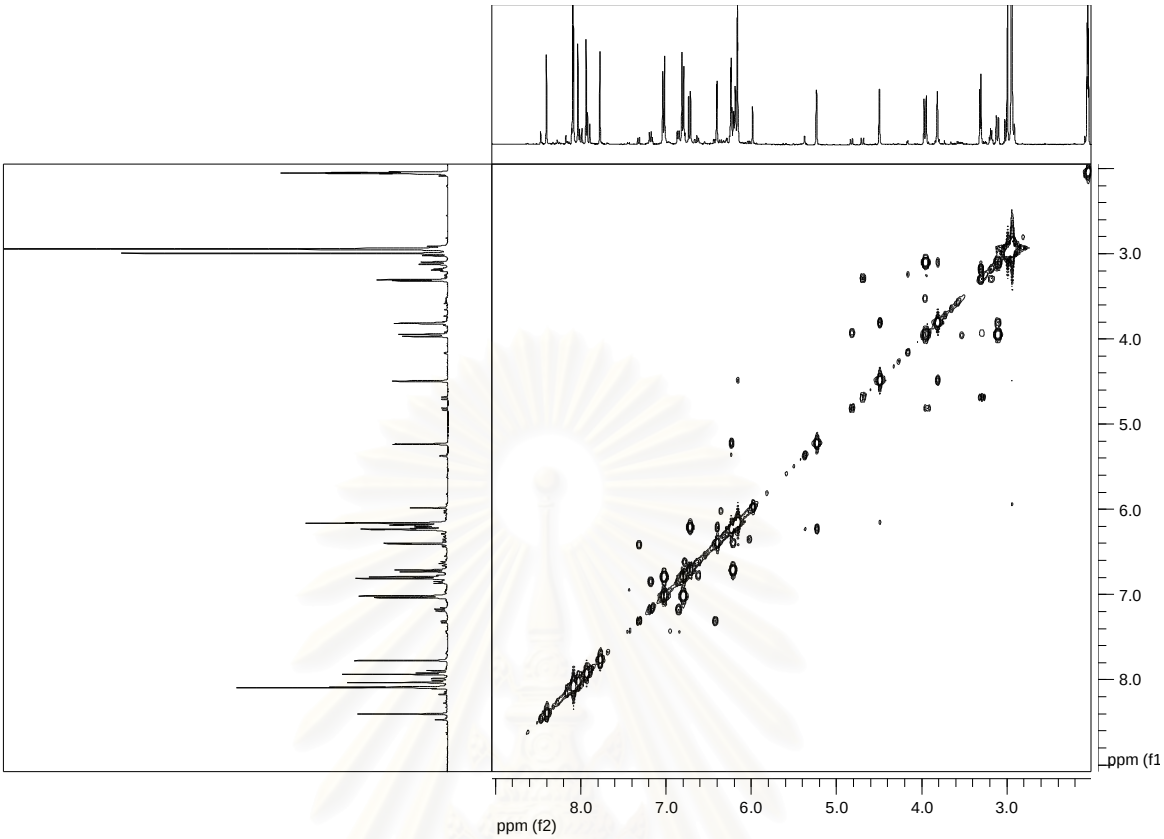

Figure A-2.3 COSY spectrum (acetone-d_6) of macrostachyol B (**7**).

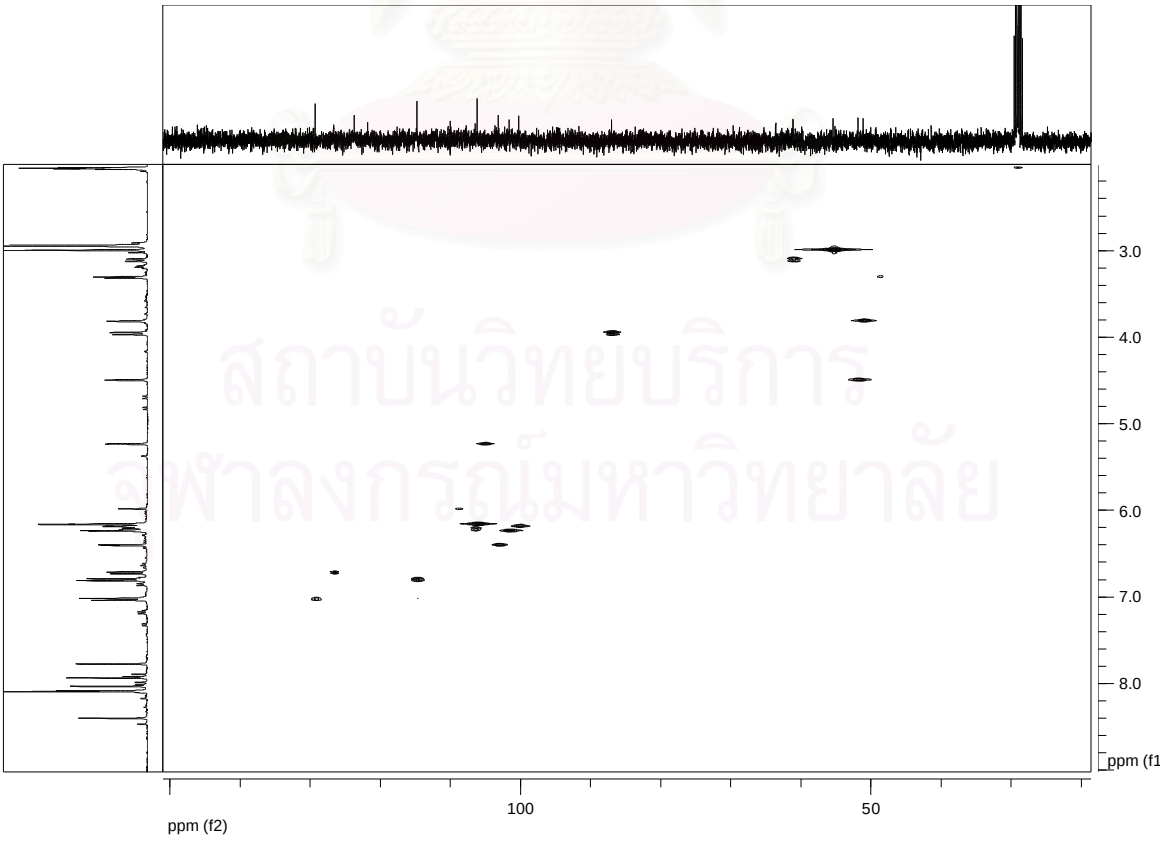

Figure A-2.4 HMQC spectrum (acetone-d_6) of macrostachyol B (**7**).

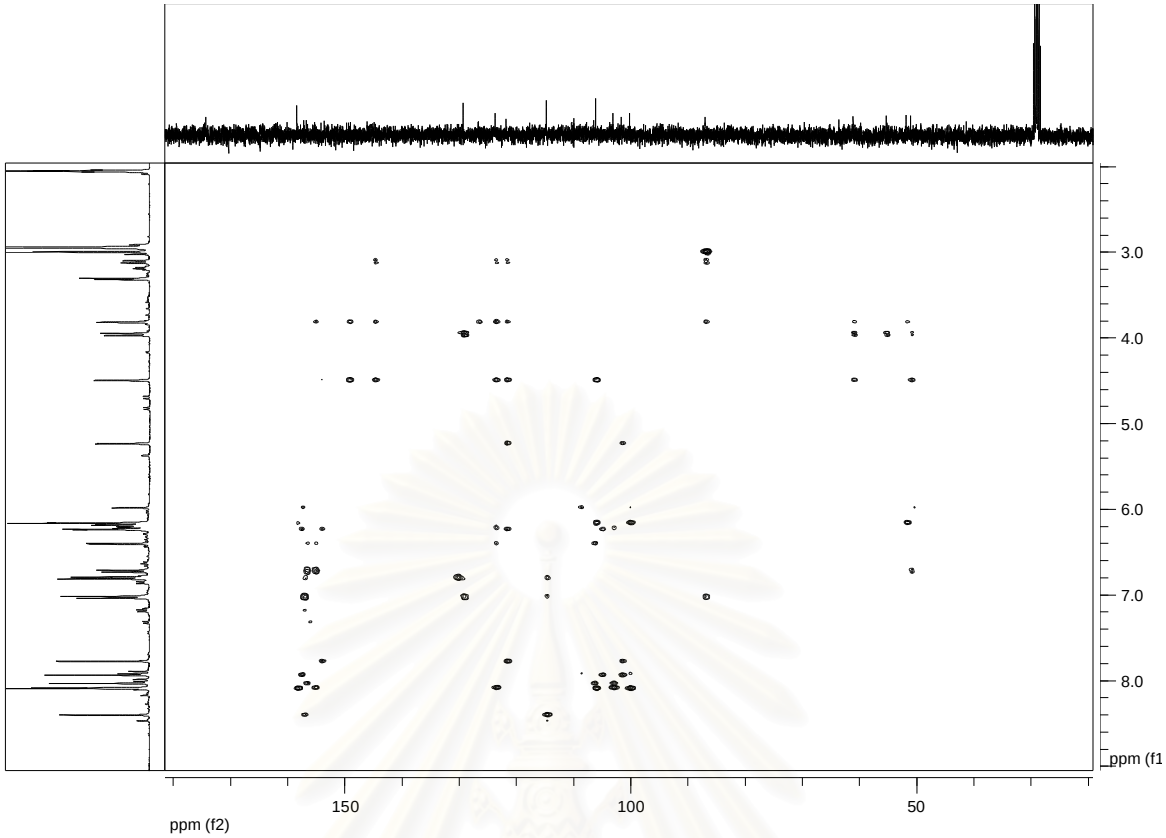

Figure A-2.5 HMBC spectrum (acetone-d_6) of macrostachyol B (**7**).

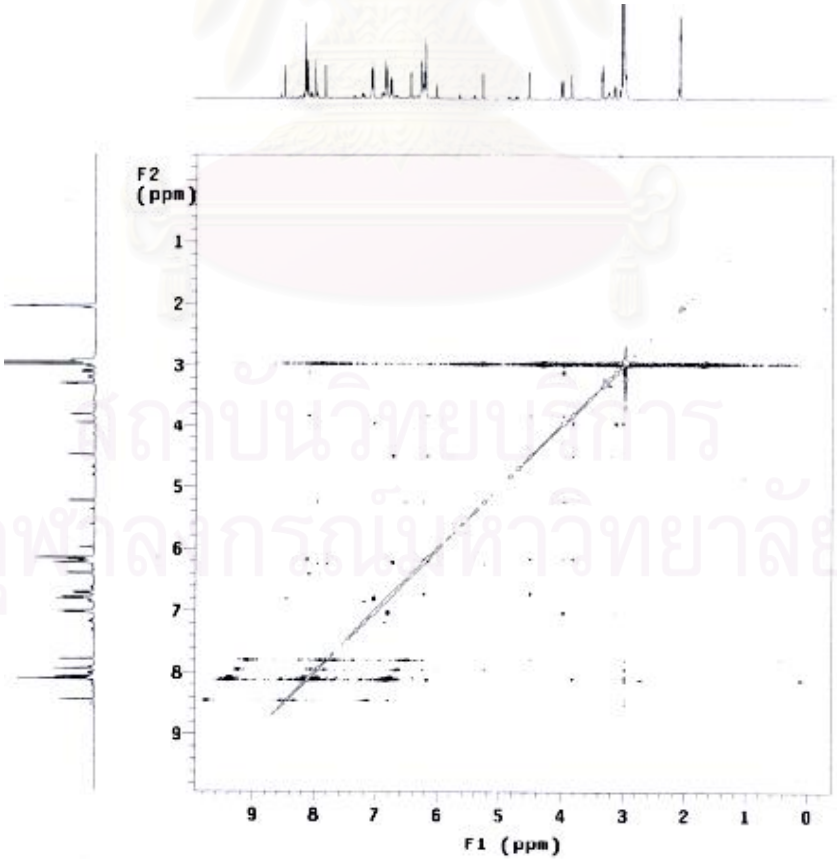

Figure A-2.6 NOESY spectrum (acetone-d_6) of macrostachyol B (**7**).

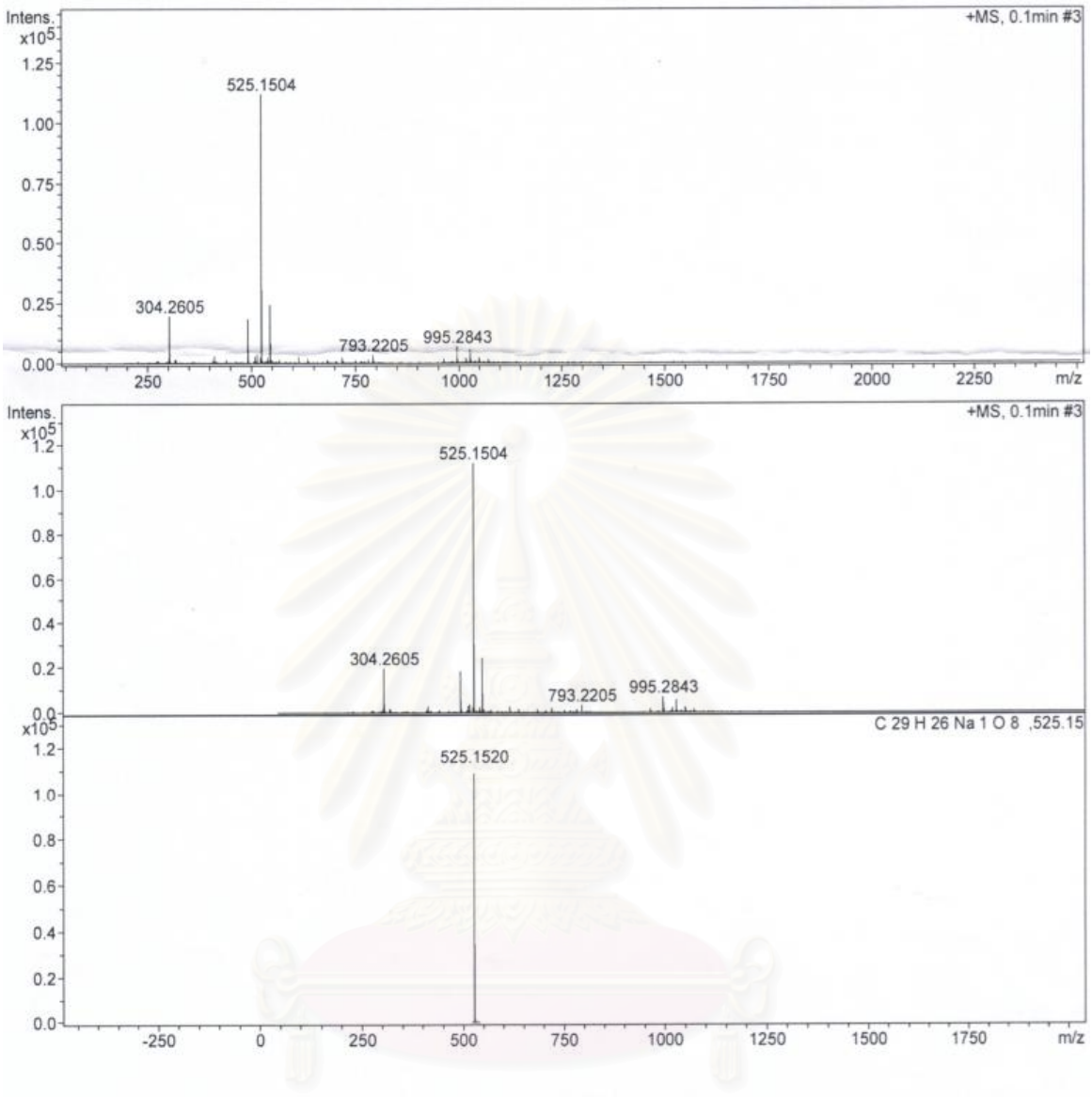

Figure A-2.7 High resolution mass spectrum of macrostachyol B (**7**).

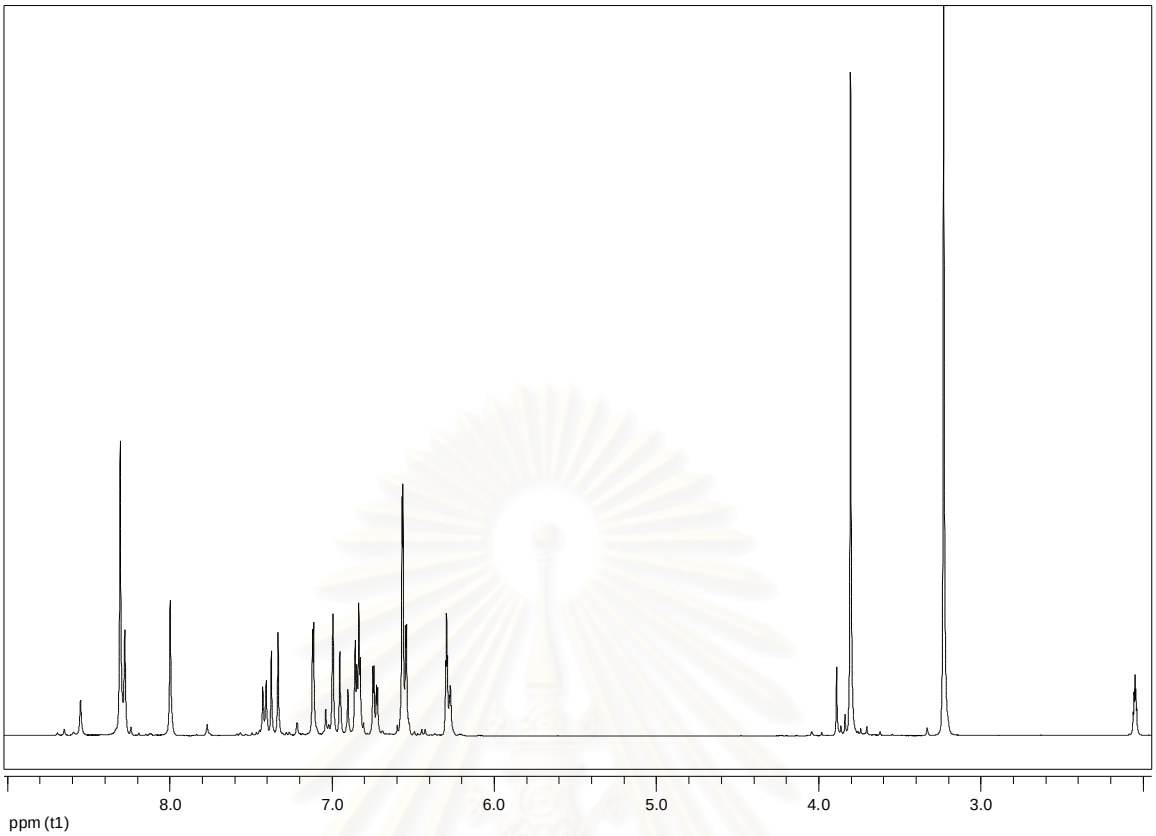

Figure A-3.1 ^{1}H NMR spectrum (acetone-d_6) of a mixture of gnetumacrosin (**9**) and resveratrol (**2**).

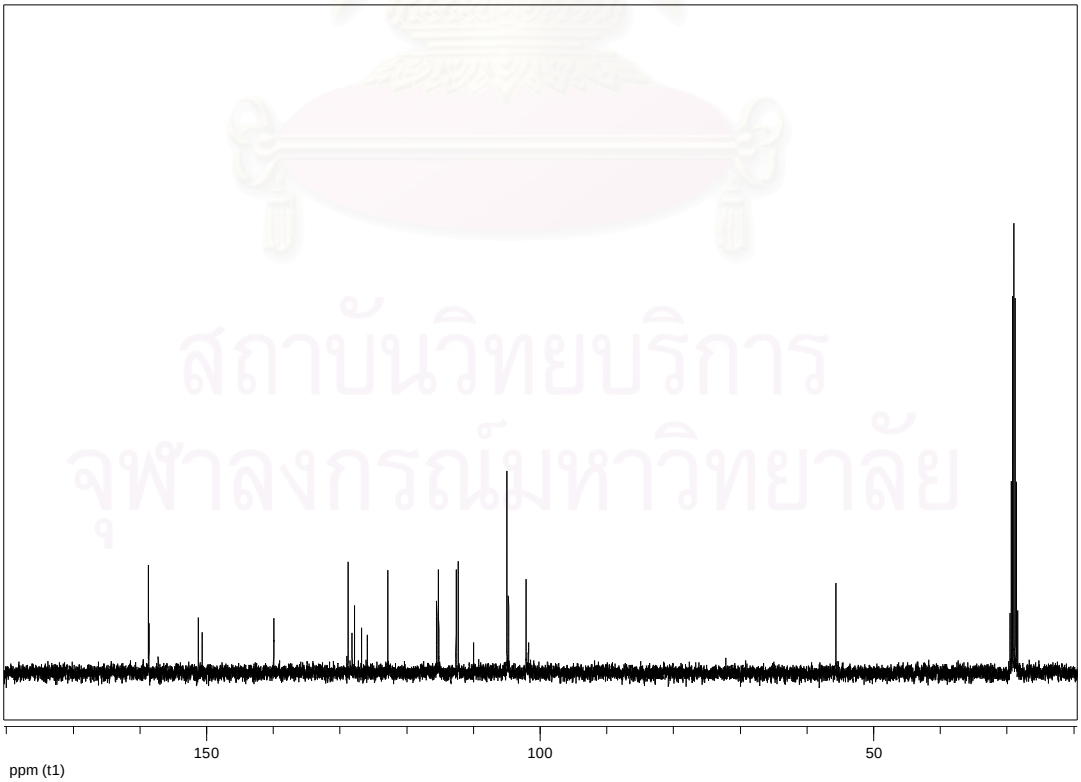

Figure A-3.2 ^{13}C NMR spectrum (acetone-d_6) of a mixture of gnetumacrosin (**9**) and resveratrol (**2**).

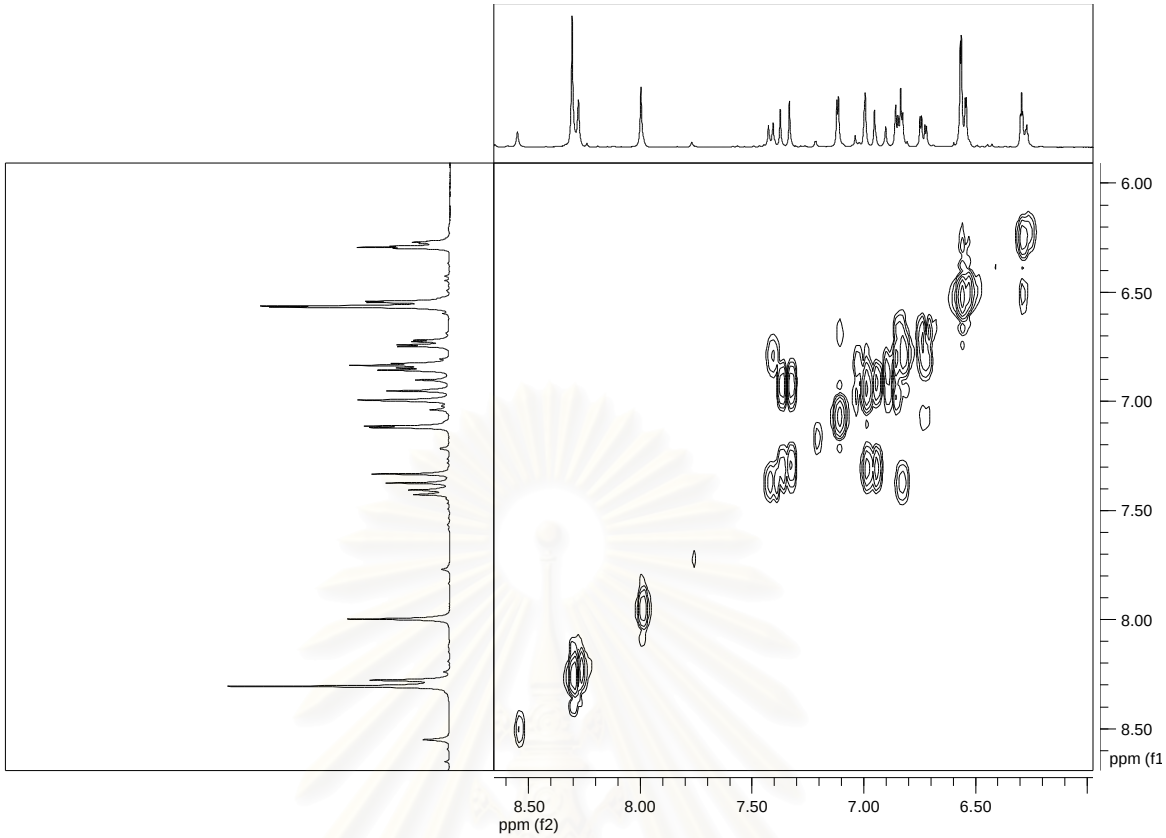

Figure A-3.3 COSY spectrum (acetone-d_6) of a mixture of gnetumacrosin (**9**) and resveratrol (**2**).

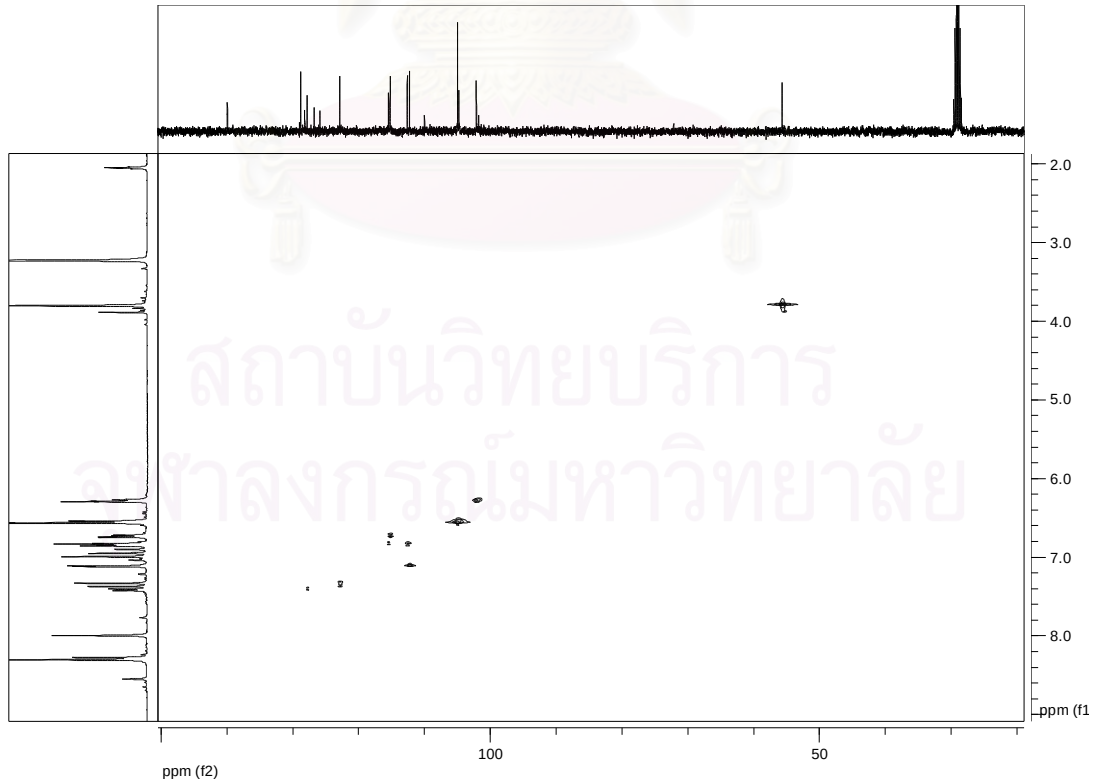

Figure A-3.4 The HMQC spectrum (acetone-d_6) of a mixture of gnetumacrosin (**9**) and resveratrol (**2**).

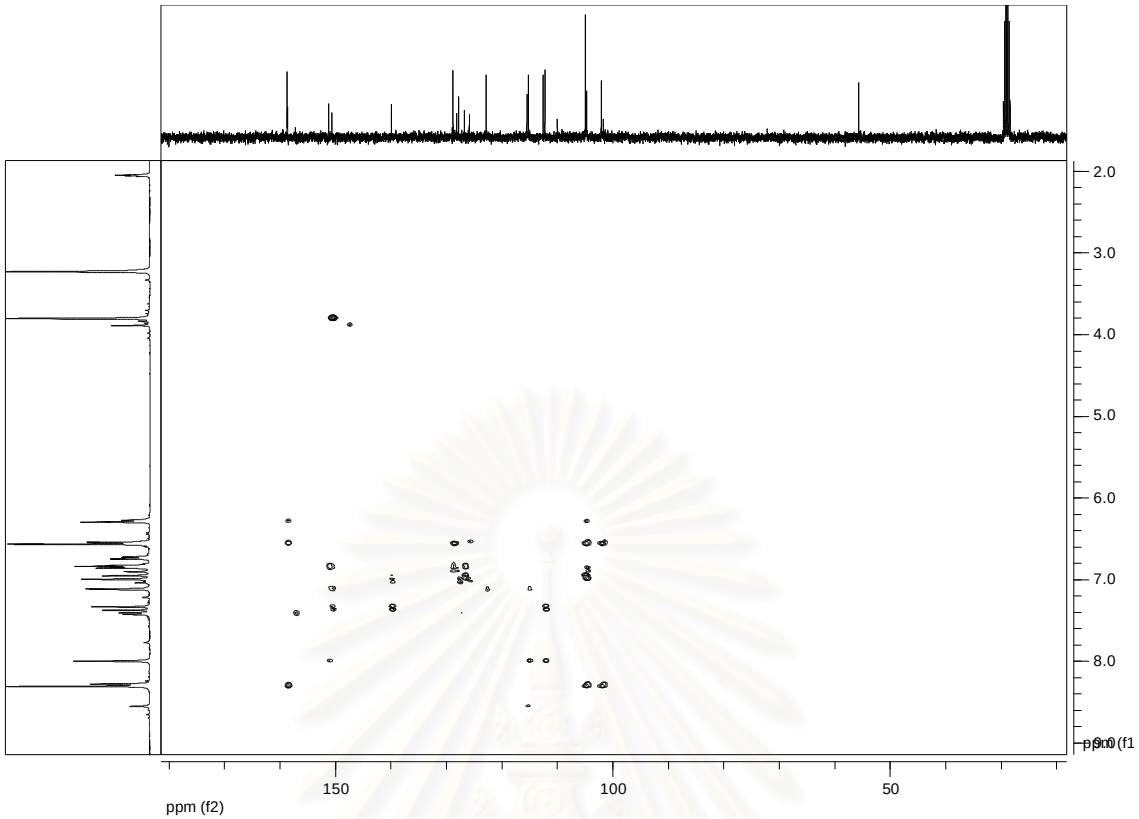

Figure A-3.5 HMBC spectrum (acetone-d_6) of a mixture of gnetumacrosin (**9**) and resveratrol (**2**).

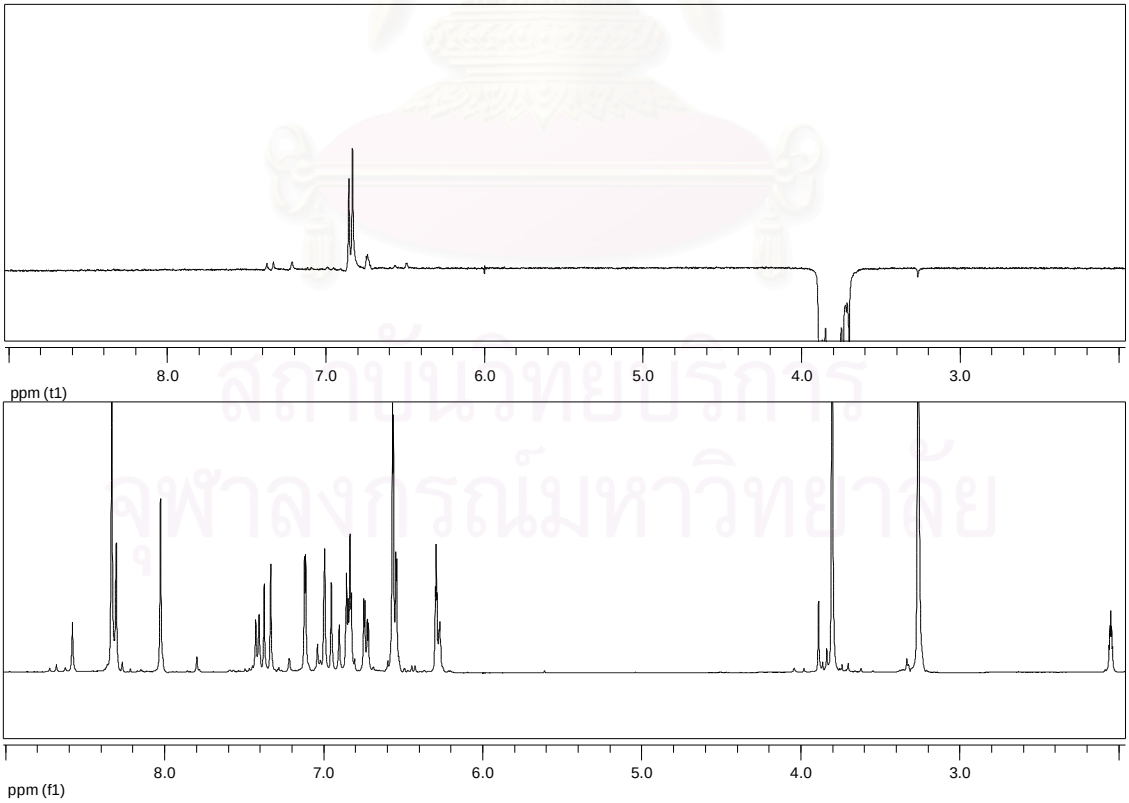

Figure A-3.6 NOE spectrum (acetone-d_6) of a mixture of gnetumacrosin (**9**) and resveratrol (**2**).

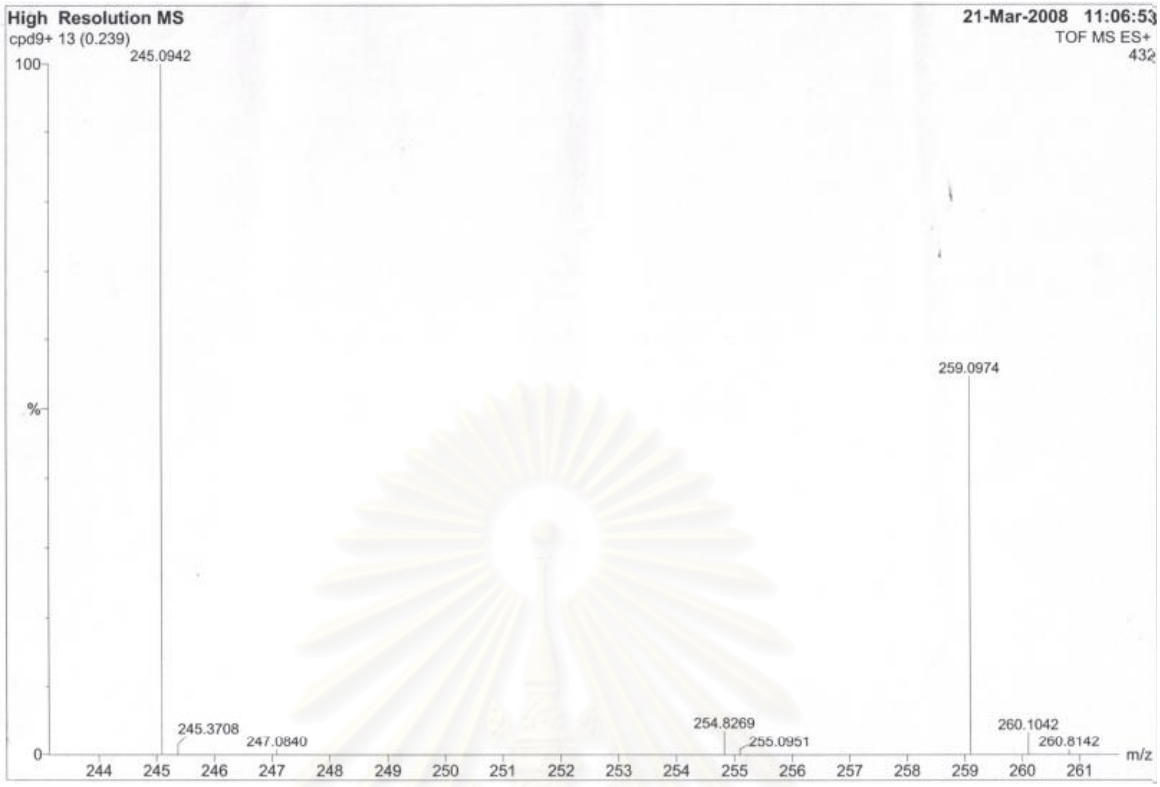

Figure A-3.7 High resolution mass spectrum of gnetumacrosin (**9**).

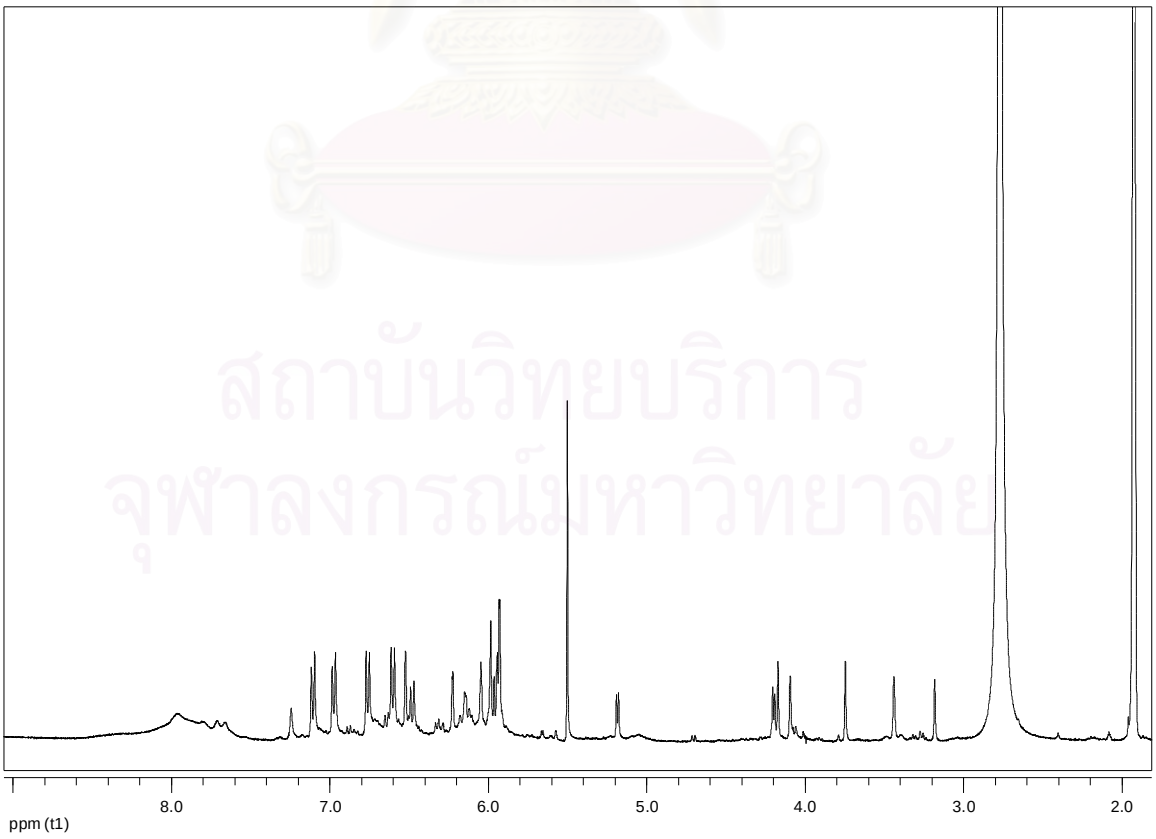

Figure A-4.1 ^{1}H NMR spectrum (acetone-d_6) of macrostachyol C (**11**).

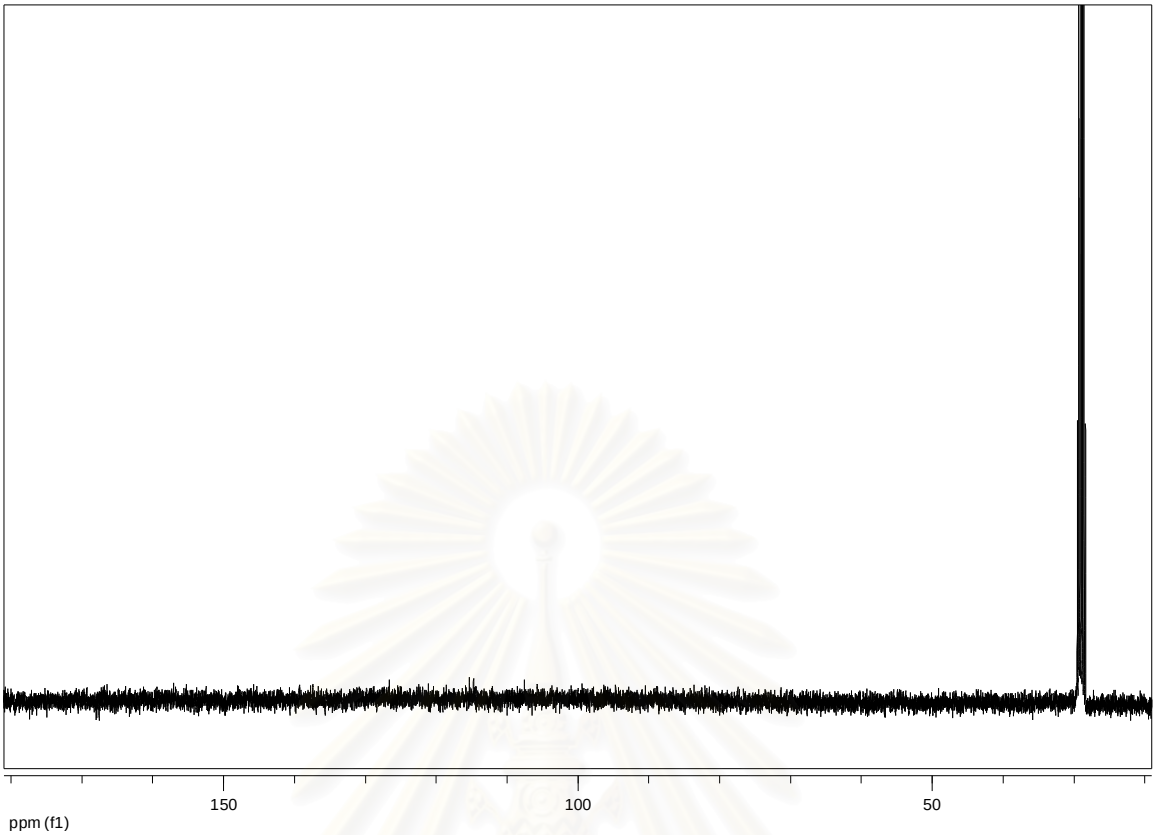

Figure A-4.2 ^{13}C NMR spectrum (acetone-d_6) of macrostachyol C (**11**).

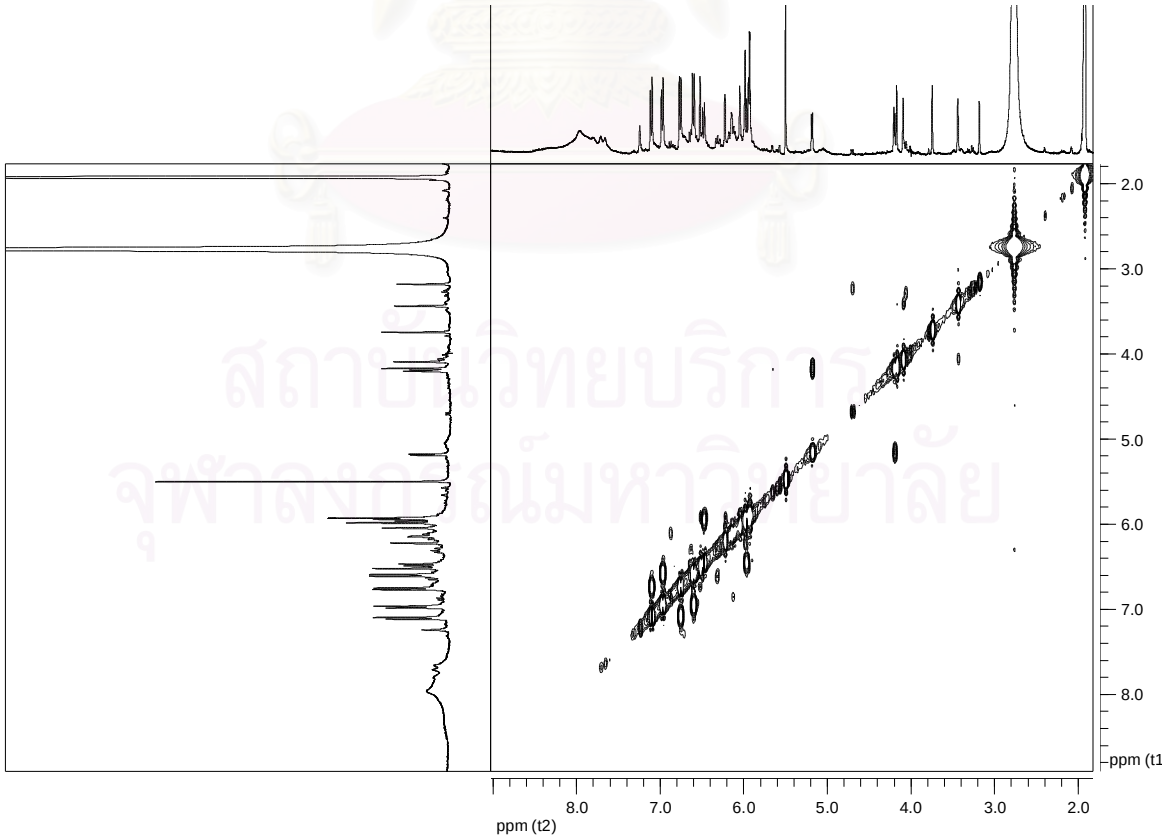

Figure A-4.3 COSY spectrum (acetone-d_6) of macrostachyol C (**11**).

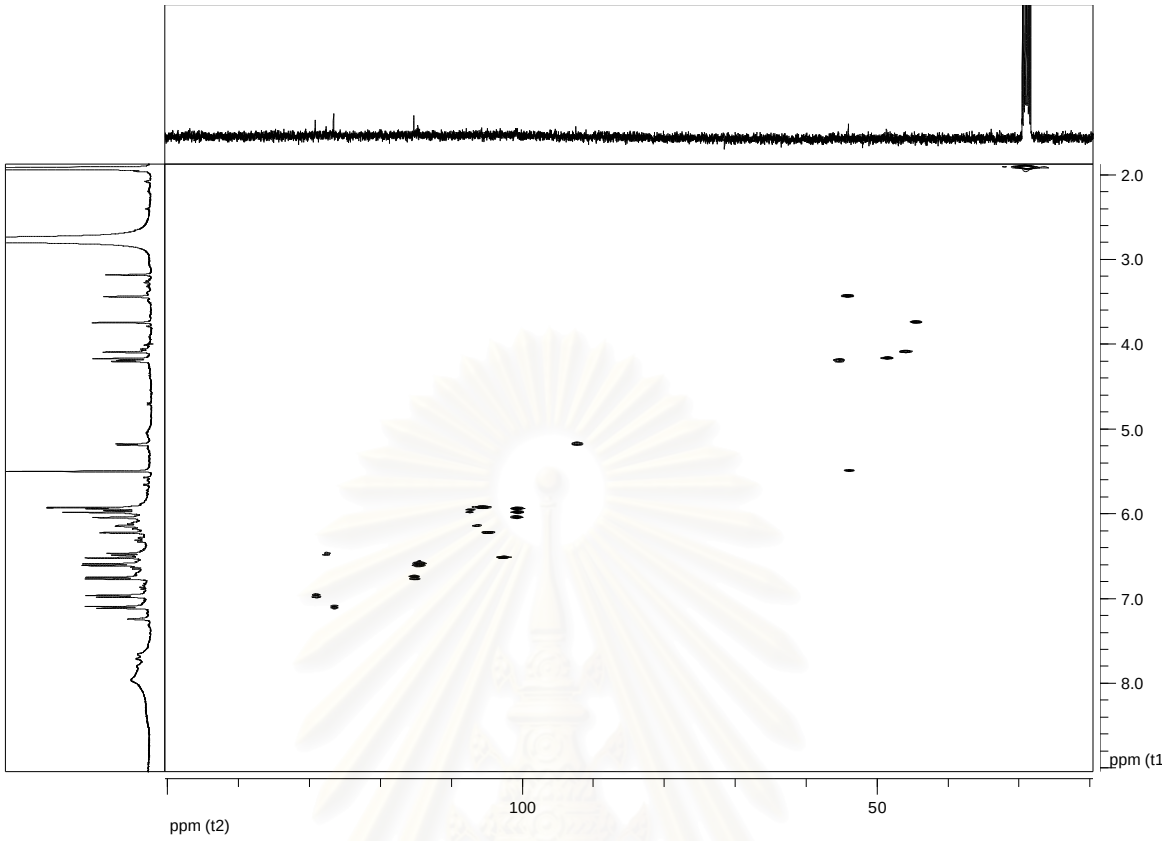

Figure A-4.4 HMQC spectrum (acetone-d_6) of macrostachyol C (**11**).

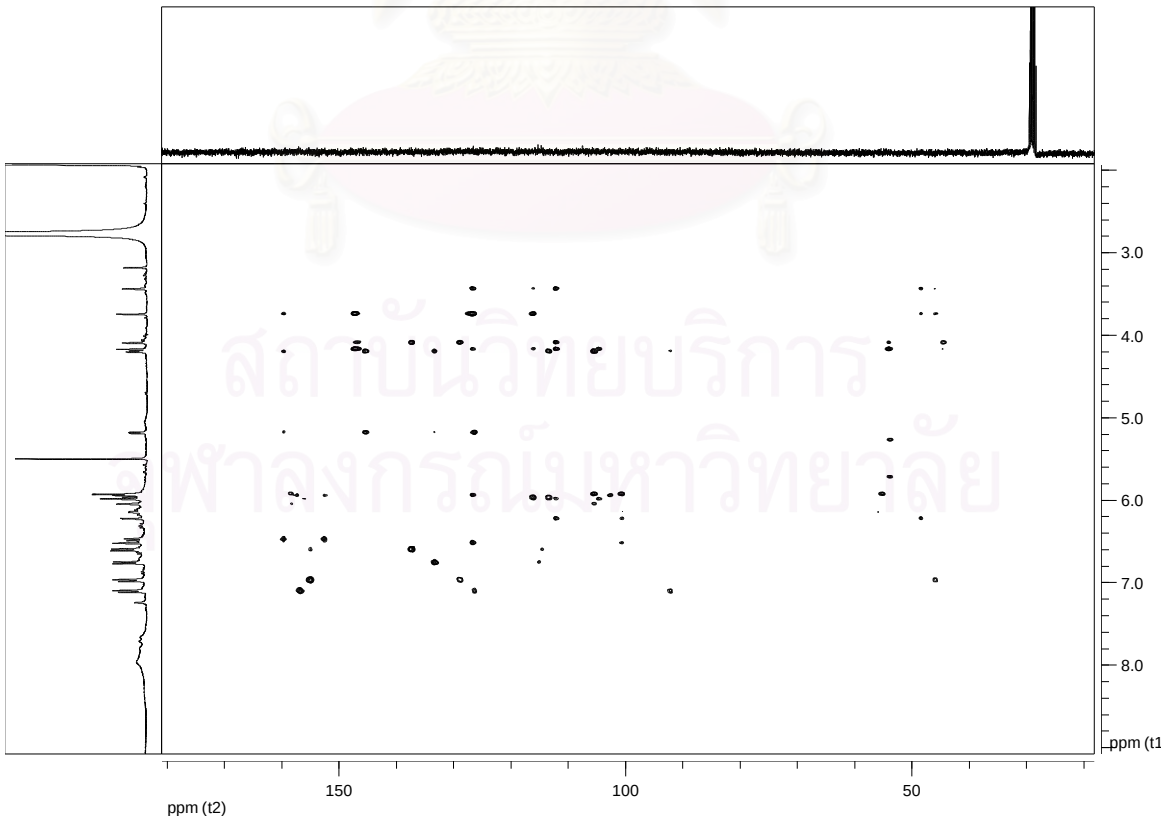

Figure A-4.5 HMBC spectrum (acetone-d_6) of macrostachyol C (**11**).

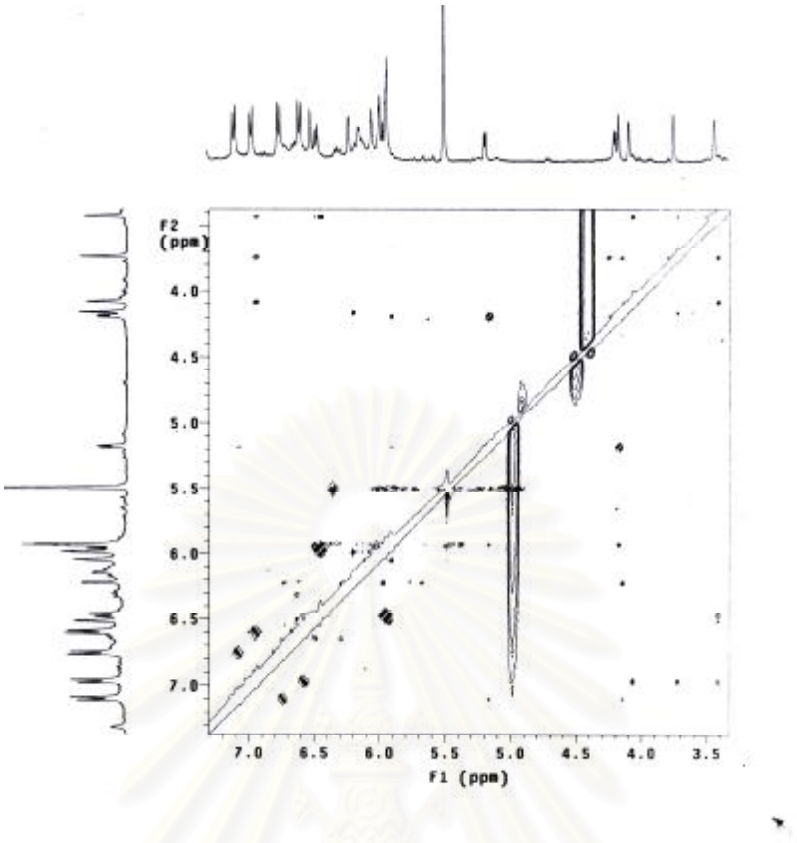

Figure A-4.6 NOESY spectrum (acetone-d_6) of macrostachyol C (**11**).

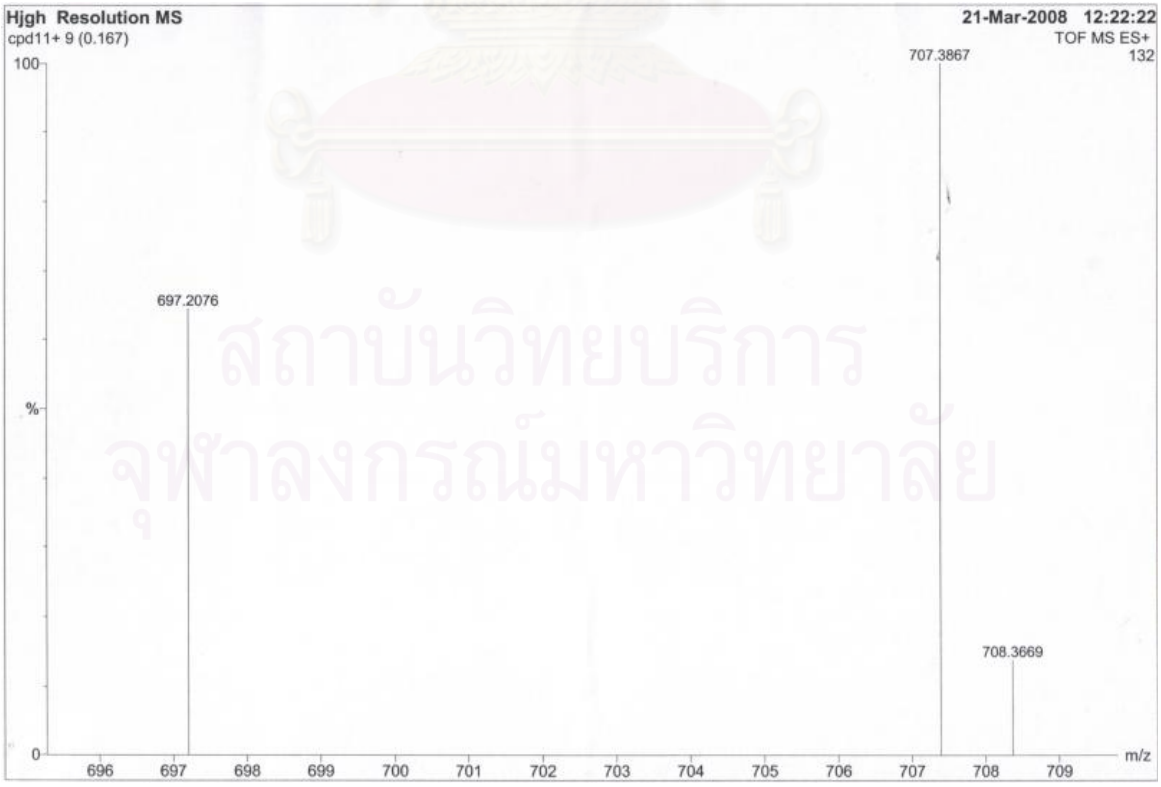

Figure A-4.7 High resolution mass spectrum of macrostachyol C (**11**).

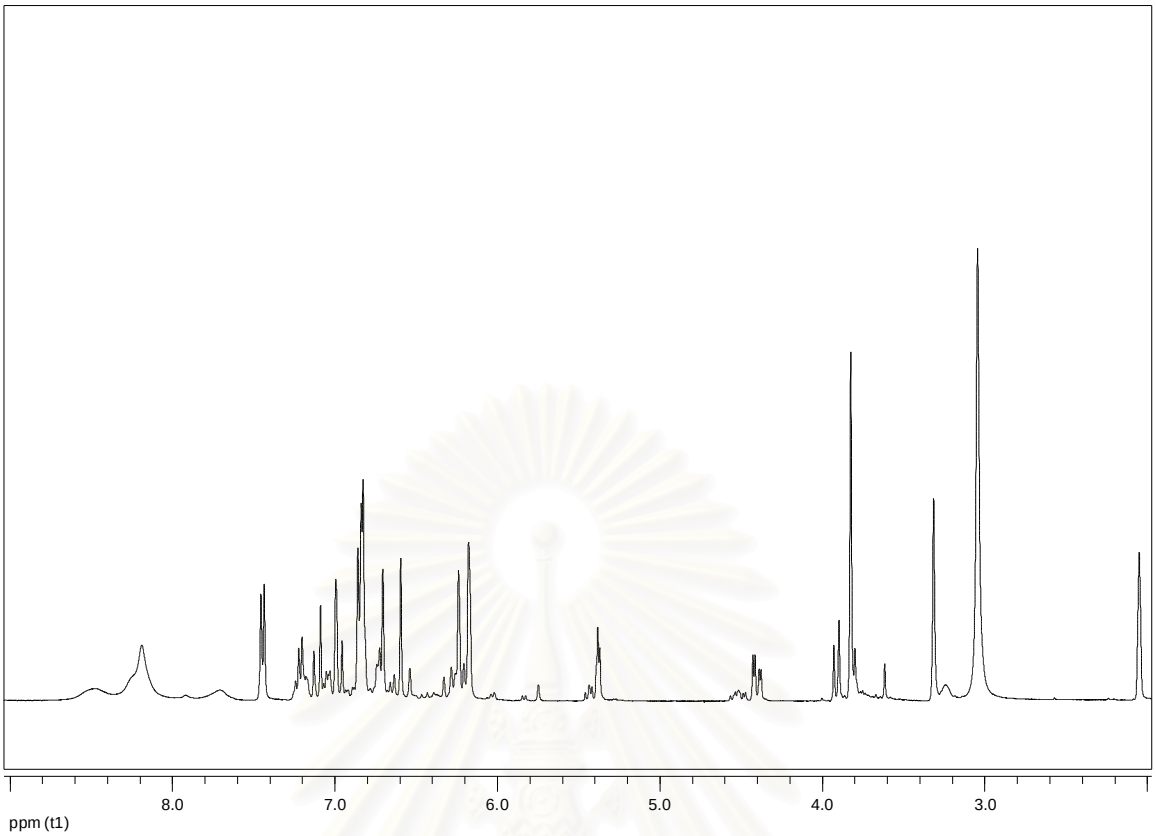

Figure A-5.1 ^{1}H NMR spectrum (acetone-d_6) of macrostachyol D (**13**).

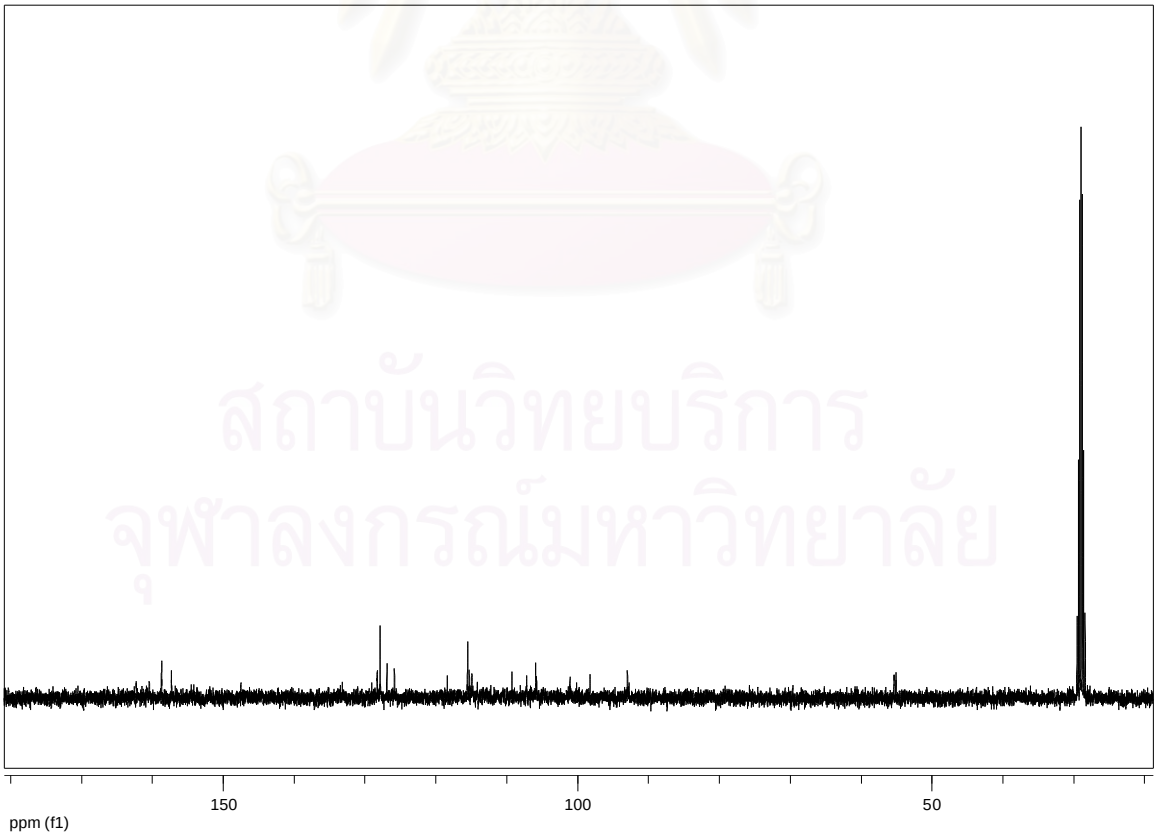

Figure A-5.2 ^{13}C NMR spectrum (acetone-d_6) of macrostachyol D (**13**).

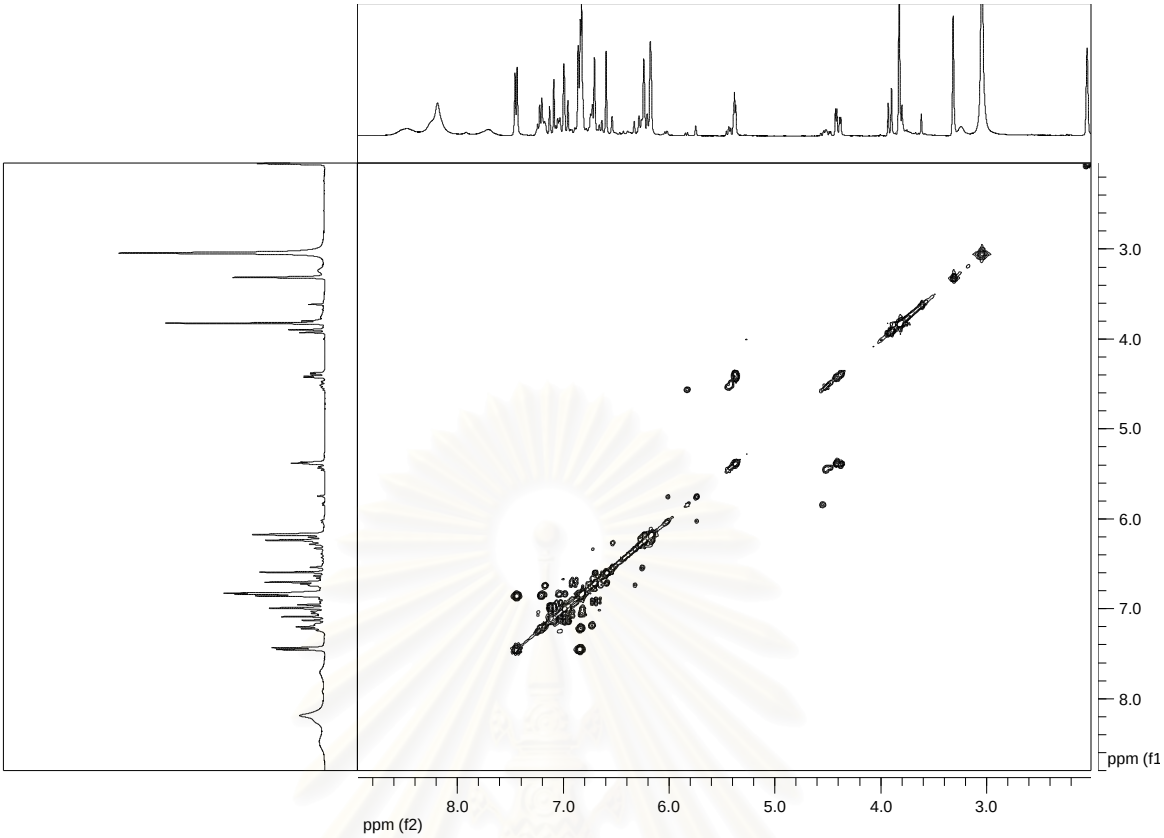

Figure A-5.3 COSY spectrum (acetone-d_6) of macrostachyol D (**13**).

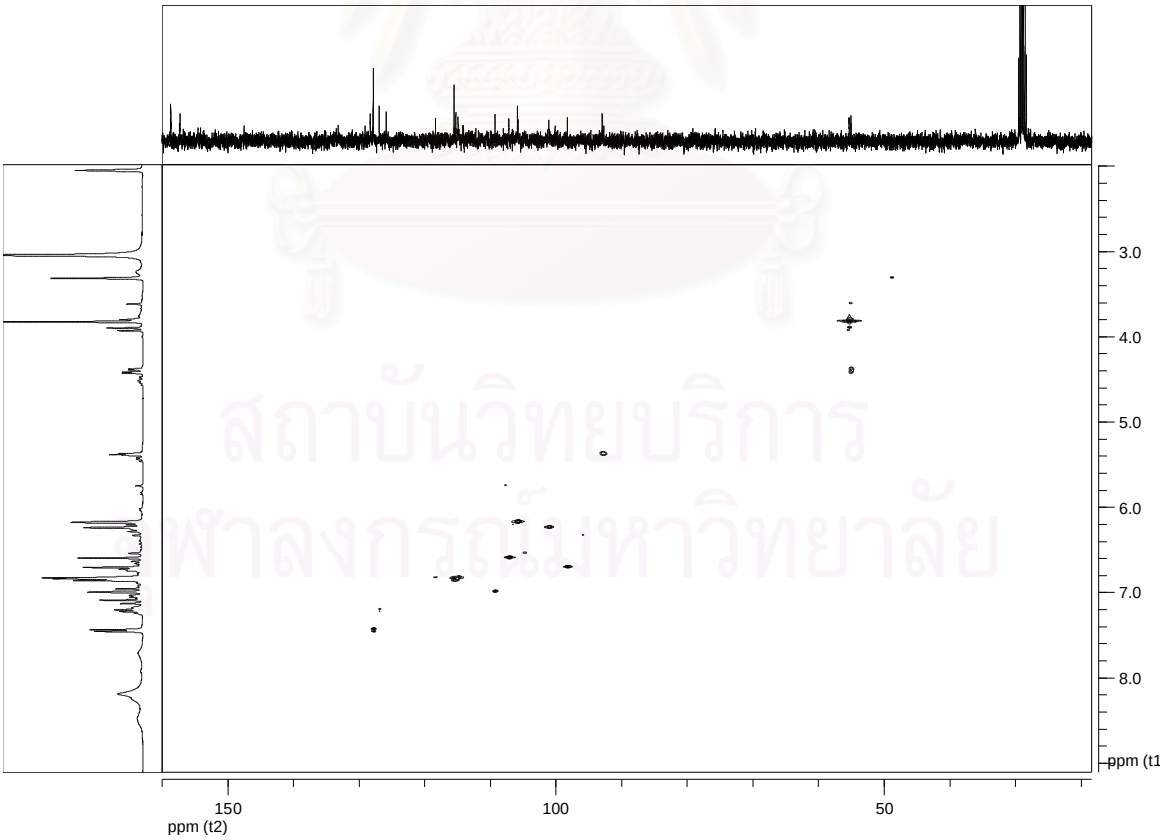

Figure A-5.4 HMQC spectrum (acetone-d_6) of macrostachyol D (**13**).

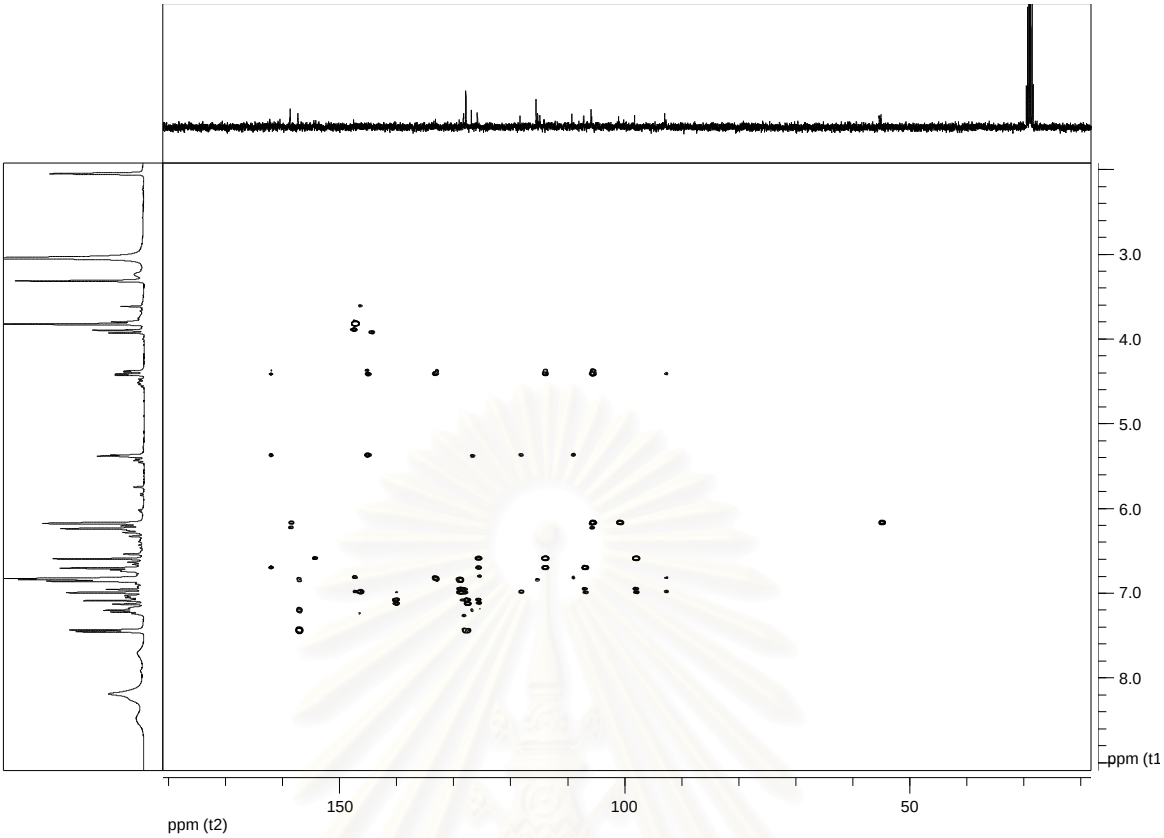

Figure A-5.5 HMBC spectrum (acetone-d_6) of macrostachyol D (**13**).

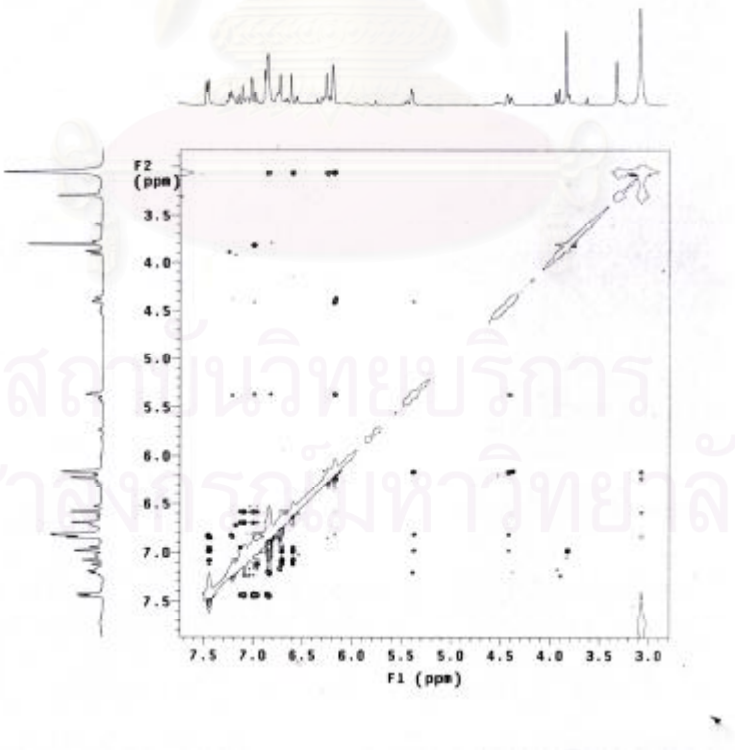

Figure A-5.6 NOESY spectrum (acetone-d_6) of macrostachyol D (**13**).

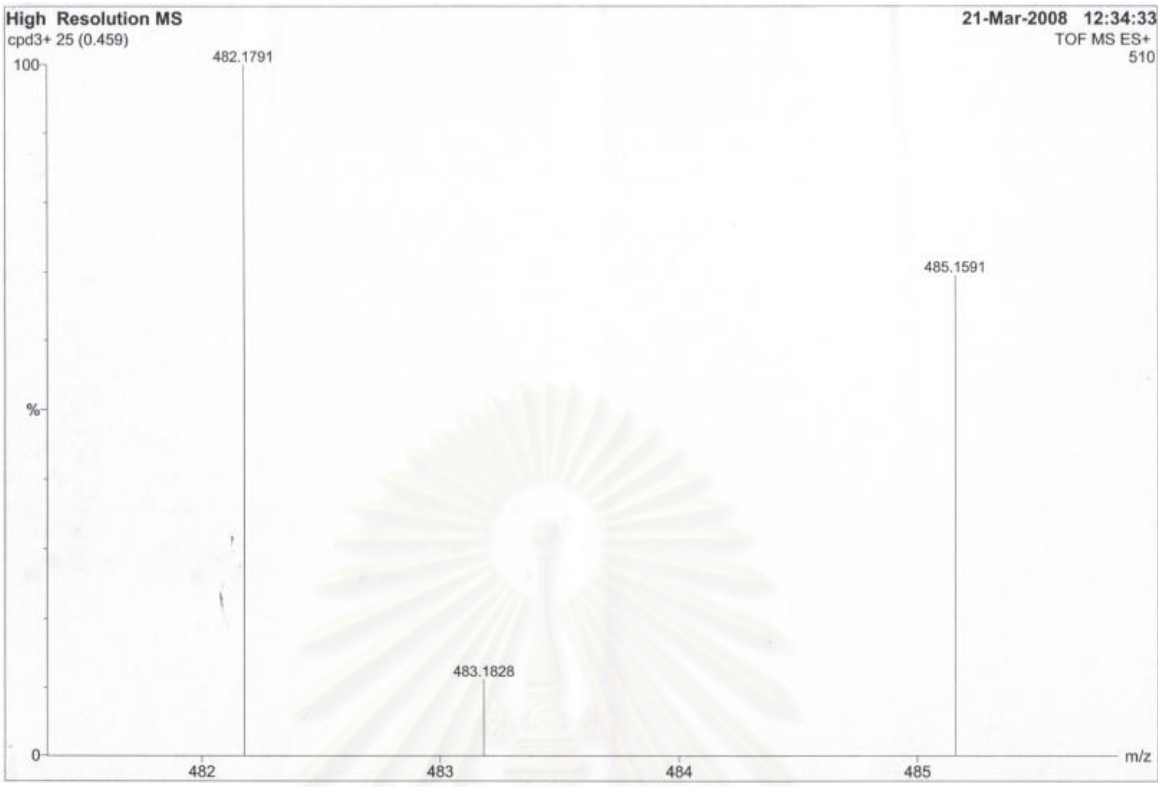

Figure A-5.7 High resolution mass spectrum of macrostachyol D (**13**).

VITA

Mr. Piyawit Sri-in was born on November 5, 1981 in, Nakhon Si Thammarat, Thailand. He graduated with Bachelor Degree of Science in Chemistry from Faculty of Science, Chulalongkorn University, in 2004. During the time he studying in Master of Science program in Department of Chemistry, he received a research fund for his thesis from the Graduate School, Chulalongkorn University.

His present address is 240/1 Moo 13, Tambon Suan Luang, Amphoe Chaloem Phra Kiat, Nakhon Si Thammarat, Thailand, 80190, Tel: 089-6727340.